Polymetallic Silyl-Iron and -Ruthenium Compounds

THE UNIVERSITY OF
WAIKATO
Te Whare Wānanga o Waikato

A thesis submitted in partial fulfilment
of the requirements for the degree
of

Masters of Science in Chemistry

at

The University of Waikato

by

Neville Kingston Masters

The University of Waikato
2010

Abstract

The synthesis of iron and ruthenium compounds which contain either end-capped silyl units Fe-Si-Si-Fe or the linear sequence Si-Ru-Ru-Si respectively were explored.

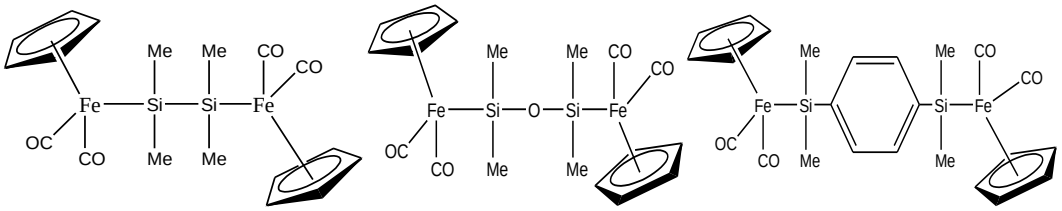

(**I**) (**II**) (**III**)

End-capped iron species, e.g. **I**, were prepared using literature methods and two new related iron containing silyl species **II** and **III** were synthesised. These were prepared as model compounds for comparison with polymeric analogues.

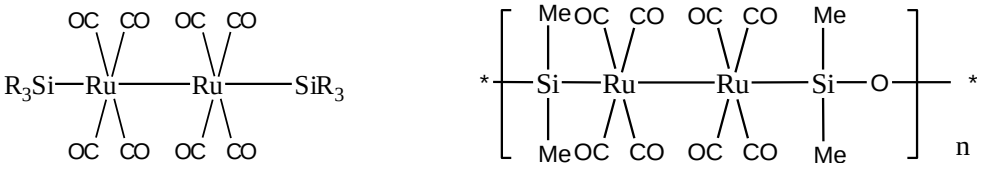

(**IV**) (**V**)

Ruthenium silyl species of the type **IV** that maintain metal – metal bonding have been prepared. As an extension to this work inorganic polymeric species such as **V** were synthesised using the same preparation techniques.

The polymeric compounds were difficult to characterise as they were unable to be chromatographed or crystallised therefore, all data was from crude mixtures. Spectroscopic techniques involved FT - IR, ESMS, LDI-TOF and NMR spectroscopy. ESMS was an ineffective technique for the polymeric compounds however, LDI-TOF mass spectrometry gave broad curves with an average molecular weight ranging from 60,000 to 200,000 for different preparations.

Flexible siloxanes such as $HSiMe_2OSiMe_2OSiMe_2H$ gave molecular cluster derivatives with bridging ligands rather than polymers.

Acknowledgements

For the completion of this thesis I would like to thank The University of Waikato staff within the chemistry department, especially my supervisor Brian Nicholson for all the support and help that I have received over these past years. Furthermore I would like to thank Alistair Wilkins for his help with the NMR spectra that have been successfully interpreted within this thesis.

Other staffing members who need appraisal are the technicians Pat Gread and Wendy Jackson, who were brilliant with training for the instrumental techniques used within the mass spectrometry suit of the chemistry department.

I would further like to thank my fellow students who have made my tertiary education very enjoyable and well worth remembering. Lastly I would like to pay a special thanks to my parents, as without them I would not have been able to achieve any of my goals over these past six years.

Table of Contents

Abstract ii
Acknowledgements iii
Table of Contents iv
List of Figures vi
List of Tables viii
Abbreviations ix

1.0 Background 1
1.1 Conventional organic polymers 1
1.2 "Decorated" one – dimensional inorganic polymers 1
1.3 Organometallic polymers 2
1.4 Metal attachment to unsaturated organic polymers 4
1.5 Polymeric material containing metal – metal bonding 5
1.6 Metallic ruthenium polymers 9
1.7 Basis for present project 22
1.8 Aim of this thesis 24

2.0 Experimental 25
2.1 General 25
2.2 Instrumental Techniques 25
2.3 Synthesis of $Na[Cp(CO)_2Fe]$ 27
2.4 Synthesis of $[(Cp(CO)_2Fe)SiMe_2]_2$ 27
2.5 Synthesis of $1,2\text{-}C_2H_4[SiMe_2(Fe(CO)_2Cp)]_2$ 28
2.6 Synthesis of $[BrSiMe_2OSiMe_2Br]$ 29
2.7 Synthesis of $O[Me_2Si(Fe(CO)_2Cp)]_2$ 29
2.8 Synthesis of $p\text{-}1,4\text{-}[BrSiMe_2(C_6H_4)SiMe_2Br]$ 30
2.9 Synthesis of $1,4\text{-}[Cp(CO)_2FeSiMe_2(C_6H_4)SiMe_2Fe(CO)_2Cp]$ 30
2.10 Synthesis of $[Et_3SiRu(CO)_4]_2$ 31
2.11 Synthesis of $[(PhSiMe_2)Ru(CO)_4]_2$ 32
2.12 Synthesis of $[(BzSiMe_2)Ru(CO)_4]_2$ 33
2.13 Attempted Synthesis of $[Ru(CO)_4SiMe_2OSiMe_2Ru(CO)_4]_n$ 34
2.14 Chemical Characterisation of Repeating Si:Ru:Ru:Si Sequence 35
2.15 Attempted Synthesis of $[Ru(CO)_4SiMe_2OSiMe_2OSiMe_2Ru(CO)_4]n$ 36
2.16 Attempted Synthesis of $Et_3Si[Ru(CO)_4SiMe_2OSiMe_2Ru(CO)_4]_nSiEt_3$ 38
2.17 Attempted Synthesis of $Et_3Si[Ru(CO)_4SiMe_2OSiMe_2OSiMe_2Ru(CO)_4]_nSiEt_3$ 39
2.18 Synthesis of $p\text{-}1,4\text{-}[Ru(CO)_4SiMe_2(C_6H_4)SiMe_2Ru(CO)_4]_n$ 39
2.19 Synthesis of $[Ru(CO)_4]_n$ 40
2.20 Miscellaneous compounds 41
2.21 Synthesis of $H_4Ru_4(CO)_4$ and $H_2Ru_4(CO)_{13}$ 41

3.0 Iron Results and Discussion 43
3.1 Introduction 43
3.2 Na[Cp(CO)$_2$Fe] (X) 43
3.3 1,2 - [Cyclopentadienyl(dicarbonyl)iron] tetramethyldisilane (Xa) 44
3.4 1,2 - [Dimethyl(cyclopentadienyl(dicarbonyl)iron)silyl] ethane (Xb) 46
3.5 1,3 - Dibromotetramethyldisiloxane (Ia) 48
3.6 1,3-Bis[cyclopentadienyl(dicarbonyl)iron] tetramethyldisiloxane (Xc) ... 49
3.7 1,4 – Bis(dimethylbromosilyl) benzene (Ib) 51
3.8 1,4 - Bis[dimethyl(cyclopentadienyl(dicarbonyl)iron)silyl] benzene(Xd) 52
3.9 Summary 55

4.0 Ruthenium Results and Discussion 57
4.1 Introduction 57
4.2 Bis [triethylsilyl(tetracarbonyl)diruthenium] (Va) 58
4.3 Bis [phenyldimethylsilyl(tetracarbonyl)diruthenium] (Vb) 67
4.4 Bis [benzyldimethylsilyl(tetracarbonyl)diruthenium] (Vc) 69
4.5 Poly [1,1,3,3-tetramethyldisiloxane(octacarbonyl)diruthenium] (VIa) 73
4.6 Attempted Chemical Characterisation of [Si-Ru-Ru-Si]$_n$ Polymer (VIa). 79
4.7 Poly[1,1,3,3,5,5-hexamethyltrisiloxane(octacarbonyl)diruthenium](VIb) 82
4.8 Bis (triethylsilyl)-poly
[1,1,3,3-tetramethyldisiloxane(octacarbonyl)diruthenium] (VIIa) 91
4.9 Bis (triethylsilyl)-poly
[1,1,3,3,5,5-hexamethyltrisiloxane(octacarbonyl)diruthenium] (VIIb) 95
4.10 Poly [(tetracarbonyl)ruthenium] (VXI) 99
4.1 Summary 100

5.0 Conclusion 101

6.0 Appendix 102

List of Figures

Figure 1: Polyvinyl ferrocene 2
Figure 2: Organometallic ferrocene polymer containing silicon 3
Figure 3: Polyvinyl ferrocene incorporated into the polymer backbone 3
Figure 4: Elemental carbon bridging two irons 4
Figure 5: Schematic of "spacer" groups between metal centres in a polymer. 4
Figure 6: Unsaturated carbon chain units between rhenium metal centres. 4
Figure 7: Internal metallic bonding within an organometallic polymer (M=Mo/Fe). 5
Figure 8: Top Schematic: Metal atom chain supported by four oligo-α-pyridylamine ligands. 6
Figure 9: ORTEP view of $[Ru_2(dpa)_4Cl_2]$. 7
Figure 10: Projection of the $Os_3(CO)_{12}(SiCl_3)_2$ with clear defined staggered arrangement between Os(1+3) and Os(2). 8
Figure 11: An ORTEP drawing of the (infinite) chain of $[Ru(CO)_4]_n$. 9
Figure 12: Major and minor product formed during thermal and photochemical reactions found by Knox and Stone (I + II respectively). 15
Figure 13: ORTEP view of $[PhMe_2SiRu(CO)_4]_2$ with each Ru containing eight equal positioned CO ligands (50 % occupancy). 18
Figure 14: 1,4 polymer schematic made by Nombel et al. 19
Figure 15: From left to right, structure of $[Ru_3(CO)_{11}(\mu\text{-}H)(\eta^1\text{-}SiR(OSiMe_3)_2)]$, $[Ru_3(CO)_{10}(\mu\text{-}H)(\eta^2\text{-}SiR(OSiMe_3)_2)]$ and $[Ru_3(CO)_{10}(\mu\text{-}H)_2(\eta^1\text{-}SiR(OSiMe_3)_2)_2]$ 20
Figure 16: (a) ORTEP view of *trans*-$[(Me_3SiO)_2RSiRu(CO)_4]_2$ and (b) view down Si-Ru-Ru-Si chain. 21
Figure 17: Metallocycle compound where M = $Ru(CO)_3$ or $Fe(CO)_3$; E = $SiMe_2$ and X = O. 22
Figure 18: The structure of $O[SiPh_2(Co(CO)_4)]_2$ with siloxane bridging two $Co(CO)_4$ groups. 23
Figure 19: Dicyclopentadienyl(tetracarbonyl)diiron $(Fp)_2$ 43
Figure 20: Structure of (Xa) 44
Figure 21: Structure of (Xb) 46
Figure 22: Bromonated siloxane derivative 48
Figure 23: Proposed structure of (Xc) 49
Figure 24: Transmittance solution cell IR spectrum of υCO region in (Xc) 50
Figure 25: Structure of (Ib) 51
Figure 26: Structure of (Xd) 52
Figure 27: Transmittance solution cell IR spectrum of υCO region in (Xd) 53
Figure 28: Structure of (Va) 58
Figure 29: Transmittance solution cell IR spectrum of υCO region in (Va) 59
Figure 30: ESMS of $[M + OMe]^-$ ion 61
Figure 31: ^1H NMR spectrum of (Va) in $CDCl_3$ 62
Figure 32: ^1H NMR spectrum of starting material Et_3SiH in $CDCl_3$ 63
Figure 33: ^{13}C NMR spectrum of (Va) in $CDCl_3$ 63
Figure 34: DEPT135 NMR spectrum of (Va) in $CDCl_3$ 64
Figure 35: 2D-XHDEPT NMR spectrum of (Va) in $CDCl_3$ 65
Figure 36: ^{13}C Coupled NMR spectrum of (Va) in $CDCl_3$ 66
Figure 37: Enlargement of Figure 36 aliphatic region 66
Figure 38: Structure of (Vb) 67

Figure 39: Proposed structure of (Vc) 69
Figure 40: Transmittance solution cell IR spectrum of υCO region in (Vc) 70
Figure 41: ESMS of [M +OMe] $^{-}$ ion for (Vc) 71
Figure 42: Proposed inorganic polymeric unit of (VIa) 73
Figure 43: Transmittance solution cell IR spectrum of υCO region in (VIa) 74
Figure 44: Full transmittance IR spectrum acquired in KBr of (VIa) 75
Figure 45: LDI-TOF mass spectrum of (VIa) on a polished steel plate 76
Figure 46: ^{13}C NMR of (VIa) in $CDCl_3$ 77
Figure 47: Coupled carbon NMR spectrum of (VIa) in $CDCl_3$ 78
Figure 48: Proposed structural arrangement of (XVIa) 79
Figure 49: Transmittance solution cell IR spectrum of υCO region in (XVIa) 80
Figure 50: Proposed inorganic polymeric unit (VIb) 82
Figure 51: Transmittance solution cell IR spectrum of υCO region in (VIb) 83
Figure 52: Major peaks in ESMS spectrum of (VIb) 84
Figure 53: Minor peaks in ESMS spectrum of (VIb) 85
Figure 54: Proposed structure of (VIb) 87
Figure 55: Proposed structure of $[HRu_4(CO)_{12}(Si_3(CH_3)_6O_2)]^-$ 88
Figure 56: ^{13}C NMR spectrum of (VIb) in $CDCl_3$ 89
Figure 57: Proposed end capped siloxane polymer structure of (VIIa) 91
Figure 58: LDI-TOF mass spectrum of (VIIa) on a polished steel plate 93
Figure 59: Proposed end capped siloxane polymer structure of (VIIb) 95
Figure 60: Structure of a singular polymeric unit for (VX) 97

List of Tables

Table 1: Organotin(carbonyl)ruthenium complexes made by Knox et al. 11
Table 2: Dimeric organosilyl(octacarbonyl)diruthenium complexes made by Knox and Stone 13
Table 3: Monomeric organosilyl(tetracarbonyl)ruthenium complexes made by Knox and Stone 14
Table 4: Organogermanium(carbonyl)ruthenium and osmium complexes made by Knox and Stone 17
Table 5: Bis (silyl) benzene complexes made by Nombel et al. 19
Table 6: List of synthesised iron compounds 42
Table 7: List of synthesised ruthenium compounds 56
Table 8: Comparative IR υCO bands for silyl and stannyl compounds found by Knox and Stone' 60
Table 9: ESMS peaks from (XVIa) spectrum 81
Table 10: Solved peaks of ESMS spectrum for (VIb) 86

Abbreviations

Fc = Ferrocene

$(Fp)_2$ = Dicyclopentadienyl(tetracarbonyl)diiron

Fp = Cyclopentadienyl(dicarbonyl)iron

Cp = Cyclopendadienyl

Cp* = (Pentamethyl)cyclopentadienyl

dppe = 1,2-Bis(diphenylphosphine)ethane

KCP = Potassium cyanoplatinate

TTF = Tetrathiofulvalene

TCNQ = Tetracyano-*p*-quinodimethane

dpa = Bis(2-pyridyl)amido

TMS = Tetramethylsilane

ORTEP = Oak Ridge Thermal Ellipsoid Plot

XRPD = X-ray Powder Diffraction

XRD = X-ray Diffraction

IR = Infrared

FT – IR = Fourier Transform Infrared

ESMS = Electrospray Mass Spectrometry

ESI = Electrospray Ionisation

LDI = Laser Desorption Ionisation

MALDI = Matrix Assisted Laser Desorption Ionisation

TOF = Time of Flight

NMR = Nuclear Magnetic Resonance

With regards to compounds mentioned by their allocated Roman numeral, structural diagrams can be found on the foldout section at the back of this thesis.

1.0 Background

1.1 Conventional organic polymers

The majority of polymers that exist today are organic such as polyethylene and polypropylene. These all contain a fundamental singular repetitive unit of organic content. These polymers have physical properties that are both benefits and flaws to their design such as being good insulators, conductors of heat and cheap to make. However, these are also their flaws for modern technology development, especially in environments that require a catalyst. As science is advancing it is effectively getting smaller and requiring the minimal use of external potential energy such as heat and electricity. Therefore, current organic polymers do not conduct electricity but are great conductors of heat however, they lose their structure and eventually oxidise. Thus the use of these polymers for modern use as cheap materials for scientific applications such as wires and catalysis are ineffective.

1.2 "Decorated" one – dimensional inorganic polymers

Inorganic polymers have been an advancing field of chemical engineering for various properties such as conductive, optical, thermal and catalytic. One – Dimensional inorganic polymers, such as potassium cyanoplatinate (KCP), have been known for many years[1, 2]. Other developments have been achieved in this field involving other KCP derivatives[3] and other metal systems similar to KCP[4]. KCP is a conductive inorganic compound; however it is not a polymer as such. Rather it is a stacked system of charged Pt monomers which gives the appearance of a polymer but no physical Pt-Pt metallic bonding exists.

[1] Miller, J. S.; Epistein, A. J., Prog. Inorg. Chem, 20 (1976) 1.
[2] Underhill, A. E; Watkins, D.M., Chem. Soc. Rev. 9 (1980) 429.
[3] Keller, B. J.; Hurst, S. K.; Dunham, S. O.; Spangler, L.; Abbott, E.H.; Peterson, E.S., Inorg. Chim. Acta, 357 (2004) 853.
[4] Mitsumi, M.; Goto, H.; Umebayashi, S.; Ozawa, Y.; Kobayashi, M.; Yokoyama, T.; Tanaka, H.; Kuroda, S.; Toriumi, K., Angew. Chim. Int. Ed. 44 (2005) 4164.

Therefore, it is better labelled as an array of ionic compounds with an electrostatic attraction for each other.

1.3 Organometallic polymers

1.3.1 Metal attachment to an organic polymer backbone

Other attempts to implement metallic properties into a polymer start with a pre-existing organic polymer and position a metal centre onto it. This is not entirely an inorganic polymer but does change polymer chemistry from being completely organic. A well known polymer attempt, involving ferrocene (Fc), resulted in having the metal sandwich "dangling" off the side of the main organic polymeric chain (refer to Figure 1)[5].

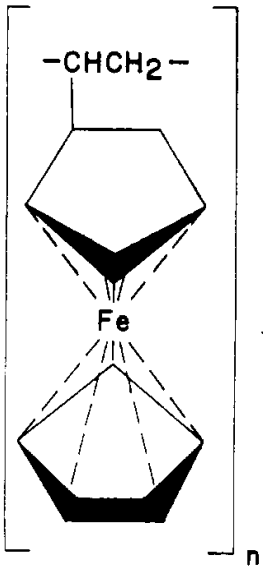

Figure 1: Polyvinyl ferrocene

[5] Arimato, F. S.; Haven, A. C. J., Am. Chem. Soc. 77 (1955) 6295.

1.3.2 Metal insertion into an organic polymer backbone

Further attempts where Fe has been replaced by another transition metal[6, 7] have been researched as well as making Fc di-substituted. Hence, the Fc "sandwich" can now be incorporated in the organic polymer backbone[8]. Further extensions to the latter involving silicon have also been achieved, increasing the overall inorganic content present in the polymer (refer to Figure 2)[9].

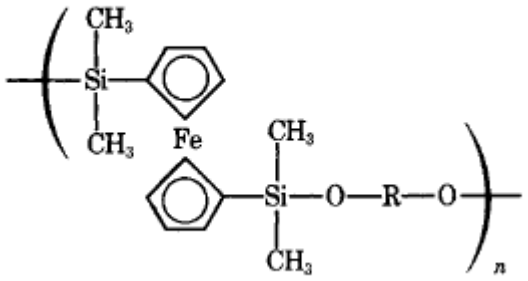

Figure 2: Organometallic ferrocene polymer containing silicon

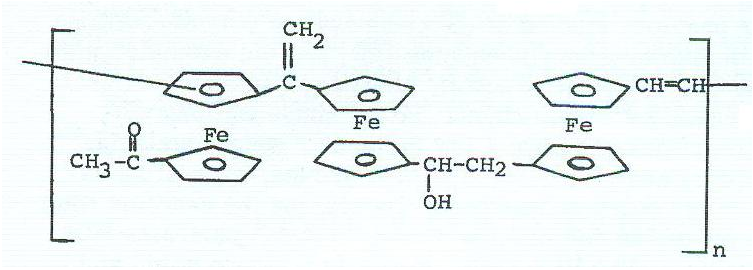

Figure 3: Polyvinyl ferrocene incorporated into the polymer backbone

[6] Rulkens, R.; Lough, A. J.; Manners, I., J. Am. Chem. Soc. 116 (1994) 797.
[7] MacLachlan, M.; Lough, A. J.; Manners, I., Macromolecules 29 (1996) 8562.
[8] Grube, P. L.; Pittman, Jr, C. U.; Sasaki, Y., J. Macromol Sci. A8 5 (1974) 923.
[9] McManus, S. P.; Patterson, W. J.; Pittman, Jr, C. U., J. Polymer Sci. 12 (1974) 837.

1.4 Metal attachment to unsaturated organic polymers

Another attempt that is also commonly employed is the use of attaching an unsaturated organic spacer between metal centres[10, 11] (refer to Figure 5). An increased quantity of spacer groups positioned between each metal results in a similar polymeric compound like the di-substituted Fc compound (refer to Figure 3)[8]. However, if the linker groups are not continued after the metal centres, but are increased between them[10], the metals effectively become terminal groups only (Figure 4 and Figure 6) and communication between them decreases[12].

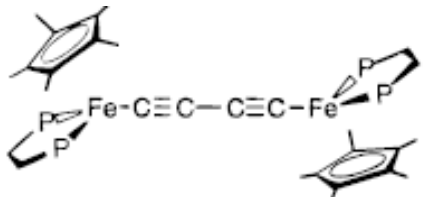

Figure 4: Elemental carbon bridging two irons

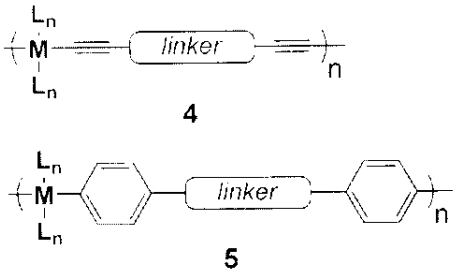

Figure 5: Schematic of "spacer" groups between metal centres in a polymer

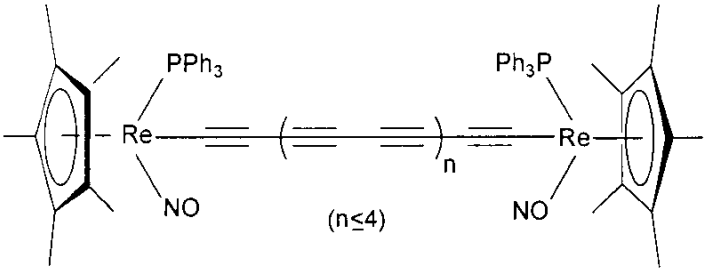

Figure 6: Unsaturated carbon chain units between rhenium metal centres

[10] Dembinski, R.; Bartik, T.; Bartik, B.; Jaeger, M.; Gladysz, J. A., J. Am. Chem. Soc. 122 (2000) 810.
[11] Bielawski, C. W.; Boydston, A. J.; Williams, K. A., Chem. Soc. Rev. 36 (2007) 729.
[12] Narvor, N. L.; Toupet, L.; Lapinte, C., J. Am. Chem. Soc. 117 (1995) 7129.

The properties of these linked organometallic compounds will effectively become dependent upon the organic spacer used between each metal centre. Aromatic and unsaturated organic compounds (refer to Figure 6)[10], or high/low electronegative containing compound arrangements (tetrathiofulvalene (TTF) and tetracyano-*p*-quinodimethane (TCNQ)) can and have been found to continue electrical conductivity[13]. However, as mentioned above, increased spacer quantity between each metal will result in independent metal centres.

1.5 Polymeric material containing metal – metal bonding

Very little has been done in the area of metal – metal bonding within a polymer, and as mentioned, these mostly consists of organic spacers joining metals together. Of a review regarding the advances in metallic polymers, only a small section was dedicated to this area involving metal – metal bonding within the polymer backbone (refer to Figure 7)[14].

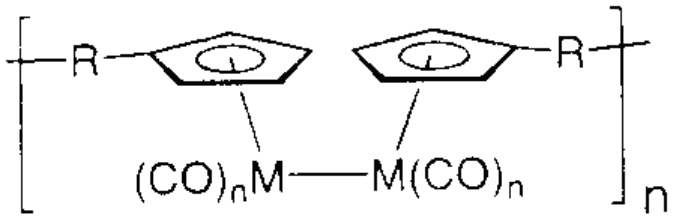

Figure 7: Internal metallic bonding within an organometallic polymer (M=Mo/Fe)

[13] Gillson, J. L.; Wheland, R. C., J. Am. Chem. Soc. (1976) 3916.
[14] Gomez-Elipe, P.; Manners, I.; Nguyen, P., Chem. Rev. 99 (1999) 1515.

1.5.1 Extended polymeric materials containing metal – metal bonds and bulky stabilising groups

Attempts that have been documented involving Cr, Ni and Co[15] which contain multiple metal – metal bonds, (refer to Figure 8) employs the use of large stabilising ligands to maintain these bonds. The formation of these compounds followed the same techniques used by another documented paper, generating a three unit long metal – metal compound involving Ru (refer to Figure 9)[16].

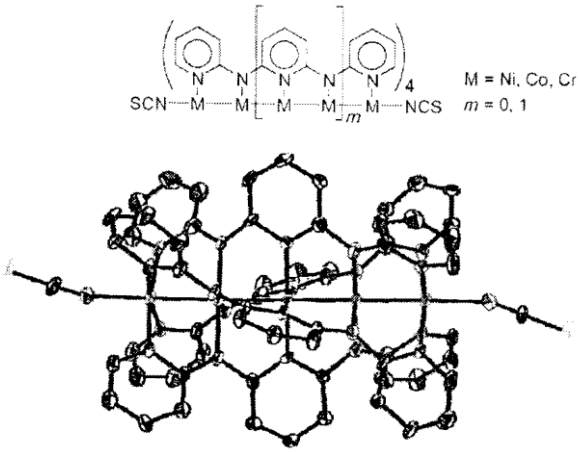

Figure 8: Top Schematic: Metal atom chain supported by four oligo-α-pyridylamine ligands. Bottom: ORTEP view of pentacobalt complex

[15] Chen, I. P.; Fu, M. D.; Tseng, W. H.; Yu, J. Y.; Wu, S. H.; Ku, C. J.; Chen, C.; Peng, S. M., Angew. Chem. Int. Ed. 45 (2006) 5814.
[16] Sheu, J. T.; Lin, C. C.; Chao, I.; Wang, C. C.; Peng, S. M., Chem. Commun. 3 (1996) 315.

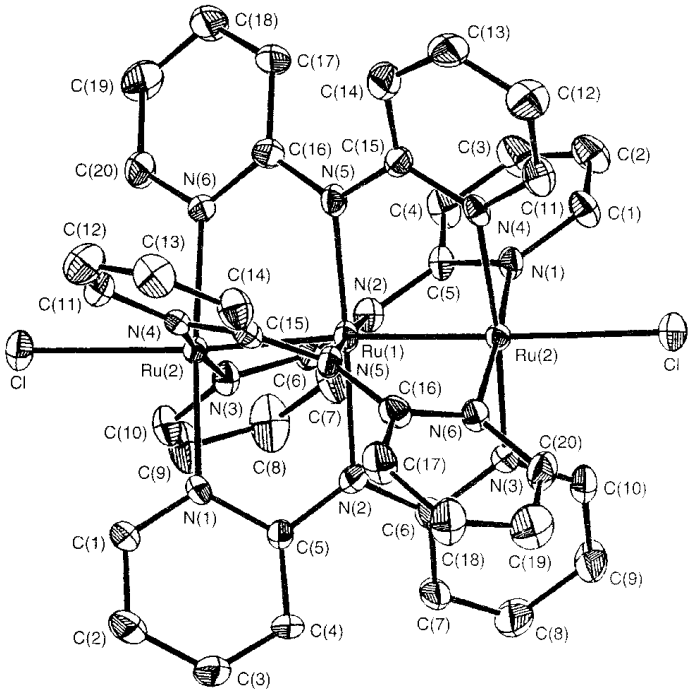

Figure 9: ORTEP view of $[Ru_2(dpa)_4Cl_2]$

These two references have succeeded in creating extended internal metal – metal bonded units through the addition of high stabilising 2,5-diamino-pyridine ligands. If it was not for these large ligands the compound would not maintain these metal – metals bonds. Therefore this area, although tending towards polymeric materials, it is not directly relevant to the present study as the chemistry does not involve the formation of stable metal – metal compounds without the help of other groups. The use of transition metal carbonyls containing metal – metal bonds would be more relevant as the carbonyl group would only become bridging under specific conditions. Otherwise the carbonyls would generally be in terminal positions only.

1.5.2 Extended polymeric materials with metal – metal bonds without bulky stabilising groups

A documented paper within the literature has used metal carbonyls, without any additional bridging carbonyls, to generate a stable compound that maintains metal – metal bonding. This paper contains the most relevant chemistry that is desired with the formation of a multi-metal linkage of osmium carbonyls and silicon groups (refer to Figure 10) [17].

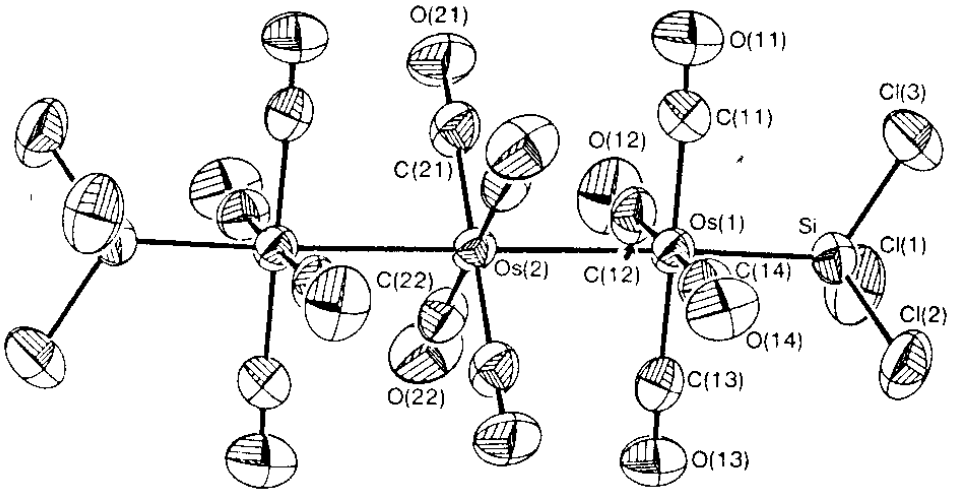

Figure 10: Projection of the $Os_3(CO)_{12}(SiCl_3)_2$ with clear defined staggered arrangement between Os(1+3) and Os(2)

This area is where this thesis intends to develop and create a new series of compounds which contain multi-metal – metal linkages whilst maintaining metal carbonyl chemistry. The chemistry discovered[17] is unique to osmium carbonyl only, as this paper attempted the same reaction with other transition metal carbonyls from the iron triad group ($Fe_3(CO)_{12}$ and $Ru_3(CO)_{12}$).

[17] Willis, A. C.; Van Buuren, G. N.; Pomeroy, R. K.; Einstein, F. W. B., Inorg. Chem. 22 (1983) 1162.

1.6 Metallic ruthenium polymers

One particular paper, involving photochemical reactions with ruthenium[18] discovered that under a carbon monoxide atmosphere $Ru_3(CO)_{12}$, in a suitable solvent, a polymeric $[Ru(CO)_4]_n$ compound was formed (Figure 11)[19].

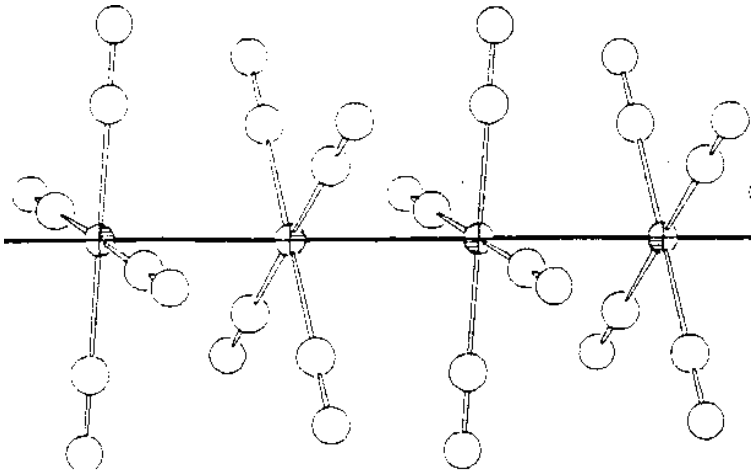

Figure 11: An ORTEP drawing of the (infinite) chain of $[Ru(CO)_4]_n$

A more recent paper achieved the same result through a modified technique to create the same metallic polymer $[Ru(CO)_4]_n$[19]. The photochemical reaction found[18] involved the use of artificial light from a UV lamp (roughly 12 hrs) absorbed by a vessel containing $Ru_3(CO)_{12}$ in THF under a carbon monoxide atmosphere. After the first 12 hrs of UV light exposure, the product formed is opaque and prevents further formation of $[Ru(CO)_4]_n$. Therefore, removal of the formed product is required and the re-establishment of carbon monoxide atmosphere is required to continue formation of more $[Ru(CO)_4]_n$. Following the same reaction conditions as conducted above, it is found that the use of natural sun light (up to 3 hrs on a sunny day however, potentially a week if cloudy)[19] is sufficient to obtain the same total yield. Hence, there is no need to stop the reaction temporarily and establish ideal conditions again.

[18] Hastings, W. R.; Baird, M. C., Inorg. Chem. 25 (1986) 2913.
[19] Masciocchi, N.; Moret, M.; Cairati, P.; Ragaini, F.; Sironi, A., J. Chem. Soc. Dalton Trans. (1993) 471.

Further investigation conducted by the latter group involving X-ray powder diffraction (XRPD) of $[Ru(CO)_4]_n$ gave structural detail on the arrangement achieved between two or more 'planar' ruthenium carbonyl units. These were found to consist of an average Ru – Ru distance of 2.860 Å, comparable to the distances in $Ru_3(CO)_{12}$ of 2.854 Å. Each planar unit is also found to have a staggered conformation (refer to Figure 11) with the Ru – Ru – CO bond angle at approximately 90^o. The polymer is completely inorganic, however some problems existed with it. These were all related to what was documented by both references and that the compound is completely insoluble in common organic solvents. This fact results in knowing that the polymer cannot be adjusted by the addition of any other groups without the destruction of it. Thus, there are no desired physical properties that exist for it currently such as conductive, catalytic, optical etc.

1.6.1 Ruthenium polymers incorporating group 14

Transition metal chemistry incorporating silicon and germanium has been an interest to The University of Waikato for many years[20, 21]. The key point of this thesis is to develop an inorganic polymeric material which contains metal – metal bonding. Incorporating silicon within this polymer will increase the overall inorganic content present within the structure.

Knox and Stone wrote a series of papers involving the reactions that occur between dodecacarbonyltriruthenium with silicon[22] and germanium[23] organohydrides, as well as dodecacarbonyltriosmium analogues[24]. Initial research conducted by Knox et al. involved the salt elimination reactions between $Ru(CO)_4^{2-}$ dianions, made using sodium dissolved in liquid ammonia, and an appropriate organotin halides (refer to Table 1)[25].

[20] Van Tiel M. L., D. Phil. Thesis, University of Waikato; (1991).
[21] McIndoe J. S., M. Sci. Thesis, University of Waikato; (1995).
[22] Knox, S. A. R.; Stone, F. G. A., J. Chem. Soc. (A) (1969) 2559.
[23] Knox, S. A. R.; Stone, F. G. A., J. Chem. Soc. (A) (1971) 2874.
[24] Knox, S. A. R.; Stone, F. G. A., J. Chem. Soc. (A) (1970) 3147.
[25] Cotton, J. D.; Knox, S. A. R.; Stone, F. G. A., J. Chem. Soc. (A) (1968) 2758.

Table 1: Organotin(carbonyl)ruthenium complexes made by Knox et al.[25]

Compound	**Colour**	**m.p/b.p (^{o}C)**	**(υCO) band frequencies (cm^{-1})**
$[Me_3Sn]_2Ru(CO)_4$	Yellow	ca. $80/10^{-2}$mm	2084s, 2024s, 2012w, 2003s
$[Et_3Sn]_2Ru(CO)_4$	Yellow	ca. $100/10^{-2}$mm	2079s, 2019s, 2009s, 1998s
$[Pr_3Sn]_2Ru(CO)_4$	Yellow	Decomp.>$150/10^{-2}$mm	2078s, 2018s, 2008s, 1997s
$[Bu_3Sn]_2Ru(CO)_4$	Yellow	Decomp.>$150/10^{-2}$mm	2077s, 2017s, 2007s, 1996s
$[Ph_3Sn]_2Ru(CO)_4$	Pale Yellow	180 – 182	2097vw, 2055vw, 2029s
$[(PhCH_2)_3Sn]_2Ru(CO)_4$	Pale Yellow	99 – 101	2089vw, 2050vw, 2021s
$Me_{10}Sn_4Ru_2(CO)_6$	Yellow	190 – 192	2036m, 2000s, 1982m
$Bu_{10}Sn_4Ru_2(CO)_6$	Yellow		2029m, 1994s, 1975m
$[Me_3Pb]_2Ru(CO)_4$	Pale Yellow		2078s, 2023w, 2018s, 2004s

It was found that organotin halides formed the monomeric ruthenium analogues $(R_3Sn)_2Ru(CO)_4$. These compounds exist, in solution, in both *cis* and *trans* forms (more the former) as shown by the υCO band frequencies observed (refer to Table 1). The peak around 2010 cm^{-1} increases in intensity as the organic group attached increases in size and is responsible for the increased formation of the *trans* isomer. Therefore, with the larger phenyl and benzyl groups attached the only isomer formed is *trans* giving rise to a the single strong stretching band.

Later research undertaken by Knox and Stone, after the above research with tin, involved investigating silane reactions with dodecacarbonyltriruthenium. It was then found that ruthenium maintained metal to metal bonding after addition of two silane units forming the linear arrangement Si-Ru-Ru-Si. The reactions investigated were conducted under thermal and photochemical conditions (refer to Table 2 and Table 3). Initial investigation involving the smaller silane unit (as opposed to the larger stannyl) was to determine the different properties of the monomeric compounds $(R_3E)_2M(CO)_4$; where R is an organic group; E is Si or Sn; and M is Ru.

Table 2: Dimeric organosilyl(octacarbonyl)diruthenium complexes made by Knox and Stone[22]

Compound	**Colour**	**m.p (^{o}C)**	**(υCO) band frequiencies (cm^{-1})**
$[Me_3SiRu(CO)_4]_2$	Bright Yellow	129 - 131	2041w, 2014s, 2005w,sh
$[Et_3SiRu(CO)_4]_2$	Bright Yellow	150 - 152	2041w, 2014s, 2005w,sh
$[Pr_3SiRu(CO)_4]_2$	Bright Yellow	79 - 81	2040w, 2014s, 2004w,sh
$[Ph_3SiRu(CO)_4]_2$			2055w, 2026s, 2016w,sh
$[(EtO)_3SiRu(CO)_4]_2$			2057w, 2028s, 2018w,sh
$[MeCl_2SiRu(CO)_4]_2$	Pale Yellow	136 - 141	2073w, 2044s, 2035w,sh
$[Cl_3SiRu(CO)_4]_2$	Pale Yellow	145 - 150	2086w, 2056s, 2050w,sh

Table 3: Monomeric organosilyl(tetracarbonyl)ruthenium complexes made by Knox and Stone[22]

Compound	**Colour**	**m.p/b.p (^{o}C)**	**(υCO) band frequiencies (cm^{-1})**
$(Me_3Si)_2Ru(CO)_4$	Yellow	50 / 10^{-2}mm	2094m, 2031s, 2015sh, 2009s
$Me_3SiRu(CO)_4GeBu_3$			2089w, 2029w, 2024w, 2013s, 2007m
$Me_3SiRu(CO)_4SnMe_3$	Yellow	50 / 10^{-2}mm	2089m, 2031s, 2026s, 2015w, 2006s
$Me_3SiRu(CO)_4SnPh_3$	Yellow	123 - 124	2024s
$Et_3SiRu(CO)_4SnMe_3$	Yellow	50 / 10^{-2}mm	2088w, 2030m, 2025m, 2014s, 2005s
$Me_3SiRu(CO)_4AuPPh_3$	Bronze	106 - 107	2059m, 1996s, 1989sh, 1970s
$Me_3SiRu(CO)_4Mn(CO)_5$	Yellow	108	2041m, 2027s, 1996w, 1977sh, 1973s
$(Me_3Si)_2Ru(CO)_2(Ph_3P)_2$	Yellow	118 - 120	2046w, 1997m, 1990sh, 1970s
$(Cl_3Si)_2Ru(CO)_2(Ph_3P)_2$			2113w, 2067m, 2060sh, 2047s
$Me_3SnRu(CO)_4SnBu_3$	Yellow	100 / 10^{-2}mm	2082m, 2022s, 2010m, 2002s
$[Me_2SnRu(CO)_4]_2$	Yellow - Orange	130	2067s, 2016s, 2010s

All reactions between $Ru_3(CO)_{12}$ and an organosilane were found to form compound (I) (refer to Figure 12)[22], in relative high yields (99% thermal and 90% photochemical). The monomeric compounds (II) were formed in relatively low yields and were found to decompose to the dimer (I).

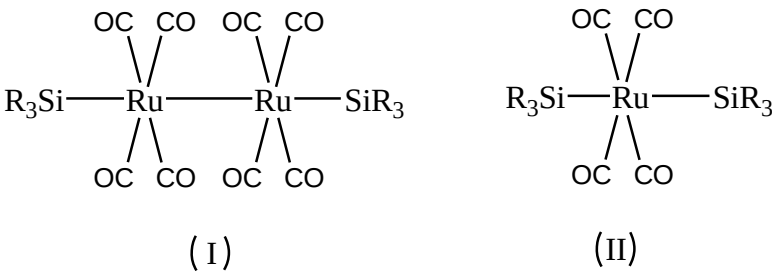

Figure 12: Major and minor product formed during thermal and photochemical reactions found by Knox and Stone (I + II respectively)

The proposed structure (refer to Figure 12) with high symmetry is assumed as a result of the "characteristic" IR fingerprint for the υCO bands containing one strong and two weak bands[22]. Further information gathered on (I), details that the two $Ru(CO)_4$ units facing each other are in a staggered arrangement. This was found by comparing the spectra obtained to a known manganese compounds, that contains a staggered arrangement, with spectroscopic data that has been interpreted ($R_3PMn(CO)_4Mn(CO)_4PR_3$)[26, 27]. The arrangement of the $Ru(CO)_4$-$Ru(CO)_4$ staggered carbonyls has also be noted[19] to be observed within the XRPD technique involving the polymeric $[Ru(CO)_4]_n$ compound.

Another important physical property that was discovered using mass spectrometry was that the cation fragment $[R_3SiRu(CO)_4]^+$ is readily observed. This led to the knowledge that the Ru – Ru bond is able to be chemically attacked. Therefore, $[R_3SiRu(CO)_4]$ fragments can be made and reacted with to generate a variety of new compounds. Using a reducing agent on these types of bis-silyl diruthenium compounds, further compounds can be made using a salt elimination reaction. Many organosilicon halide compounds are known[22], [28] and therefore, the potential

[26] Osborne, A. G.; Stiddard, M. H. B., J. Chem. Soc. (1964) 634.
[27] Lewis, J.; Manning, A. R.; Miller, J. R., J. Chem. Soc. (A) (1966) 634.
[28] Bazant, V.; Chvalovsky, V.; Rathousky, J., Organosilicon Compounds V1+V2(P1) (1965).

to form new ruthenium silyl complexes can be assumed plausible (refer to Table 3). It was known that salt elimination reactions between ruthenium anions and tin halides were readily achieved[25]. As mentioned earlier, the monomeric tin analogues readily exist in mostly *cis* conformation until the R group is too large.

The mono-ruthenium Si – Ru – Sn compounds behave in a similar manner in solution with an equal arrangement of both *cis* and *trans* forms present. However, as the attached groups increase in size the latter is more observed.

Knox and Stone continued research involving dodecacarbonyltriruthenium with group 14 compounds incorporating germanium analogues[23]. It was found that with this work both the monomer and dimer compounds could be formed; as well as some new hexa-cyclic and multi-bridging compounds (refer to Table 4). This finally led to a series of conclusions, involving four research papers from Knox and Stone, regarding the iron triad group and group 14 hydrides.

I : Increased thermal stability of metal carbonyls in the order (Fe < Ru < Os)[25].

II : Formation of dimer preferred to monomer in order of stability (Si > Ge > Sn)[23].

Of the dimer analogues, Si, Ge and Sn have been synthesised with ruthenium carbonyl. The Sn dimer analogue is the only one where the linear *trans* arrangement has eclipsed carbonyls. This compound was only formed in minute quantities. However, it has been completely characterised by Howard et al. using X-ray diffraction (XRD)[29].

[29] Howard, J. A. K.; Kellett, S.C.; Woodward, P., J. Chem. Soc. Dalton Trans. (1975) 2332.

Table 4: Organogermanium(carbonyl)ruthenium and osmium complexes made by Knox and Stone[23]

Compound	Colour	m.p/b.p (^oC)	(υCO) bands frequencies (cm^{-1})
$(Me_3Ge)_2Ru(CO)_4$	Yellow	(75 / 10^{-2} mm)	2093w,2035m, 2029s, 2014s
$[Me_3GeRu(CO)_4]_2$	Yellow	126 - 127	2046w, 2017s, 2008w
$[Me_2GeRu(CO)_3]_3$	Orange	140 – 150 dec.	2046s, 2038w, 2017s, 2011w, 1986m
$(Me_2Ge)_3[Ru(CO)_3]_2$	Lemon	150 – 160 dec.	2029s, 1991s,br
$[Me_3GeRu(CO)_3GeMe_3]_2$	Yellow	180 – 190 dec.	2046w, 2008s, 1994m
$(Me_3Ge)_2Ru(CO)_2(Ph_3P)_2$	White	112 – 114	2047w, 1998m, 1990m,sh, 1976s
$(Cl_3Ge)_2Ru(CO)_4$	White	90 – 100 dec.	2162w, 2117m, 2104s
$(Me_3Ge)_2OsCO)_4$	Pale Yellow	(ca. 60 / 10^{-2} mm)	2096w, 2031m, 2017sh, 2012
$Me_3GeOs(CO)_4H$	Colourless	(ca. 20 / 10^{-2} mm)	2118w, 2052m, 2036sh, 2032s, 1950w
$[Me_2GeOs(CO)_3]_3$	Lemon	220 – 240 dec.	2052s, 2043w, 2014s, 2008w, 1984s
$(Me_2Ge)_3[Os(CO)_3]_2$	Yellow		2021s, 1990s,br
$[Me_3GeOs(CO)_3GeMe_3]_2$	Pale Yellow	150 – 160 dec.	2048w, 2002s, 1988m
$(Me_3Ge)_2Os(CO)_2(Ph_3P)_2$	White	112 – 117	2049w, 1989m, 1981sh, 1971s
$Me_3GeRu(CO)_4SnMe_3$	Yellow	(ca. 70 / 10^{-2} mm)	2089m, 2028s, 2017w, 2010s
$Me_3GeRu(CO)_4AuPPh_3$	Cream	95 – 105 dec.	2060m, 1996s, 1991sh, 1975s
$Me_3GeRu(CO)_4Re(CO)_5$	Lemon	107 – 109	2119vw, 2053m, 2015s, 1995w, 1981m, 1974m
$Hg[Ru(CO)_4GeMe_3]_2$	Rose Pink	71	2090w, 2068s, 2063sh, 2024sh, 2019sh, 2016s, 2006s, 2002sh

1.6.2 Extended polymeric ruthenium compounds involving bis (silyl) benzenes

More current research involving dodecacarbonyltriruthenium and silanes is in an article from Japan[30]. This research document investigated polymeric materials which contained the liner *trans* Si-Ru-Ru-Si backbone structure that was found by Knox and Stone[22]. The differences between these two research documents are strongly dependent on the type of silane used to complete the backbone. Nombel et al. altered the chemistry that was developed by Knox and Stone, by implementing the use of bi-functional silane compounds. This would result in polymeric materials which contained more than one group of four linear Si-Ru-Ru-Si inorganic backbone units.

The bi-functional silane reactants were 1,3 or 1,4 – bis (silyl) benzenes, resulting in forming three new *trans* silyl ruthenium compounds (refer to Table 5 and Figure 14). A model compound was made (refer to Figure 13) which was used to determine the possible layout and structural arrangement that the bi-substituted silanes may take[30].

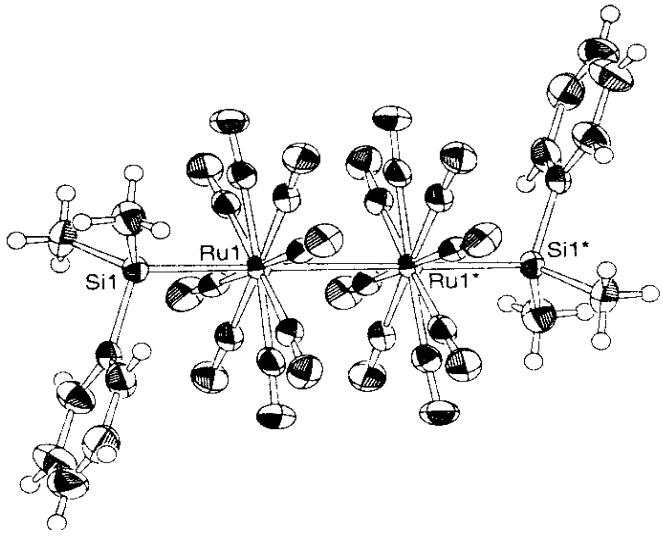

Figure 13: ORTEP view of $[PhMe_2SiRu(CO)_4]_2$ with each Ru containing eight equal positioned CO ligands (50 % occupancy).

[30] Nombel, P.; Hatanaka, Y.; Shimada, S.; Tanaka, M., Chem. Letters (1999) 159.

The reaction for the model compound was thermally conducted, as done for Knox's silicon compounds, and the same conditions were followed for all other di-silanes. The reactions generated three different compounds with different properties which unequivocally contained the same linear arrangement as that of the model compound (refer to Figure 14, note 1,3 isomer also known)[30]. The conditions for this assumption is based on the characterisation data collected and compared to the IR from [Ph $Me_2SiRu(CO)_4]_2$ in Table 5. Further data collected involving ^{1}H, ^{13}C and ^{29}Si NMR, X-ray diffraction and extended KBr IR data for the model and bis-benzene polymers[30].

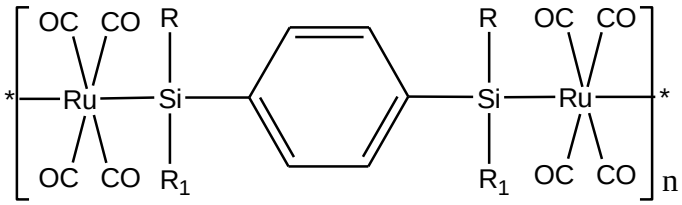

Figure 14: 1,4 polymer schematic made by Nombel et al.

Table 5: Bis (silyl) benzene complexes made by Nombel et al.[30]

Benzene	R	R'	State	Mr	Solubility	(υCO) bands cm^{-1}
1,3 – C_6H_4	Me	Me	Yellow solid	15000	THF and CH_2Cl_2	2004
1,4 – C_6H_4	Me	Ph	Yellow solid	11000	THF and Hexane	2005
1,4 – C_6H_4	Me	Me	Yellow solid		Insoluble	
[Ph $Me_2SiRu(CO)_4]_2$			Yellow solid	696	Hexane	2000

The model compound contains a high disorder of the carbonyls between the two facing $Ru(CO)_4$ units. This has also been found involving other ruthenium compounds that containing two facing Ru-Ru carbonyl groups[31].

Nombel's research involving bi-functional silanes has resulted in the apparent possibility for the creation of organometallic polymers that incorporate ruthenium and silicon. However, the chemistry still requires the use of the substituted benzene rings between each inorganic Si-Ru-Ru-Si linear arrangement. Therefore, the chemistry is similar to when an unsaturated hydrocarbon spacer

[31] Braunstein, P.; Glasworthy, J. R.; Massa, W., J. Chem. Soc. Dalton Trans. (1997) 4677.

group is inserted into the backbone[10, 11]. The polymers are therefore not completely desired or wanted to be gained from this thesis, as the organic aromatics involved are considered to be too much organic material.

1.6.3 Extended ruthenium polymers and catalysis compounds

The optimum result would be to have one single carbon linking group or none, where the carbon is replaced by another element (preferentially a metal). The use of siloxanes can potentially result in this conclusion. Braunstein et al. has documented ruthenium carbonyl compounds containing bulky siloxanes and further detailing the high disorder of the Ru – Ru carbonyls[31].

The reactions involving these bulky siloxanes ($HSiR(OSiMe_3)_2$ R=Me or $OSiMe_3$) with dodecacarbonyltriruthenium resulted in several products to be formed (refer to Figure 15 and Figure 16)[31].

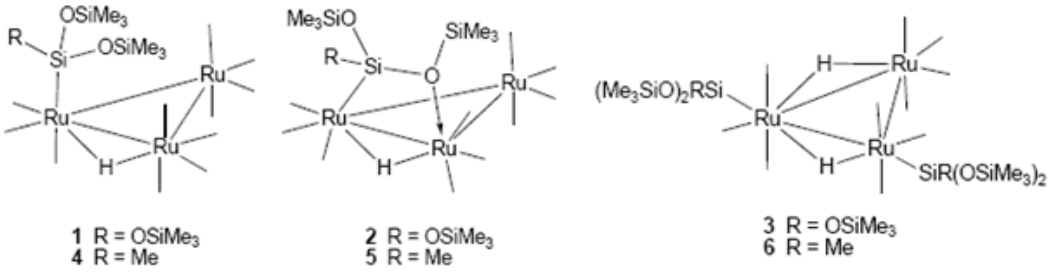

1 R = $OSiMe_3$
4 R = Me

2 R = $OSiMe_3$
5 R = Me

3 R = $OSiMe_3$
6 R = Me

Figure 15: From left to right, structure of $[Ru_3(CO)_{11}(\mu\text{-}H)(\eta^1\text{-}SiR(OSiMe_3)_2)]$, $[Ru_3(CO)_{10}(\mu\text{-}H)(\eta^2\text{-}SiR(OSiMe_3)_2)]$ and $[Ru_3(CO)_{10}(\mu\text{-}H)_2(\eta^1\text{-}SiR(OSiMe_3)_2)_2]$

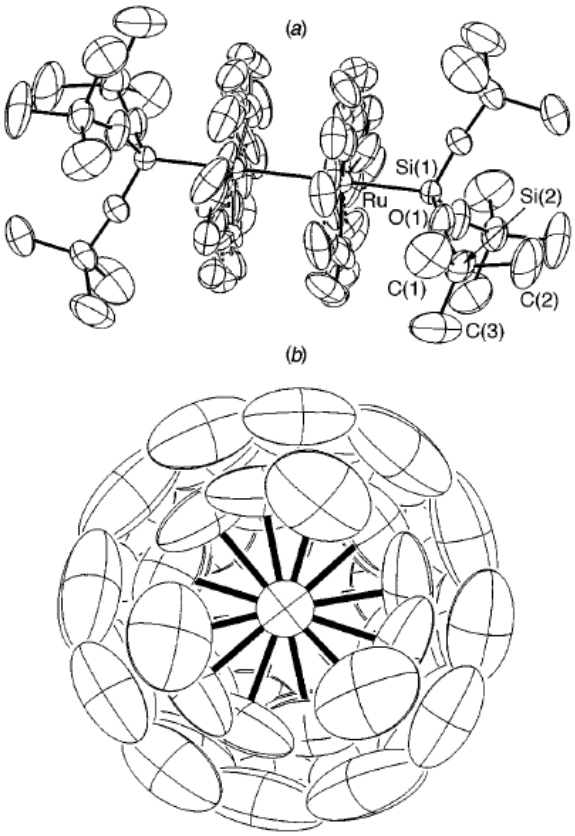

Figure 16: (a) ORTEP view of *trans*-$[(Me_3SiO)_2RSiRu(CO)_4]_2$ and (b) view down Si-Ru-Ru-Si chain.

These trinuclear species are formed for short periods only as additional decomposition pathways over time, or as a result of contact with acid or silica, lead to the dinuclear siloxy products (refer to Figure 16)[31]. Data for these compounds proposed configurations were found using IR, mass spectrometry and ^1H NMR spectroscopic methods[31]. The data regarding configuration of the carbonyls is highly disordered for all dinuclear ruthenium species[30].

A known bi-product observed within all of these reactions is the formation of $H_4Ru_4(CO)_{12}$[22, 30, 31]. This is formed through the reaction of ruthenium carbonyl in the presence of hydrogen gas[32].

[32] Knox, S. A. R.; Koepke, J. W.; Andrews, M. A.; Kaesz, H. D., J. Am. Chem. Soc. (1975) 3942.

1.7 Basis for present project

Since siloxane compounds are known to combine well with ruthenium carbonyls, and that the Si-Ru-Ru-Si structure from Knox and Stone is strongly adopted, the investigation into the use of di and trisiloxanes and disilanes with dodecacarbonyltriruthenium should provide positive results. Combining the research gathered from Knox, Stone[22], Nombel[30] and Braunstein[31] the synthesis of a completely inorganic polymer chain is possible. The use of di and trisiloxanes will result in a series of *trans* linear Si-Ru-Ru-Si arranged units in the backbone that are all linked together by oxygen atoms. Research conducted thus far, involving siloxane chemistry, is used to create specific types of compounds for either catalytic or polymeric use. The former consists of small siloxane transition metal complexes which are "end-capped". These compounds adopt two types of arrangements, either bridging (refer to Figure 18) or cyclic (refer to Figure 17) configuration between two separate metal centres[33, 34].

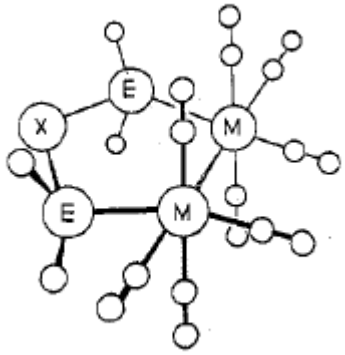

Figure 17: Metallocycle compound where M = $Ru(CO)_3$ or $Fe(CO)_3$; E = $SiMe_2$ and X = O.

[33] Greene, J.; Curtis, M. D., J. Am. Chem. Soc. 17 (1978) 2324.
[34] McIndoe, J. S.; Nicholson, B. K., J. Organomet. Chem. 648 (2002) 237.

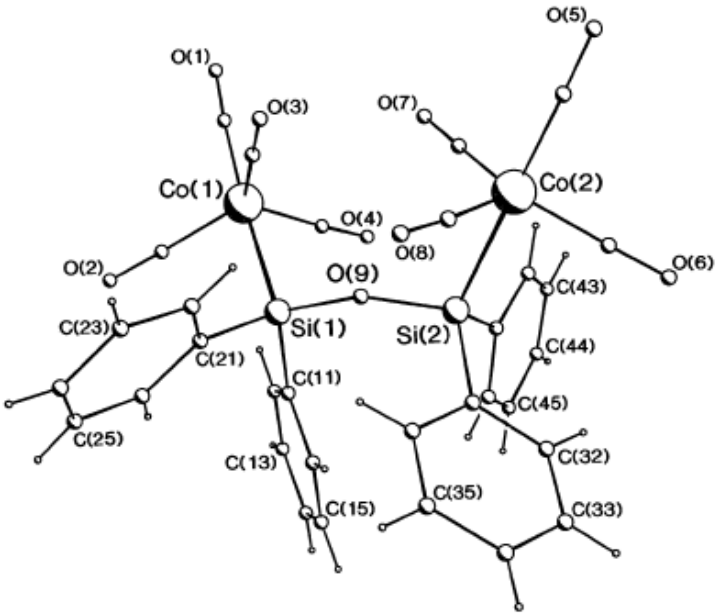

Figure 18: The structure of $O[SiPh_2(Co(CO)_4)]_2$ with siloxane bridging two $Co(CO)_4$ groups.

General silicon chemistry has found that siloxanes have an angle between the three atoms (Si-O-Si) of roughly 106.5°[35]. However; this angle is dependent on the size of the R groups attached to the silicon atoms[36]. It has been found that the angle stays relatively bent if R = Me however, larger groups result in the angle tending towards 180° (R = Ph)[36]. Therefore, observing Figure 17 and Figure 18 it is clear to see the possible catalytic use of these compounds with highly strained and potentially pseudo-stable bonds.

Therefore, it is believed that by using ruthenium and siloxanes or disilanes, a new type of polymeric material can be achieved. Obtaining repeating four member units linked by oxygen can give polymers based on the chemistry from Knox, Stone, Nombel, Braunstein and Suwinska. These papers give the idea whereby the linear Si-Ru-Ru-Si units are present, but also the Si-O-Si bond angle would become linear too with the attachment of a large ruthenium metal. Note however, the latter bond angle of 180° is not rigid and can be subjected to some degree of movement or flexibility. Therefore, with the level of linearity occurring within this compound it is hard to ignore the potential polymer possibilities.

[35] Zolota, A. A.; Frolow, F.; Milstein, D., J. Chem. Soc., Chem. Commun. (1989) 1826.
[36] Suwinska, K.; Palenik, G. J.; Gerdil, R., Acta. Crystollogr., 42C (1986) 615.

There is one minor detail however, that exists with the use of silicon, this being the tendency to form tetrahedral arrangements. Thus, although the compound contains the potential for a lot of linear arrangement it can potentially "coil back" on itself to form large cyclic compounds.

1.8 Aim of this thesis

The chemistry of ruthenium is what this study will be discussing, through the use of thermal reactions between dodecacarbonyltriruthenium and mono or disubstituted silane or siloxane compounds. The techniques that will be used to acquire these compounds will consist of those originally developed by Knox and Stone[22]. Therefore, through thermal and salt elimination reactions more products containing the *trans*-linear sequence that maintains metal – metal bonding will be attempted. Other papers concerning potential polymer chain formation will also be consulted and work conducted under the same conditions stated.

The main priority of this thesis is to develop a continuing polymeric chain consisting of as little organic material in the main backbone whilst maintaining metal – metal bonding. The potential for this does exist in theory, with the use of disilanes and siloxanes when reacted thermally. Before starting directly with ruthenium polymeric materials, the simpler dimer compounds will first need to be understood. Furthermore, before generating the polymeric type materials, end-capped models will need to be investigated first. This will be conducted using salt elimination reactions between $Na[Cp(CO)_2Fe]$ and an appropriate silicon halide. This will give an insight, much like the compound in Figure 13, into the arrangement, and somewhat the properties, that may occur for the ruthenium silicon compounds.

2.0 Experimental

2.1 General

All glassware used was acid and base washed, all solvents used were commercial drum grade and were not purified further.

2.2 Instrumental Techniques

2.2.1 FT – IR Spectroscopy

Samples were prepared within a solution cell using petroleum spirits, unless otherwise stated, all solid samples were prepared in KBr, which was dried overnight at 100^{o}C. All spectra were acquired using a Perkin Elmer Spectrum 100 FT – IR spectrometer, with the data processed using Perkin Elmer Spectrum software.

2.2.2 Electrospray Mass Spectrometry

All samples were run on a Bruker MicrOTOF mass spectrometer and were conducted in negative ion mode only with ESI source and TOF detector left at default settings. The mass spectrometer was calibrated, prior to use, using a sodium formate solution.

2.2.3 LDI-TOF Mass Spectrometry

Samples were dissolved in THF, unless stated otherwise, and were laid directly on a polished steel target (Bruker Daltonics) and allowed to air dry.

The samples were analysed on a Bruker AutoFlex II mass spectrometer using the linear detector and pulsed ion extraction between 100 and 300 ns. Positive ions were accelerated at 20 kV. A total of between 300 and 500 shots were collected from various locations on the sample spot. Protein calibration standard II (Bruker Daltonics) was utilised in order to ensure accurate mass calibration of the instrument.

Spectra were annotated in FlexAnalysis (Bruker Daltonics).

2.2.4 NMR Spectroscopy

^{1}H and $^{13}C\{^{1}H\}$ NMR spectra were acquired using a 300 or 400 MHz Bruker Avance series machine. All spectra were acquired at ambient temperatures (303 K), in 5mm tubes and using $CDCl_3$ as the lock solvent. ^{1}H NMR spectra were calibrated to the lock solvent peak occurring at 7.26 ppm, with ^{13}C NMR spectra calibrated to the lock solvent peak appearing at 77.16 ppm.

Spectra were resolved using Bruker Avance software with linear prediction also being used for two dimensional spectra.

2.2.5 Isotope Pattern Calculator

All calculated mass spectrometry peaks were acquired and compared to the isotope pattern generated using Bruker Daltonics MicrOTOF IsotopePattern V.1.2 (Build 192).

2.3 Synthesis of $Na[Cp(CO)_2Fe]$

A Schlenk flask containing a sodium amalgam (0.1 g Na; 5 mL Hg) had added to it a 60 mL THF solution containing $(Fp)_2$ (0.2 g; 0.57 mmoles). This was stirred under a di-nitrogen atmosphere for 3 hrs to give the sodium cyclopentadienyl(dicarbonyl)iron(-I), $Na[Cp(CO)_2Fe]$, which was used without further characterisation[37].

2.4 Synthesis of $[(Cp(CO)_2Fe)SiMe_2]_2$

A Schlenk flask containing 10 mL THF and $[ClSiMe_2]_2$ (0.1 g; 0.53 mmoles) had a 60 mL THF solution containing $Na[Cp(CO)_2Fe]$ (0.23 g; 1.3 mmoles) added. The solution was left to stir overnight (8 – 10 hrs) before having the solvent removed under vacuum. The remaining solid was re-dissolved in petroleum spirits and filtered before this solvent was also removed under vacuum, giving a crude yield of 30 %. The remaining solid was chromatographed using silica, eluting with a 3:1 petroleum spirits:CH_2Cl_2 mixture. Three bands were observed; the fastest, a pale yellow band near the solvent front, is a trace quantity of ferrocene. The slowest band was a dark red band of $(Fp)_2$. The second fastest band, bright yellow, was the desired compound and was extracted using petroleum spirits.

IR Spectroscopic Data			
υCO (hexane, cm^{-1})		Literature Data υCO (hexane, cm^{-1})[38]	
1999(s)	1947(s)	1997(s)	1945(s)
υCO (KBr, cm^{-1})			
2054(w)	1991(vs)	1936(vs)	
NMR Spectroscopic Data ($CDCl_3$)		Literature Data ($CDCl_3$)[38]	
^{1}H NMR signal (ppm)		^{1}H NMR signals (ppm)	
0.35 (CH_3)		0.45 (CH_3)	
4.7 (Cp)		4.79 (Cp)	
^{13}C NMR signal (ppm)			
4.2 (CH_3)			
83.4 (Cp)			

[37] King, R. B.; Bisnette, M. B., J. Organometal. Chem. 2 (1964) 15.

2.5 Synthesis of 1,2-$C_2H_4[SiMe_2(Fe(CO)_2Cp)]_2$

A Schlenk flask containing a THF solution of 1,2-$C_2H_4[SiMe_2Cl]_2$ (0.2 g; 0.9 mmoles) had a THF solution containing $Na[Cp(CO)_2Fe]$ (0.39 g; 2.1 mmoles) added. The solution was left to stir overnight (8 – 10 hrs) before having the solvent removed under vacuum. The remaining solid was re-dissolved and filtering using petroleum spirits before having this solvent removed under vacuum, giving a crude yield of 56 %. The remaining solid was then chromatographed using silica, eluting with a 3:1 petroleum spirits:CH_2Cl_2 mixture. Three bands were observed, like that within the previous example, with the second fastest eluting yellow band extracted using petroleum spirits.

IR Spectroscopic Data	
υCO (hexane, cm^{-1})	Literature Data υCO (hexane, cm^{-1})[37]
1997(s) 1944(s)	2005(s) 1948(s)
NMR Spectroscopic Data ($CDCl_3$)	Literature Data ($CDCl_3$)[37]
^{1}H NMR signal (ppm)	^{1}H NMR signals (ppm)
0.04 (CH_3)	0.32 (CH_3)
0.43 (CH_2)	0.86 (CH_2)
4.7 (Cp)	4.5 (Cp)
^{13}C NMR signal (ppm)	
-0.3 (CH_3)	
9.9 (CH_2)	
80.2 (Cp)	

2.6 Synthesis of [$BrSiMe_2OSiMe_2Br$]

A round bottomed flask containing 60 mL CCl_4 and [$HSiMe_2OSiMe_2H$] (0.76 g; 5.66 mmoles) was refluxed under a di-nitrogen atmosphere with N-bromosuccinimide (2.41 g; 13.5 mmoles) at 60 ^oC for 3 hrs. Filtration of the crude solvent mixture was conducted through a filterstick under di-nitrogen atmosphere. The solvent was removed under vacuum, leaving the product which was reacted without further purification. An IR spectrum showed the υSiH (hexane, cm^{-1}) bond had been completely reacted, with the absence of a band at 2029 cm^{-1}.

2.7 Synthesis of $O[Me_2Si(Fe(CO)_2Cp)]_2$

A Schlenk flask containing a 10 mL THF solution with $O[SiMe_2Br]_2$ (0.76 g; 5.66 mmoles) had a THF solution containing $Na[Cp(CO)_2Fe]$ (2.4 g; 14 mmoles) added. The solution was left to stir overnight (8 – 10 hrs) before having the solvent removed under vacuum. The remaining solid was re-dissolved using petroleum spirits and filtered. The solvent was removed under vacuum, giving a crude yield of 20 %. The remaining solid was chromatographed using silica, eluting with a 1:1 petroleum spirits:CH_2Cl_2 solvent mixture. The second dark yellow band was extracted using petroleum spirits.

IR Spectroscopic Data

υCO (hexane, cm^{-1})

2050(vw) 2012(s) 1957(s)

υCO (KBr, cm^{-1})

1998(s) 1943(s)

Other significant IR bands (KBr, cm^{-1})

2962(w) 1261(vs) 1095(vs) 1020(vs) 803(vs)

NMR Spectroscopic Data ($CDCl_3$)

^1H NMR signal (ppm)	^{13}C NMR signal (ppm)
0.5 (CH_3)	1.3 (CH_3)
4.7 (Cp)	80.4 (Cp)

2.8 Synthesis of p-1,4-[$BrSiMe_2(C_6H_4)SiMe_2Br$]

A flask containing 1,4-bis(dimethylsilyl)benzene (0.874 g; 4.5 mmoles) was refluxed in CCl_4 (20 mL) under a di-nitrogen atmosphere with N-bromosuccinimide (1.92 g; 10.8 mmoles) at 60 ^oC for 6 hrs. Filtration of the crude solvent mixture was conducted through a filterstick and under a di-nitrogen atmosphere. The solvent was removed under vacuum, leaving the product which was reacted without further purification. The IR spectrum showed the υSiH (hexane, cm^{-1}) bond had been completely reacted, with the absence of a band at 2029 cm^{-1}.

2.9 Synthesis of 1,4-[$Cp(CO)_2FeSiMe_2(C_6H_4)SiMe_2Fe(CO)_2Cp$]

A Schlenk flask containing 1,4-[$BrSiMe_2(C_6H_4)SiMe_2Br$] (ca. 0.87 g; 2.6 mmoles) had a THF solution containing $Na[Cp(CO)_2Fe]$ (2.4 g; 11.32 mmoles) added. The solution was left to stir overnight (8 – 10 hrs) before having the solvent removed under vacuum. The remaining solid was re-dissolved and filtered using 1:1 petroleum spirits:CH_2Cl_2 solvent mixture. The solvent was removed under vacuum, giving a crude yield of 30 %. The remaining solid was chromatographed using silica, eluting with a 1:3 petroleum spirits:CH_2Cl_2 solvent mixture. Three bands appeared, as observed in previous examples, with the second fastest eluting yellow band being extracted using CH_2Cl_2.

IR Spectroscopic Data

υCO (hexane, cm^{-1})

1998(s) 1984(vw) 1946(s) 1915(vw)

NMR Spectroscopic Data ($CDCl_3$)

^1H NMR signal (ppm)	^{13}C NMR signal (ppm)
0.6 (CH_3)	1.0 (CH_3)
4.5 (Cp)	84 (Cp)
7.5 (Aromatic)	132 (Aromatic)
	212 (CO)

2.10 Synthesis of $[Et_3SiRu(CO)_4]_2$

$Ru_3(CO)_{12}$ (0.15 g; 0.24 mmoles) and Et_3SiH (0.21 g; 2.0 mmoles) were placed into an ampoule containing hexane (15 mL). The ampoule was sealed and heated at 85 ^oC for 48 – 96 hrs[22]. The ampoule was opened and the solvent was removed under vacuum, giving a crude yield >90 %. This was chromatographed using silica, eluting with petroleum spirits. The fastest moving yellow band was extracted using petroleum spirits.

IR Spectroscopic Data

υCO (hexane, cm^{-1})		Literature Data υCO (hexane, cm^{-1})[22]	
2042(w)	2017(vs)	2041(w)	2014(s)
		2005(w,sh)	

NMR Spectroscopic Data ($CDCl_3$)

^1H NMR signals (ppm)	^{13}C NMR signals (ppm)
1.0 (CH_2 + CH_3)	8.7 (CH_3)
	11.9 (CH_2)
	208.1 (CO)

^{13}C DEPT135 signals (ppm, J = 125 Hz)

8.6 (CH_3)

11.8 (CH_2)

^{13}C + ^1H 2D NMR signals (ppm, J = 125 Hz)

(8.7 (^{13}C) 1.0 (^1H) CH_3)

(11.8 (^{13}C) 1.0 (^1H) CH_2)

^{13}C Coupled signals (ppm)

Quartet (J = 125 Hz) of triplets (J = 5.5 Hz) (CH_3)

Triplet (J = 116 Hz) of quartets (not resolved) (CH_2)

208 (CO)

ESMS major signals (MeOH + NaOMe, *m/z*; Negative Ion Mode)

M = $[Et_3SiRu(CO)_4]_2$

$[M+OMe]^-$ Found: 688.973 Calculated: 688.976

2.11 Synthesis of $[(PhSiMe_2)Ru(CO)_4]_2$

$Ru_3(CO)_{12}$ (0.15 g; 0.24 mmoles) and $PhSiMe_2H$ (0.27 g; 2.0 mmoles) were placed into an ampoule containing hexane (15 mL). The ampoule was sealed and heated at 90 – 95 ^oC for 72 hrs. The ampoule was opened and the solvent was removed under vacuum, giving a crude yield of 67 %. This was chromatographed using silica, eluting with petroleum spirits. The second fastest moving yellow band was extracted with petroleum spirits.

IR Spectroscopic Data

υCO (hexane, cm^{-1})

2048(w) 2020(vs)

υCO (KBr, cm^{-1})		Literature Data υCO (KBr, cm^{-1})[30]	
2060(m)	2007(vs)	2000(s)	1992(vs)
1992(vs)			

NMR Spectroscopic Data ($CDCl_3$)

^1H NMR signals (ppm)	^{13}C NMR signals (ppm)
0.8 (CH_3)	6.8 (CH_3)
Multiplet 7.2	Multiplet 130
	206.5 (CO)

ESMS major signals (MeOH + NaOMe, *m/z*; Negative Ion Mode)

M = $[PhMe_2SiRu(CO)_4]_2$

$[M+OMe]^-$ Found: 728.917 Calculated: 728.913

2.12 Synthesis of $[(BzSiMe_2)Ru(CO)_4]_2$

$Ru_3(CO)_{12}$ (0.15 g; 0.24 mmoles) and $BzSiMe_2H$ (0.38 g; 2.0 mmoles) were placed into an ampoule containing hexane (15 mL). The ampoule was sealed and heated at 90 – 95 ^oC for 50 – 72 hrs. The ampoule was opened and the solvent was removed under vacuum, giving a crude yield of 90 %. This was chromatographed on silica, eluting with petroleum spirits. The fastest eluting band was $H_4Ru_4(CO)_{12}$ where the majority of the product remained at the starting position. Extraction of a pure compound by this method was difficult due to the slow mobility. Re-crystallisation techniques were implemented using warm petroleum spirits to dissolve the crude mixture, and cooling to -25 ^oC overnight. The supernatant was removed and the process repeated several times, giving bright yellow needle crystals of $[BzMe_2SiRu(CO)_4]_2$.

IR Spectroscopic Data

υCO (hexane, cm^{-1})

2046(w) 2019(vs)

NMR Spectroscopic Data ($CDCl_3$)

^1H NMR signals (ppm)	^{13}C NMR signals (ppm)
0.5 (CH_3)	5.9 (CH_3)
2.6 (CH_2)	34.3 (CH_2)
Multiplet 7.2	Multiplet 140
	206.9 (CO)

ESMS major signals (MeOH + NaOMe, *m/z*; Negative Ion Mode)

M = $[BzMe_2SiRu(CO)_4]_2$

$[M+OMe]^-$ Found: 756.924 Calculated: 756.945

Micro Analysis

Calc. for $C_{26}H_{26}O_8Ru_2Si_2$	C: 43.09 %; H: 3.62 %
Found	C: 42.42 %; H: 3.59 %

2.13 Attempted Synthesis of $[Ru(CO)_4SiMe_2OSiMe_2Ru(CO)_4]_n$

$Ru_3(CO)_{12}$ (0.15 g; 0.24 mmoles) and 1,1,3,3 tetramethyldisiloxane (0.21 g; 1.5 mmoles) were placed into an ampoule containing hexane (15 mL). The ampoule was sealed before being heated at 85 – 90 ^oC for 72 hrs. The ampoule was opened and the solvent was removed under vacuum, giving a dark yellow oil with a crude yield of 60 – 75 %. The crude mixture was unable to be chromatographed using silica or alumina, eluting with common organic solvents due to irreversible binding to the inert phase. All characterisation techniques used and data obtained are from the crude product.

IR Spectroscopic Data

υCO (hexane, cm^{-1})

2095(m) 2081(m) 2067(m) 2040(vs) 2011(vs)
1995(w,sh)

υCO (KBr, cm^{-1})

2082(m) 2041(s) 2010(s)

Other significant bands (KBr, cm^{-1})

2963(m) 1638(w) 1617(w) 1412(w)
1261(vs) 1094(vs) 1026(vs)
801(vs)

NMR Spectroscopic Data ($CDCl_3$)

^1H NMR signals (ppm)	^{13}C NMR signals (ppm)
0.0 multiple singlets (strong)	1.2 strong
0.1 strong	1.3 medium
0.57 strong	11.2 strong
0.59 weak	12.2 medium

^{13}C Coupled signals (ppm)

1.0 Quartet (J = 118 Hz) (strong)
1.1 Quartet (J = 118 Hz) (medium)
11.0 Quartet (J = 118 Hz) (strong)

LDI – TOF MS signals (*m/z*; Positive Ion Mode)

50,000(br) maxima (medium mass range 20,000 – 180,000)

2.14 Chemical Characterisation of Repeating Si:Ru:Ru:Si Sequence

A Schlenk flask containing a sodium amalgam [Na (0.05 g; 8.6 mmoles), Hg (5 mL)] had added to it a THF solution containing $[Ru(CO)_4SiMe_2OSiMe_2Ru(CO)_4]_n$ (0.1 g; 0.18 mmoles). The solution was stirred at room temperature for 15 min before being transferred under a di-nitrogen atmosphere into another Schlenk flask containing a THF solution of triphenyltin chloride (0.096 g; 0.25 mmoles). The solution was left to stir at 0 ^oC for 2 hrs before the solvent was removed under vacuum. The remaining solid was dissolved in a 1:1 petroleum spirits:CH_2Cl_2 solvent mixture and filtered. The solvent was again removed under vacuum with further characterisation being conducted without further purification.

IR Spectroscopic Data

υCO (hexane, cm^{-1})

2097(w) 2080(w) 2032(vs) 2017(vs)

υCO (KBr, cm^{-1})

2015(vs)

Other significant bands (KBr, cm^{-1})

1260(s) 1076(s) 1020(s)

Further characterisation could not be achieved.

2.15 Attempted Synthesis of $[Ru(CO)_4SiMe_2OSiMe_2OSiMe_2Ru(CO)_4]n$

$Ru_3(CO)_{12}$ (0.15 g; 0.24 mmoles) and 1,1,3,3,5,5 hexamethyltrisiloxane (0.36 g; 1.6 mmoles) were placed into an ampoule containing hexane (15 mL). The ampoule was sealed before being heated at 85 – 90 ^oC for 48 hrs. The ampoule was opened and the solvent was removed under vacuum giving a yellow oil with a crude yield of 70 %. The crude mixture was chromatographed using silica, eluting with a 1:1 petroleum spirits:CH_2Cl_2 solvent mixture. The fastest eluting yellow band was extracted using the same mixture, giving a pale yellow solid.

IR Spectroscopic Data

υCO (hexane, cm^{-1})

2095(s) 2066(w) 2032(s,br) 2011(s,br) 1990(w,sh)

υCO (KBr, cm^{-1})

2060(vs) 2017(vs) 1999(vs)

Other significant bands (KBr, cm^{-1})

2963(m) 2918(m) 2850(m) 1463(w,sh) 1416(w)

1261(vs) 1100(s) 1053(s)

892(m) 859(m) 803(vs)

NMR Spectroscopic Data ($CDCl_3$)

^1H NMR signals (ppm)

0.1 (Si^2-$(CH_3)_2$)

0.6 (Ru-$Si^{1/1'}$-$(CH_3)_2$)

^{13}C NMR signals (ppm)

1.3 (Si^2-$(CH_3)_2$)

11.2 (Ru-$Si^{1/1'}$-$(CH_3)_2$)

197.6 + 191.7 (CO)

ESMS major signals (MeOH + NaOMe, *m/z*; Negative Ion Mode)

$M^1 = Ru_3(CO)_{11}(Si_3(CH_3)_6O_2)$

$[M^1+OMe]^-$	Found: 849.751	Calculated: 849.739
$[M^1–CO+OMe]^-$	Found: 821.758	Calculated: 821.744

$M^2 = HRu_4(CO)_{14}(Si_3(CH_3)_6O_2)$

$[M^2+OMe]^-$	Found: 1035.647	Calculated: 1035.637
$[M^2–CO+OMe]^-$	Found: 1007.653	Calculated: 1007.642
$[M^2–2CO+OMe]^-$	Found: 979.668	Calculated: 979.655

$M^3 = H_4Ru_4(CO)_{14}(Si_3(CH_3)_6O_2)_2$

$[M^3+OMe]^-$	Found: 1244.712	Calculated: 1244.721

LDI – TOF MS signals (*m/z*; Positive Ion Mode)

50,000(br) maxima (medium mass range 20,000 – 180,000).

2.16 Attempted Synthesis of $Et_3Si[Ru(CO)_4SiMe_2OSiMe_2Ru(CO)_4]_nSiEt_3$

$Ru_3(CO)_{12}$ (0.1 g; 0.16 mmoles), 1,1,3,3 tetramethyldisiloxane (0.23 g; 1.7 mmoles) and Et_3SiH (0.15 g; 1.3 mmoles) were added to an ampoule containing hexane (15 mL). The ampoule was sealed before being heated at 85 ^oC for 90 hrs. The ampoule was opened and the solvent was removed under vacuum, giving a dark brown oil with a crude yield of 60 %. The crude product was unable to be chromatographed on silica or alumina and further experiments were conducted without purification. Therefore, all characterisation techniques involve the crude product.

IR Spectroscopic Data

υCO (hexane, cm^{-1})

2103(s,br) 2082(w) 2040(s) 2033(s) 2011(vs)
1999(w)

υCO (KBr, cm^{-1})

2079(m) 2015(s,sh) 2008(vs)

Other significant bands (KBr, cm^{-1})

2958(s) 2863(s) 2803(m)
1260(vs) 1095(vs) 1025(vs)
842(m) 800(vs)

NMR Spectroscopic Data ($CDCl_3$)

^1H NMR signals (ppm)

0.1 singlet (CH_3) strong
0.5 quartet (CH_2) weak
0.9 triplet (CH_3) weak

^{13}C NMR signals (ppm)

-0.3 (CH_3) weak
1.0 (CH_3) strong
6.2 (CH_2) strong
6.7 (CH_3) strong
189 (CO) weak

^{13}C Coupled signals (ppm)

1.0 Quartet (J = 118 Hz) (strong)

LDI – TOF MS signals (*m/z*; Positive Ion Mode)

200,000(br) maxima (extra large mass range 50,000 – 500,000).

2.17 Attempted Synthesis of $Et_3Si[Ru(CO)_4SiMe_2OSiMe_2OSiMe_2Ru(CO)_4]_nSiEt_3$

$Ru_3(CO)_{12}$ (0.15 g; 0.24 mmoles), 1,1,3,3,5,5 hexamethyltrisiloxane (0.34 g; 2.0 mmoles) and Et_3SiH (0.11 g; 1.0 mmoles) were added to an ampoule containing hexane (15 mL). The ampoule was sealed and heated at 85 – 95 ^oC for 72 hrs. The ampoule was opened and the solvent removed under vacuum, giving a brown oil with a crude yield of roughly 40 %. The product was chromatographed using silica, eluting with 1:1 petroleum spirits:CH_2Cl_2 solvent mixture. The fastest band was extracted using CH_2Cl_2 giving a brown/yellow solid.

Further characterisation could not be achieved, all data obtained using IR, ESMS and NMR concurred with that found for the attempted synthesis of $[Ru(CO)_4SiMe_2OSiMe_2OSiMe_2Ru(CO)_4]_n$.

2.18 Synthesis of p-1,4-$[Ru(CO)_4SiMe_2(C_6H_4)SiMe_2Ru(CO)_4]_n$

$Ru_3(CO)_{12}$ (0.13 g; 0.2 mmoles) and 1,4-bis(dimethylsilyl)benzene (0.25 g; 1.5 mmoles) were placed into an ampoule containing hexane (15 mL). The ampoule was sealed before being heated at 85 ^oC for 90 hrs. The ampoule was opened and the solvent was removed under vacuum. The solid was insoluble in common organic solvents. Washing of the solid with petroleum spirits several times resulted in removal of the by-product contaminant.

IR Spectroscopic Data

υCO, supernatant (hexane, cm^{-1})

2047(w) 2019(m)

υCO, solid (KBr, cm^{-1})	Literature Data υCO (KBr, cm^{-1})[30]
2050(m) 2005(vs) 1995(s)	2005(vs,br) 2000(vs,br)

Further characterisation could not be achieved.

2.19 Synthesis of $[Ru(CO)_4]_n$

A Schlenk flask containing $Ru_3(CO)_{12}$ (0.10 g; 0.16 mmoles) was partially dissolved in 15 mL of THF. The solution and flask were saturated with $CO_{(g)}$ and left in natural sunlight for several days. The solvent was removed under vacuum giving an orange solid of polymeric $[Ru(CO)_4]_n$.

IR Spectroscopic Data

υCO (KBr, cm^{-1})		Literature Data υCO (KBr, cm^{-1})[18]	
1995(vs)	1974(vs)	1999(vs)	1970(vs)
591(m)	507(vs)	600(m)	500(s)
400(m)			

Further characterisation could not be achieved.

2.20 Miscellaneous compounds

2.21 Synthesis of $H_4Ru_4(CO)_4$ and $H_2Ru_4(CO)_{13}$

During reactions between $Ru_3(CO)_{12}$ and the silanes or siloxanes, $H_4Ru_4(CO)_{12}$ and $H_2Ru_4(CO)_{13}$ compounds are formed as secondary products and fit the isotope pattern for a compound containing four ruthenium atoms (refer to Appendix 4). The compounds are formed when ruthenium carbonyl is heated in the presence of liberated hydrogen[32], the latter is formed in the same manner however, under more forcing conditions[41].

IR Spectroscopic Data

υCO (hexane, cm^{-1})

2095(vw) 2081(s) 2066(vs) 2032(vs) 2028(s,sh) 2011(s)

Literature Data υCO for $H_4Ru_4(CO)_{12}$ (hexane, cm^{-1})[32]

2081(s) 2067(vs) 2030(m) 2024(s) 2009(w)

ESMS major signals (MeOH + NaOMe *m/z*; Negative Ion Mode)

$[H_3Ru_4(CO)_{12}+OCH_3]^-$	Found: 775.601	Calculated: 775.625
$[H_3Ru_4(CO)_{12}]^-$	Found: 744.583	Calculated: 744.659
$[H_3Ru_4(CO)_{11}]^-$	Found: 716.588	Calculated: 716.595
$[HRu_4(CO)_{13}]^-$	Found: 770.559	Calculated: 770.569
$[HRu_4(CO)_{12}]^-$	Found: 742.574	Calculated: 742.571
$[HRu_4(CO)_{11}]^-$	Found: 714.579	Calculated: 714.581

Table 6: List of synthesised iron compounds

Key:		
Iron Compounds:	**Chemical Formula**	**Given Symbol:**
Dicyclopentadienyl(tetracarbonyl)diiron	$Cp_2Fe_2(CO)_4$	$(Fp)_2$
Sodium-Cyclopentadienyl(dicarbonyl)iron(-I)	$Na[CpFe(CO)_2]$	(X)
1,2-Bis[cyclopentadienyl(dicarbonyl)iron] tetramethyldisilane	$[CpFe(CO)_2SiMe_2]_2$	(Xa)
1,2-Bis[dimethyl(cyclopentadienyl(dicarbonyl)iron)silyl] ethane	$(C_2H_4)[SiMe_2Fe(CO)_2Cp]_2$	(Xb)
1,3-Dibromotetramethyldisiloxane	$O[SiMe_2Br]_2$	(Ia)
1,3-Bis[cyclopentadienyl(dicarbonyl)iron] tetramethyldisiloxane	$O[SiMe_2Fe(CO)_2Cp]_2$	(Xc)
1,4-Bis(dimethylbromosilyl) benzene	$(C_6H_4)[SiMe_2Br]_2$	(Ib)
1,4-Bis[dimethyl(cyclopentadienyl(dicarbonyl)iron)silyl] benzene	$(C_6H_4)[SiMe_2Fe(CO)_2Cp]_2$	(Xd)

3.0 Iron Results and Discussion

3.1 Introduction

Using iron organometallic compounds, a series of salt elimination reactions can generate new iron organometallic-silicon containing compounds. To create these, $(Fp)_2$ was used as it is capable of being characterised easily by various instrumental techniques. The purpose of these iron-silicon compounds is to obtain spectroscopic data regarding their structural arrangement and physical characteristics. In knowing these, the iron analogues can somewhat be translated into what can be expected for the polymeric ruthenium – silicon compounds.

3.2 $Na[Cp(CO)_2Fe]$ (X)

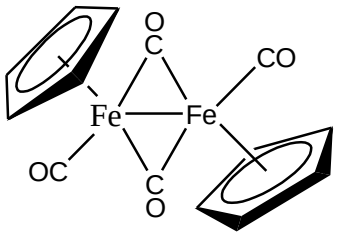

Figure 19: Dicyclopentadienyl(tetracarbonyl)diiron $(Fp)_2$

A sodium amalgam (0.2 g Na; 10 mL Hg) was prepared under a di-nitrogen atmosphere with a THF solution containing $(Fp)_2$ added to it (refer to Figure 19). The solution was stirred for 3 hrs to obtain a yellow solution of $Na[Cp(CO)_2Fe]$[37]. The anion was used without further purification or characterisation in a salt elimination reaction with a halogenated silicon compound.

3.3 1,2 - [Cyclopentadienyl(dicarbonyl)iron] tetramethyldisilane (Xa)

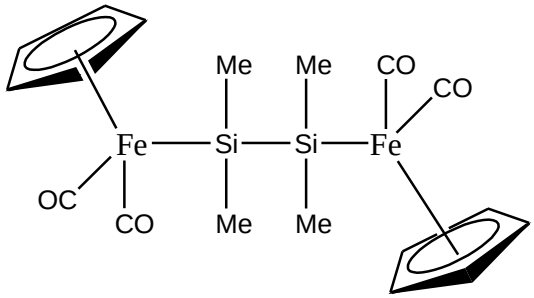

Figure 20: Structure of (Xa)

This compound was synthesised as a model for the M-Si-Si-M sequenced complexes (M = Fe) to generate a rudimentary overview for metallic end-capped silicon groups. It has been reported previously the spectroscopic data of (Xa) which involved IR, electron impact mass spectrometry and ^{1}H NMR spectroscopic data[38]. Further synthesis of other metallic end-capped silicon compounds will also be conducted to determine the spectroscopic changes that differ from the model (Xa).

A THF solution containing an excess of $(Fp)_2$ was made into its anion, $Na[Cp(CO)_2Fe]$, by stirring for 3 hrs in a Schlenk flask under a di-nitrogen atmosphere in a sodium amalgam. The anion was transferred under a di-nitrogen atmosphere into a neighbouring Schlenk flask containing a THF solution of 1,2-dichlorotetramethyldisilane. The reactants were stirred overnight, resulting in a salt elimination reaction to synthesise compound (Xa) (refer to Figure 20). The THF was removed under vacuum to give a red solid which was washed with petroleum spirits and filtered. The solvent was removed under vacuum to give a yellow – red solid with a crude yield of 30 %. The compound was chromatographed using silica, eluting with a 3:1 petroleum spirits:CH_2Cl_2 solvent mixture. The second fastest eluting yellow band was extracted using petroleum spirits, which was later removed under vacuum to give a bright yellow film of (Xa).

[38] King, R. B.; Pannell, K. H.; Bennett, C. R.; Ishaq, M., J. Organometal. Chem. 19 (1969) 327

3.3.1 IR Spectroscopy Data

An IR solution cell spectrum was obtained using petroleum spirits with the υCO region investigated. Two strong bands were observed at 1999 cm^{-1} and 1947 cm^{-1} which correlate well with the literature data (1997 cm^{-1} and 1949 cm^{-1})[38].

An ESMS experiment was attempted to find a peak correlating with a $[M+OMe]^-$ (M = (Xa)) ion which had a calculated *m/z* of 500. The spectrum acquired did not exhibit any peaks that resembled the synthesised (Xa) compound. The literature mass spectrometry data was acquired using electron impact mass spectrometry, a much higher energy spectral analysis method cf. ESMS. Therefore, ESMS does not appear to be an appropriate method for these types of metallic end capped compounds.

3.3.2 NMR Spectroscopy Data

A ^1H NMR spectrum was acquired of (Xa) in $CDCl_3$ with two peaks observed at 0.35 ppm and 4.7 ppm which are assigned to Fe-Si-CH_3 and the Fe-Cp ring respectively. This correlates well with the literature data of 0.45 ppm and 4.79 ppm for the same groups respectively found by King[38].

^{13}C NMR data was acquired, where two peaks at 4.2 ppm and 83.4 ppm were observed and assigned to Fe-Si-CH_3 and the Fe-Cp ring respectively.

3.4 1,2 - [Dimethyl(cyclopentadienyl(dicarbonyl)iron)silyl] ethane (Xb)

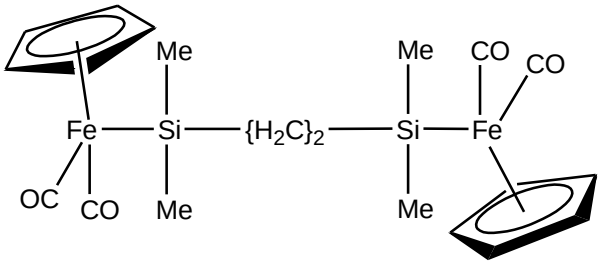

Figure 21: Structure of (Xb)

Further changes to the bridging unit between each end-capped iron – silicon compound through incorporating more organic content between the silicons, to determine the resulting change in spectra. The compound (Xb) (refer to Figure 21) was synthesised in the same manner as that achieved by King et al. and conducted for compound (Xa)[38].

An overnight salt-elimination reaction was achieved between $Na[Cp(CO)_2Fe]$ and $ClMe_2Si(CH_2)_2SiMe_2Cl$ in THF. The solvent was removed under vacuum giving a red solid which was washed with petroleum spirits and filtered. The solvent was again removed under vacuum to give a red-yellow solid with a crude yield of 56 %. The compound was further purified by chromatography using silica, eluting with a 3:1 petroleum spirits:CH_2Cl_2 solvent mixture. The second fastest eluting yellow band was extracted using petroleum spirits, with the solvent removed under vacuum giving a bright yellow solid of (Xb).

3.4.1 Spectroscopic Data

A solution cell IR spectrum was acquired in petroleum spirits and the υCO region was investigated. Two strong bands were observed at 1997 cm^{-1} and 1944 cm^{-1} which correlate well with the literature data (2005 cm^{-1} and 1948 cm^{-1}). This υCO band pattern is characteristic for these types of iron carbonyl compounds, as found by King et al. and as observed in the previous example.

NMR spectroscopy determined the positions for the three separate organic environments. A ^{1}H NMR spectrum showed three key peaks appearing at 0.04 ppm, 0.43 ppm and 4.7 ppm which are assigned to Fe-Si-CH_3, Fe-Si-CH_2 and the Fe-Cp ring respectively. These do not correlate well with the literature data found 0.32 ppm, 0.86 ppm and 4.5 ppm for the same groups respectively.

Three further NMR experiments were conducted, ^{13}C NMR, DEPT135 and HSQC to help assists with interpreting the ^{1}H NMR spectrum. Within these three spectra three peaks are observed in each. These were observed within the ^{13}C NMR spectrum at -0.3 ppm, 9.9 ppm and 80.2 ppm which were assigned to Fe-Si-CH_3, Fe-Si-CH_2 and the Fe-Cp ring respectively, with no signal observed for Fe-CO. Within the DEPT135 spectrum, the peaks at -0.3 ppm and 80 ppm remained in the positive phase with the other at 9.9 ppm becoming inverted, which effectively backs up the data observed in the ^{13}C NMR. The HSQC spectrum showed that the peaks appearing within the ^{13}C spectra correlate with those observed within the ^{1}H spectra for their respective groups.

Within the ^{1}H NMR spectra it is unclear why the data gathered does not correlate with that found within the literature but does correlate with that found within the other acquired spectra.

3.5 1,3 - Dibromotetramethyldisiloxane (Ia)

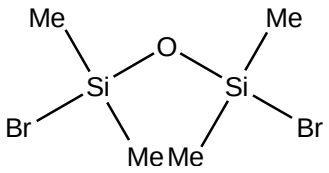

Figure 22: Bromonated siloxane derivative

To achieve further end-capped iron silicon derivatives which were not mentioned to be achieved by King et al. An attempted synthesis involving a siloxane compound was prepared following the same methods that were used to synthesis the previous literature examples[38].

The parent silicon hydride needed to be converted into its corresponding halide, achieved through the removal of the hydrogen, replacing it with a halide. 1,1,3,3-tetramethyldisiloxane and N-bromosuccinimide were refluxed under a di-nitrogen atmosphere in CCl_4 at 60 ^{o}C for 3 hrs. The solution was filtered under a di-nitrogen atmosphere followed by removal of the solvent under vacuum. A yellow-white liquid of (Ia) was obtained, which was used without further purification.

The corresponding halogenated siloxane compound (Ia) had an IR solution cell spectrum acquired in petroleum spirits, observing the full removal of the υSi-H band at 2029 cm^{-1}.

3.6 1,3-Bis[cyclopentadienyl(dicarbonyl)iron] tetramethyldisiloxane (Xc)

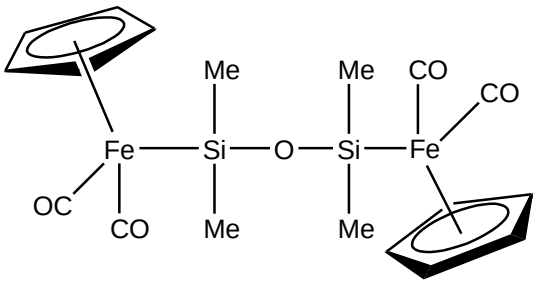

Figure 23: Proposed structure of (Xc)

The third synthesised metallic end-capped derivative using $Na[Cp(CO)_2Fe]$ was acquired to determine the spectroscopic change that would occur for these type of compounds. The addition of an electronegative atom between the iron metal centres should alter the metal carbonyl IR bands and the ^1H NMR spectra cf. previous literature examples (refer to Figure 23).

A Schlenk flask containing a THF solution of $Na[Cp(CO)_2Fe]$ was transferred under a di-nitrogen atmosphere into another Schlenk flask containing a THF solution of (Ia). The solution was stirred overnight, resulting in a salt elimination reaction to synthesise (Xc).

The THF was removed under vacuum to give a red solid which was washed with petroleum spirits and filtered. The solvent was removed under vacuum to give a yellow – red solid with a crude yield of 20 %. The solid was chromatographed using silica, eluting with 1:1 petroleum spirits:CH_2Cl_2 solvent mixture. The second fastest dark yellow band was extracted using a 3:1 petroleum spirits:CH_2Cl_2 solvent mixture which was then removed under vacuum giving a dark yellow solid of (Xc).

3.6.1 IR Spectroscopic Data

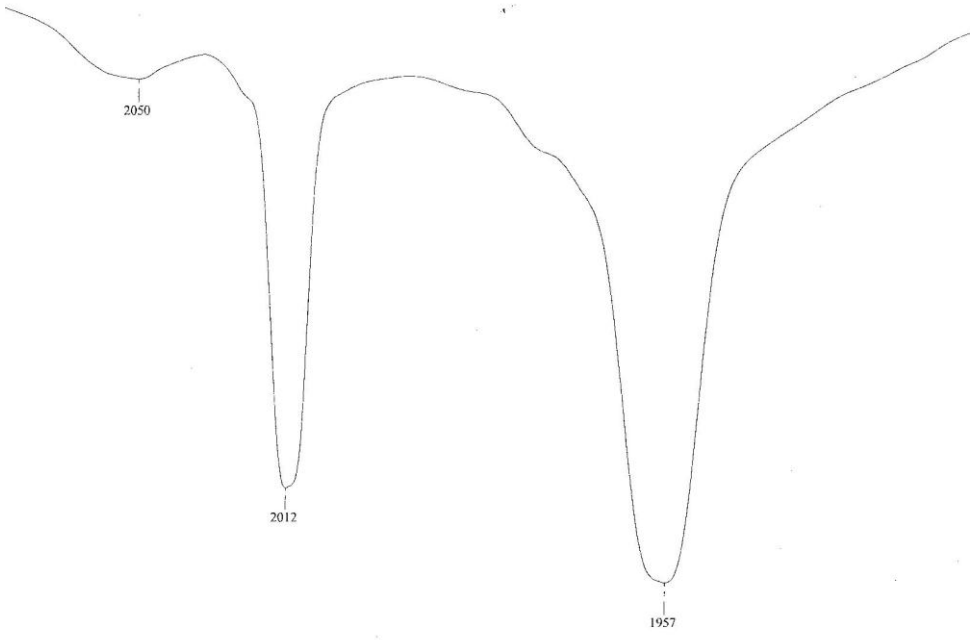

Figure 24: Transmittance solution cell IR spectrum of υCO region in (Xc)

An IR solution cell spectrum was acquired in petroleum spirits with the υCO region investigated. As for previous literature compounds, (Xc) also exhibited two strong iron carbonyl bands at 2012 cm^{-1} and 1957 cm^{-1} (refer to Figure 24).

A full KBr IR spectrum was acquired and showed bands for C-H, Si-CH_3, Si-O-Si and Si-C. The silicon – oxygen was resolved into its symmetric and asymmetric modes, which is not observed within the parent siloxane.

3.6.2 NMR Spectroscopy Data

The ^{1}H NMR spectrum of (Xc) shows two singlet signals at 4.7 ppm and 0.5 ppm which are from the Fe-Cp ring and Fe-Si-CH_3 protons respectively. These signals are assigned based on literature data found for compound (Xa) and (Xb). Therefore, (Xc) is assumed to adopt similar ^{1}H NMR positioned signals for the Fe-Si-CH_3 and Fe-Cp groups[38].

Further characterisation is assisted with the ^{13}C NMR spectrum with two signals observed at 1.3 ppm and 80.4 ppm which are assigned to Fe-Si-CH_3 and the Fe-Cp ring respectively.

3.7 1,4 – Bis(dimethylbromosilyl) benzene (Ib)

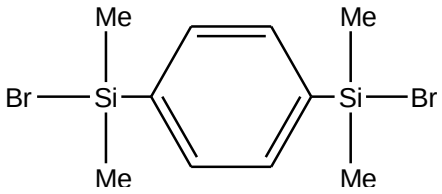

Figure 25: Structure of (Ib)

As conducted for 1,1,3,3-tetramethyl-1,3-dibromodisiloxane (Ia) (refer to Figure 22), a parent silicon hydride was converted into its corresponding halide. 1,4-bis[dimethylsilyl]benzene and N-bromosuccinimide were refluxed under a di-nitrogen atmosphere in CCl_4 at 60 ^{o}C for 6 hrs. The solution was filtered under a di-nitrogen atmosphere followed by removal of the solvent under vacuum. A pale yellow solid of (Ib) was synthesised, which was used without further purification.

The corresponding halogenated siloxane compound (Ib) had an IR solution cell spectrum acquired in petroleum spirits, observing the full removal of the υSi-H band at 2029 cm^{-1}.

3.8 1,4 - Bis[dimethyl(cyclopentadienyl(dicarbonyl)iron)silyl] benzene (Xd)

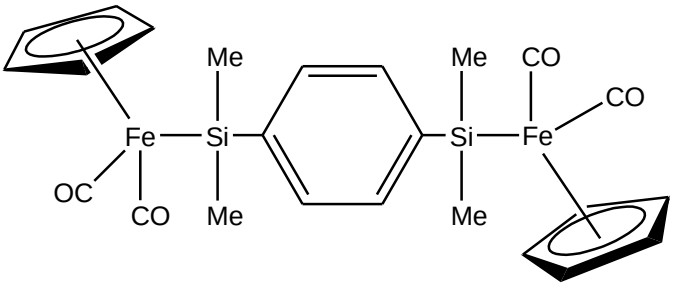

Figure 26: Structure of (Xd)

Advancing further from compound (Xb), with an increased quantity of organic content between the iron metal centres, the compound (Xd) maintains linkage through a para-substituted aromatic ring (refer to Figure 26).

A Schlenk flask containing a THF solution of $Na[Cp(CO)_2Fe]$ anion was transferred under a di-nitrogen atmosphere into another Schlenk flask containing the solid (Ib). The solution was stirred overnight resulting in a salt elimination reaction synthesising (Xd). The solvent was removed under vacuum to give a dark red solid, which was washed with a 1:1 petroleum spirits:CH_2Cl_2 solvent mixture and filtered. The solvent was removed under vacuum to give a brown solid, with a crude yield of 30 %. The solid was chromatographed using silica, eluting with a 1:3 petroleum spirits:CH_2Cl_2 solvent mixture. The fastest eluting yellow band was extracted using CH_2Cl_2 which was later removed under vacuum to give a pale yellow solid.

3.8.1 IR Spectroscopy Data

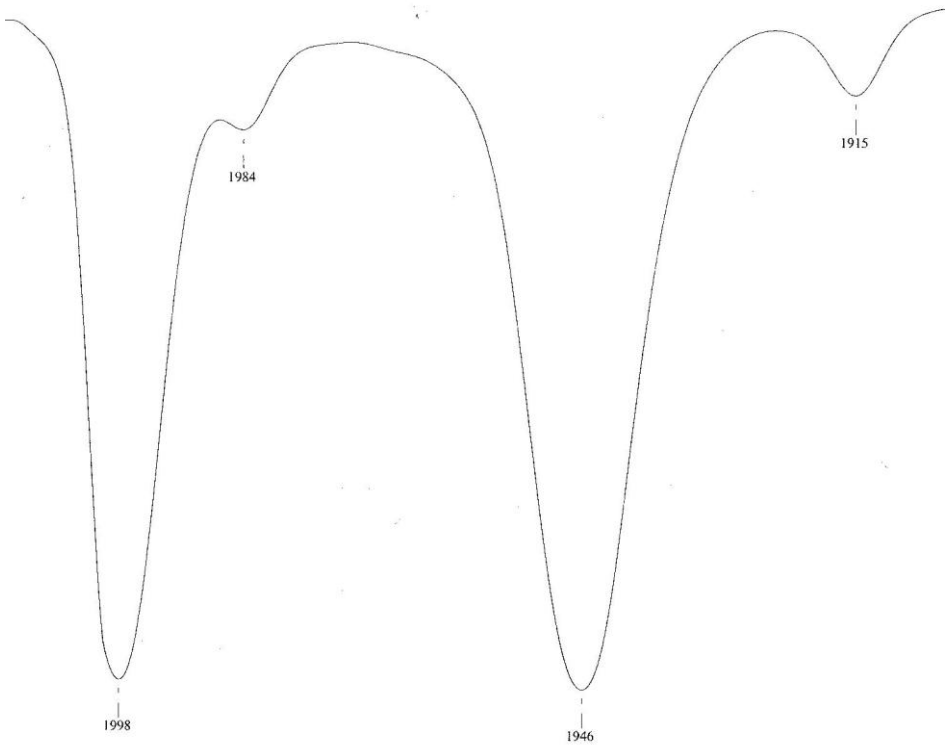

Figure 27: Transmittance solution cell IR spectrum of υCO region in (Xd)

An IR solution cell was acquired in petroleum spirits, investigating the υCO region which showed two strong bands at 1998 cm^{-1} and 1946 cm^{-1} (refer to Figure 27). This band pattern is expected for these types of compounds as discussed for previous examples.

3.8.2 NMR Spectroscopic Data

The NMR data acquired was very similar to the previous examples discussed however, (Xd) contained aromatic signals unlike the other iron-silicon compounds.

The ^{1}H NMR contained three peaks, appearing at 7.5 ppm, 4.5 ppm and 0.6 ppm which was expected as the aromatic ring signals for $C^{2/6}$ + $C^{3/5}$ at 7.5 ppm are equivalent, due to the para-substituted groups being the same. The other two signals are for the Fe-Cp ring and Si-CH_3 signals respectively as found in other examples.

^{13}C NMR data acquired showed the expected signals for (Xd) appearing at 212 ppm, 132 ppm, 84 ppm and 1 ppm. These have been assigned to Fe-CO, aromatic carbons, Fe-Cp and Si-CH_3 groups respectively based on data acquired for other previous examples.

3.9 Summary

Previously reported complexes $FpSiMe_2SiMe_2Fp$ (Xa) and $FpSiMe_2CH_2CH_2SiMe_2Fp$ (Xb) have been prepared and new data measured. NMR data for (Xb) did not concur with that observed within the literature[38] for reasons that are not clear. All NMR data obtained for this thesis show that the ^1H and ^{13}C NMR signals are for the compound (Xb).

As an extension to the work achieved by King et al., two new end – capped iron silyl compounds that were not previously made were prepared and characterised. These are $FpSiMe_2OSiMe_2Fp$ (Xc) and $FpSiMe_2C_6H_4SiMe_2Fp$ (Xd), both new compounds consisted of similar appearances to that of their known literature counterparts. Groups within these two compounds were assigned based by comparison with literature compounds.

Although all of these compounds were able to be prepared and were reasonably stable, they were difficult to purify completely because of some decomposition in solution. Hence reliable micro-analytical data could not be obtained, and none crystallised in a form suitable for X-ray crystallography.

Table 7: List of synthesised ruthenium compounds

Key:		
Compound:	**Chemical Formula**	**Given Symbol:**
Dimers		
Bis [triethylsilyl(tetracarbonyl)diruthenium]	$[Et_3SiRu(CO)_4]_2$	(Va)
Bis [phenyldimethylsilyl(tetracarbonyl)diruthenium]	$[PhMe_2SiRu(CO)_4]_2$	(Vb)
Bis [benzyldimethylsilyl(tetracarbonyl)diruthenium]	$[PhCH_2Me_2SiRu(CO)_4]_2$	(Vc)
Polymers		
Poly [1,1,3,3-tetramethyldisiloxane(octacarbonyl)diruthenium]	$[Ru(CO)_4SiMe_2OSiMe_2Ru(CO)_4]_n$	(VIa)
Poly [1,1,3,3,5,5-hexamethyltrisiloxane(octacarbonyl)diruthenium]	$[Ru(CO)_4SiMe_2OSiMe_2OSiMe_2Ru(CO)_4]_n$	(VIb)
Poly [1,4-(dimethylsilyl)benzene(octacarbonyl)diruthenium]	$[Ru(CO)_4SiMe_2(C_6H_4)SiMe_2Ru(CO)_4]_n$	(VX)
End Capped		
Bis [triethylsilyl(octacarbonyl)diruthenium]1,1,3,3-tetramethyldisiloxane	$Et_3Si[Ru(CO)_4SiMe_2OSiMe_2Ru(CO)_4]_nSiEt_3$	(VIIa)
Bis [triethylsilyl(octacarbonyl)diruthenium]1,1,3,3,5,5-tetramethyltrisiloxane	$Et_3Si[Ru(CO)_4SiMe_2OSiMe_2OSiMe_2Ru(CO)_4]_nSiEt_3$	(VIIb)
Bis [(tetracarbonyl)diruthenium](-II)1,1,3,3-tetramethyldisiloxane	$[Ru(CO)_4SiMe_2OSiMe_2Ru(CO)_4](-II)$	(XVa)
Bis [triphenyltin(tetracarbonyl)diruthenium]1,1,3,3-tetramethyldisiloxane	$O[SiMe_2Ru(CO)_4SnPh_3]_2$	(XVIa)

4.0 Ruthenium Results and Discussion

4.1 Introduction

A series of experiments were conducted in an attempt to synthesis an inorganic polymer which maintained metal – metal bonding. Inorganic compounds which are known to maintain these bonds are of the type $[R_3EM(CO)_4]_2$, where M = Os or Ru, E = Si and R = small aliphatic organic groups. These have been previously made by Knox and Stone[22]. However, the known compounds are all three or four units long only. Therefore, an extension to the research already present within the literature is to continue from these small dimer type compounds and make them polymeric.

The simpler dimer compounds previously made were synthesised, so that the optimal required conditions were found for the known ruthenium-silane compounds, (Va) + (Vb). Continuing on, using the same method and conditions that resulted in the synthesis of these compounds, an extension of the smaller dimer compounds was attempted. These dimer compounds were used as the rudimentary model compounds for the spectroscopic data found for the inorganic polymers, whereby a structure could be proposed. With the correct reaction conditions established, an attempt to synthesise polymeric ruthenium – disiloxane compounds, which maintain metal – metal bonding, will be the newest addition to the literature data.

4.2 Bis [triethylsilyl(tetracarbonyl)diruthenium] (Va)

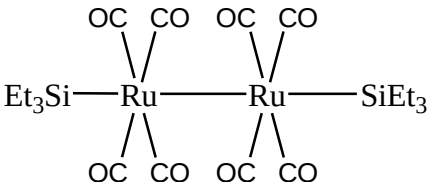

Figure 28: Structure of (Va)

Following the method described by Knox and Stone[22], Et_3SiH and $Ru_3(CO)_{12}$ were placed into an ampoule containing hexane. The ampoule was sealed under vacuum and heated at 85 ^oC for 96 hrs resulting in a bright yellow solution of (Va). As found by Knox and Stone, this gave high yields of $[Et_3SiRu(CO)_4]_2$ (Va) (refer to Figure 28). The compound was purified using silica eluting with petroleum spirits, the fastest yellow band was extracted with petroleum spirits which was cooled to give yellow crystals.

A significant by-product was $H_4Ru_4(CO)_{12}$ which was identified by mass spectrometry. This compound is an expected reaction product for $Ru_3(CO)_{12}$ in the presence of hydrogen gas[32].

4.2.1 IR Spectroscopy Data

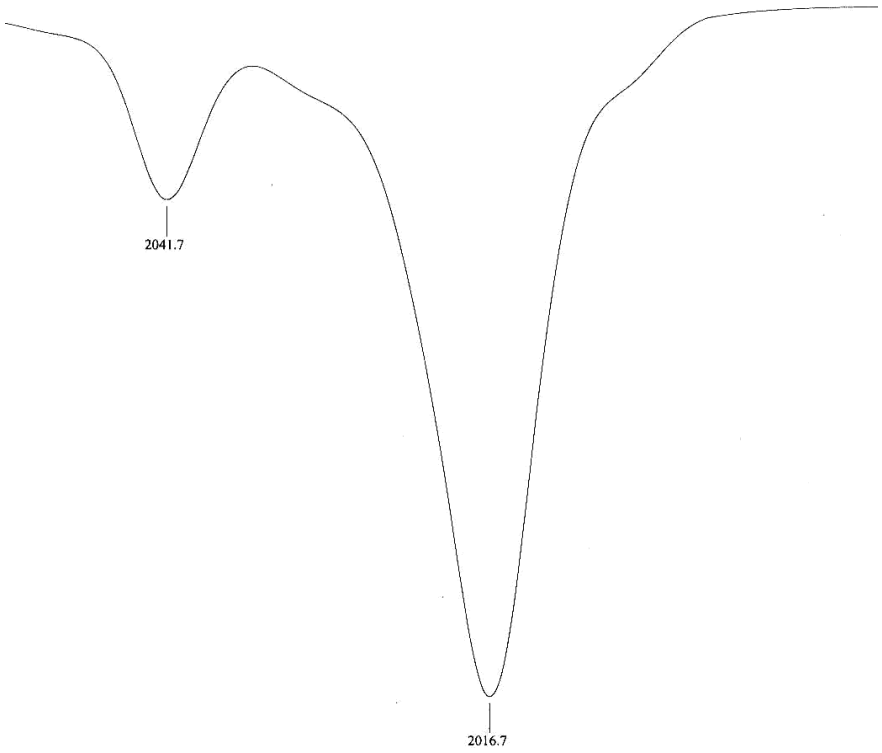

Figure 29: Transmittance solution cell IR spectrum of υCO region in (Va)

An IR solution cell spectrum was acquired and the compound's υCO stretching region was investigated. The data obtained was compared to the existing literature data, and correlates well (refer to Table 8, $[Et_3SiRu(CO)_4]_2$). The IR spectrum (refer to Figure 29) is a characteristic ruthenium carbonyl fingerprint for these types of *trans*-linear-sequenced compounds.

Table 8: Comparative IR υCO bands for silyl and stannyl compounds found by Knox and Stone[22, 23]

Compound		**υCO band frequencies (cm^{-1})**			
Monomer (tetracarbonyl)ruthenium					
$(Me_3Si)_2Ru(CO)_4$	*cis*	2094m	2031s	2015sh	2009s
$Me_3SiRu(CO)_4SnPh_3$	*trans*	2024s			
Dimer (octacarbonyl)diruthenium					
$[Et_3SiRu(CO)_4]_2$	*trans*	2041w	2014s	2005w,sh	
Monomer (tetracarbonyl)ruthenium tin					
$[Me_3Sn]_2Ru(CO)_4$	*cis*	2084s	2024s	2012w	2003s
$[Ph_3Sn]_2Ru(CO)_4$	*trans*	2097vw	2055w	2029s	

The linear Si-Ru-Ru-Si sequence is distinguished by the pattern of weak-strong-weak; whereas a *cis*-conformation would consist of two or more strong υCO bands within this region. The formation of more than one strong υCO band generally occurs for these types of compounds where R = Me. The smaller R-groups have a lower steric hindrance and therefore, can adopt both forms unlike their larger counterparts (refer to Table 8).

4.2.2 Electrospray Mass Spectrometry Data

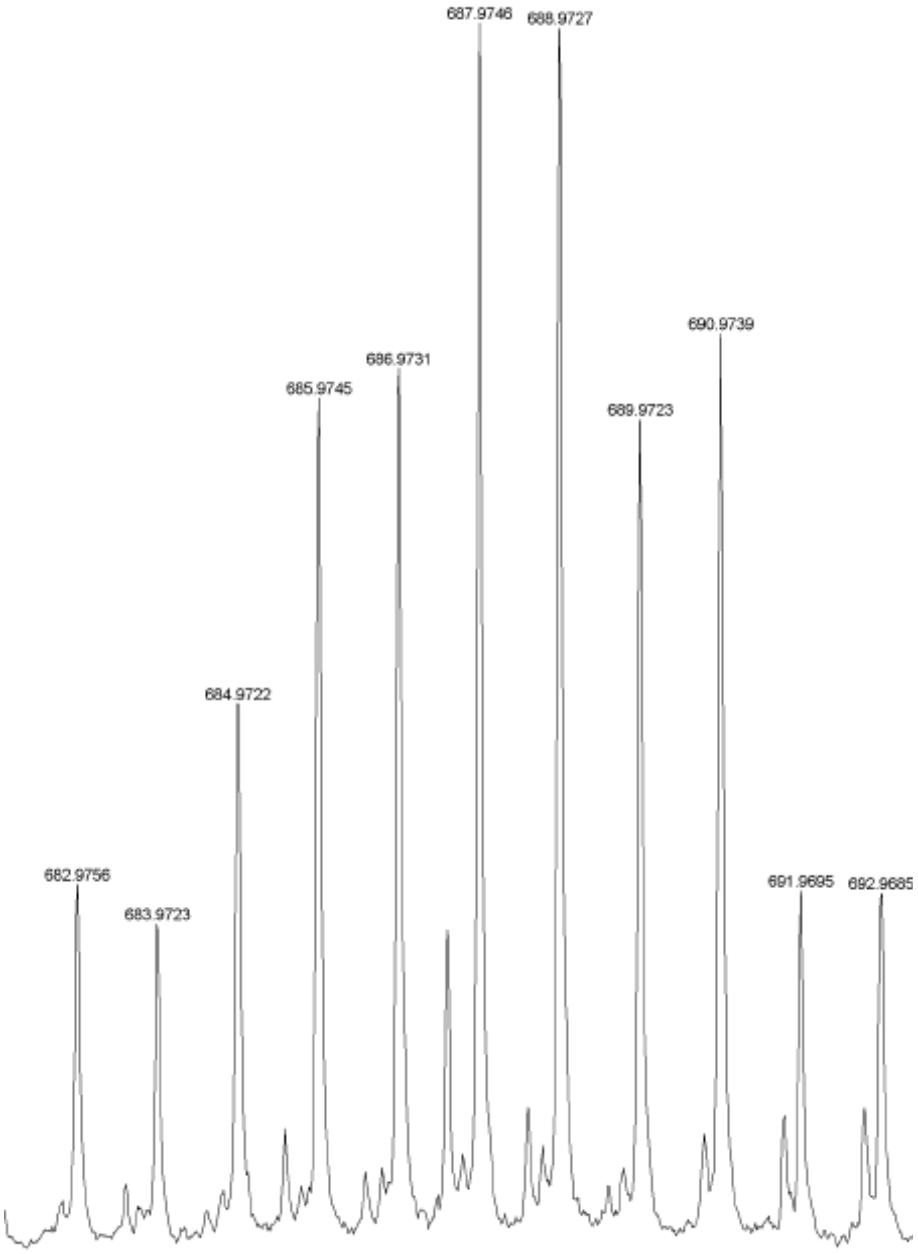

Figure 30: ESMS of [M + OMe]$^-$ ion

The dimer (octacarbonyl)diruthenium compounds, $[Et_3SiRu(CO)_4]_2$, are neutral molecules in solution. Therefore, addition of sodium methoxide is needed for ionisation to occur using ESMS. The methoxide attaches to one of the carbonyl groups generating a $[M+OMe]^-$ ion. For compound (Va) a peak at *m/z* 688.973 was observed, a close match to that calculated at *m/z* 688.976.

An enlargement of this peak, at *m/z* 688 (refer to Figure 30); gives the characteristic polynomial isotope pattern for a compound which contains two ruthenium atoms (refer to Appendix 2).

Within this spectrum there is also the appearance of the by-product $H_4Ru_4(CO)_4$ which gives a strong $[H_3Ru_4(CO)_{12}+OCH_3]^-$ peak, and related fragment compounds, between *m/z* 716 – 774. There were also other unassigned lower *m/z* peaks appearing within the spectrum.

4.2.3 NMR Spectroscopic Data

4.2.3.1 ^{1}H NMR Data

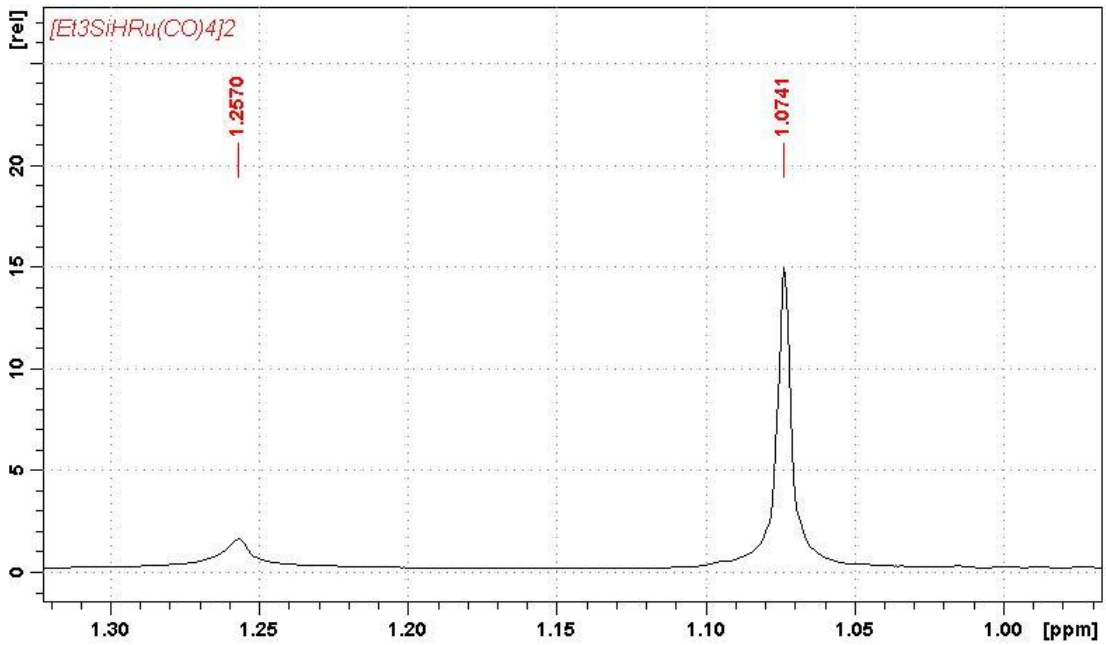

Figure 31: ^{1}H NMR spectrum of (Va) in $CDCl_3$

A ^{1}H NMR obtained for (Va) showed only a single strong peak at 1.0 ppm (refer to Figure 31). This was unexpected since the parent Et_3SiH ^{1}H NMR spectrum (refer to Figure 32) gave the more expected quartet and triplet for an ethyl group.

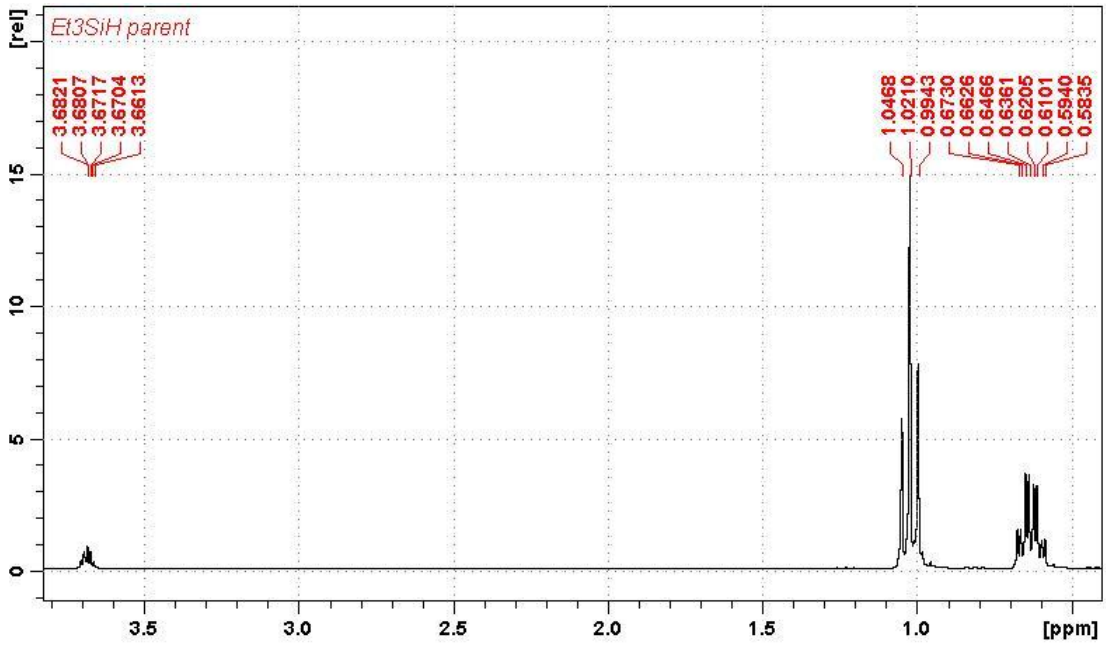

Figure 32: ^{1}H NMR spectrum of starting material Et_3SiH in $CDCl_3$

4.2.3.2 ^{13}C NMR Data

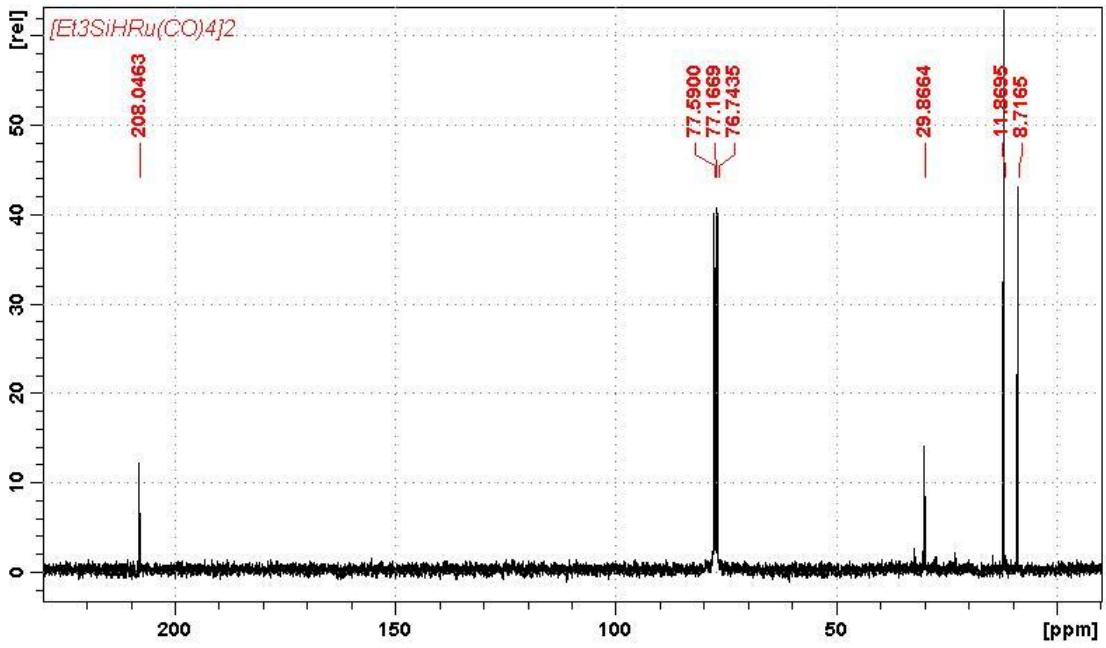

Figure 33: ^{13}C NMR spectrum of (Va) in $CDCl_3$

^{13}C NMR spectra acquired showed three peaks present at 208 ppm, 11.8 ppm and 8.7 ppm which have been assigned to CO, CH_2 and CH_3 respectively (refer to Figure 33). Unlike the ^{1}H NMR spectrum the ^{13}C NMR can see all identifiable group that belonging to the compound (Va).

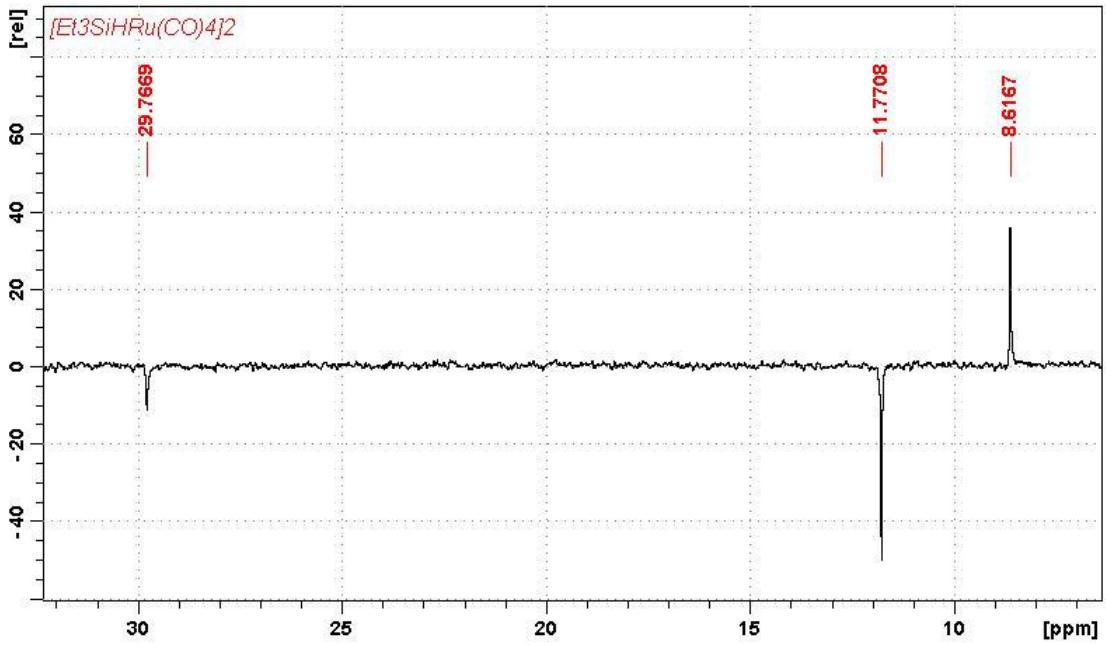

Figure 34: DEPT135 NMR spectrum of (Va) in $CDCl_3$

Other NMR spectra for (Va), involving a ^{13}C DEPT135, showed the two downfield peaks at 11.8 ppm and 8.6 ppm remained and have been assigned to the CH_2 and CH_3 groups respectively (refer to Figure 34).

These three NMR spectra combined could not give a conclusive result, primarily due to the ^{1}H NMR spectrum only containing a singlet at 1.0 ppm as opposed to the theoretical quartet and triplet expected for an ethyl group or that found in the parent silane (refer to Figure 32).

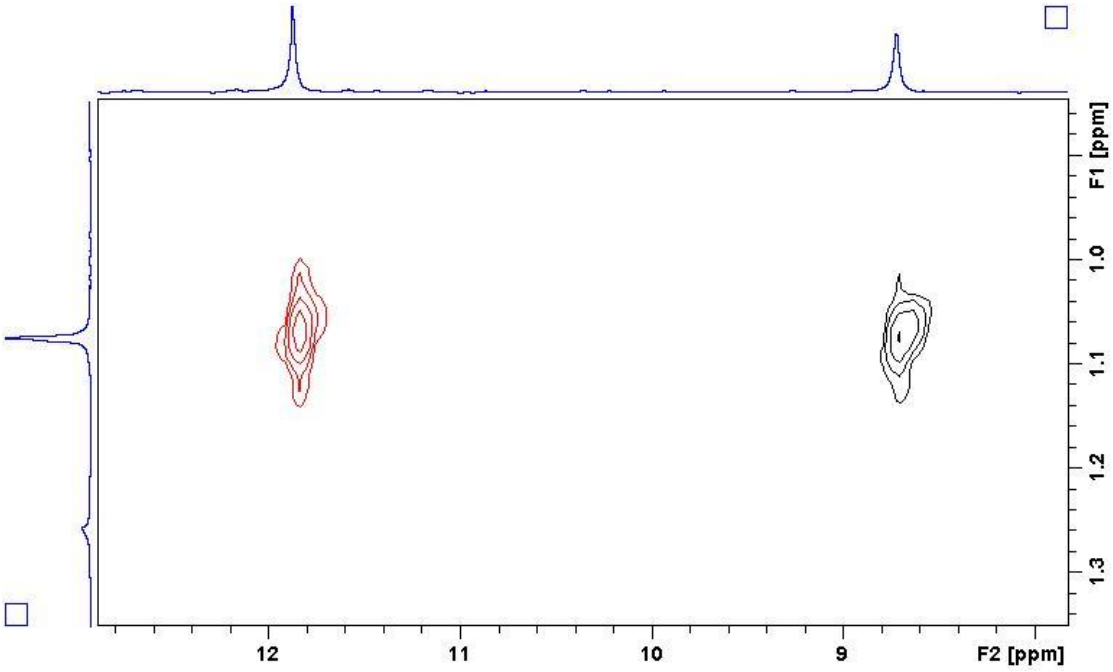

Figure 35: 2D-XHDEPT NMR spectrum of (Va) in $CDCl_3$

A two dimensional NMR ^{1}H and ^{13}C DEPT135, with J = 125Hz, was conducted (refer to Figure 35). Two peaks are observed and show that these peaks are equivalent along the y-axis (^{1}H). These peaks are associated with the CH_2 and CH_3 carbons; therefore the ^{1}H spectrum can now be interpreted. Formation of the dimer compound, (Va), causes an accidental degeneracy of the CH_2 and CH_3 proton signals. The CH_2 and CH_3 groups can easily be identified using the two dimensional spectra whereby the peaks in red are CH_2 and those in black are CH_3.

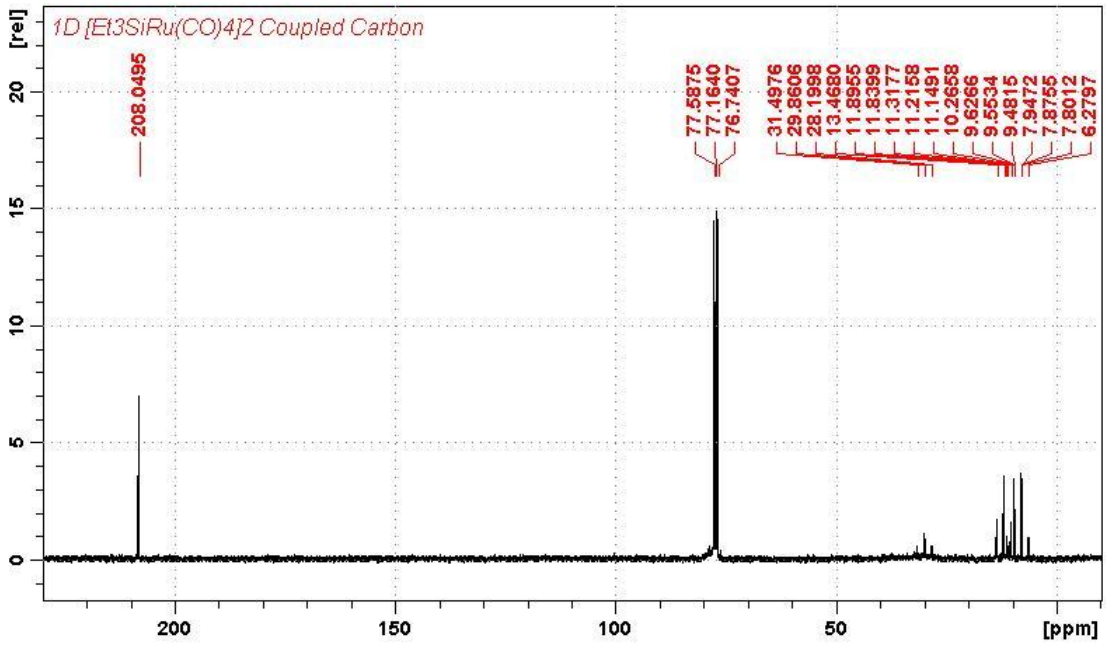

Figure 36: ^{13}C Coupled NMR spectrum of (Va) in $CDCl_3$

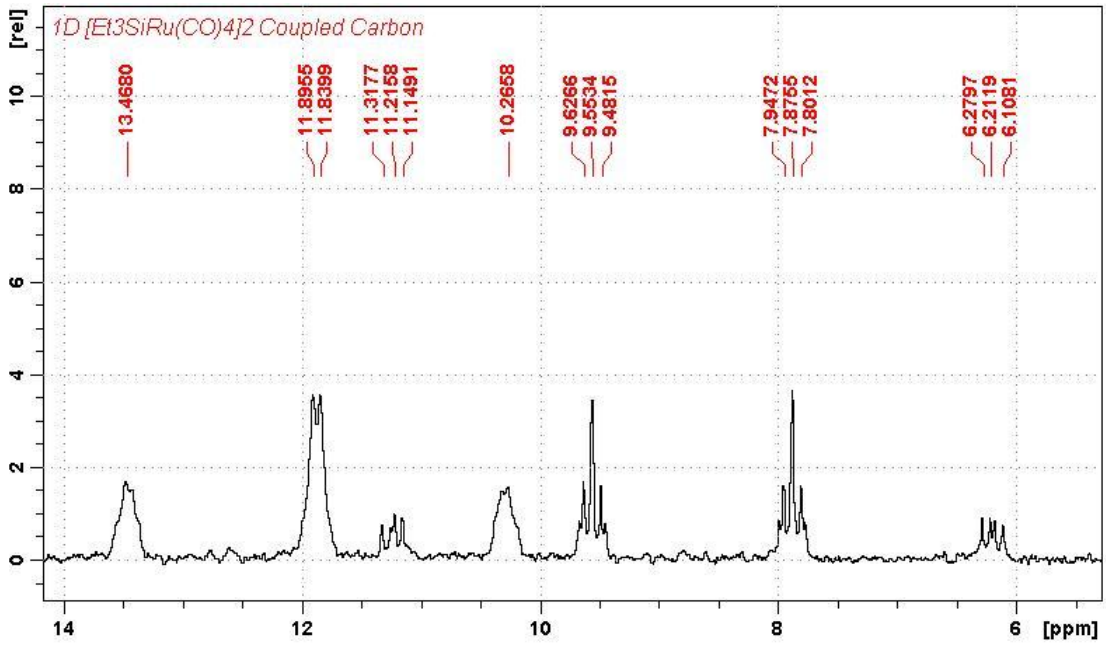

Figure 37: Enlargement of Figure 36 aliphatic region

Furthermore using ^{13}C-^{1}H coupled NMR spectroscopy; two separate series of peaks are observed around 12 ppm and 9 ppm. The series of peaks at 12 ppm consists of a triplet (J = 116 Hz) of doublets (unresolved). The coupling constant between these doublets is relatively low, unlike that found in normal aliphatic hydrocarbons, where J = 125 Hz. The other series of peaks observed at 9 ppm is a quartet (J = 125 Hz) of triplets (J = 5.5 Hz). The coupled carbon spectrum shows that the triplet of doublets is the CH_2 group due to the lowered coupling constant

value. The value is notable of directly bound aliphatic hydrocarbons to a silicon atom. Therefore, it can be further stated that the triplet of doublet at 12 ppm belongs to the Si-CH_2 and the quartet of triplets at 9.0 ppm is the CH_2-CH_3.

4.3 Bis [phenyldimethylsilyl(tetracarbonyl)diruthenium] (Vb)

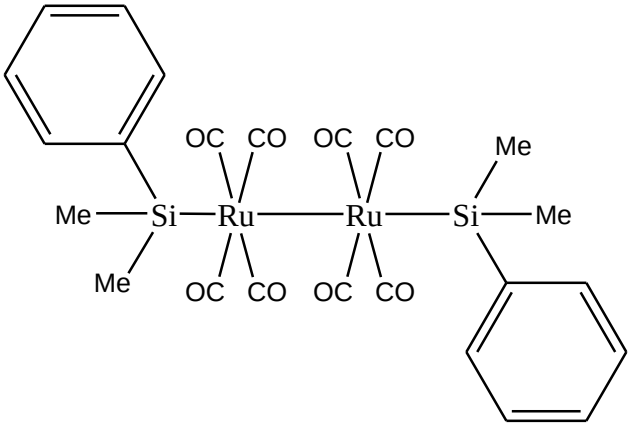

Figure 38: Structure of (Vb)

Following methods that were used for (Va), $PhMe_2SiH$ and $Ru_3(CO)_{12}$ were placed an ampoule containing hexane and sealed under vacuum. The ampoule was heated at 90 ^oC for 72 hrs to give a bright yellow solution of the synthesised (Vb). As found by Nombel et al. this compound afforded lower yields, cf. (Va), with only 60 – 70 % formation of the desired $[PhMe_2SiRu(CO)_4]_2$ compound[30]. The compound was purified using silica, eluting with petroleum spirits. The second fastest yellow band was extracted using petroleum spirits and then cooled to give bright yellow crystals.

This compound along with (Va), was prepared as a model compound for the larger dimer ruthenium compounds which incorporate aryl components for polymeric linkages.

4.3.1 Spectroscopic Data

Solution and KBr IR spectra were both obtained, two υCO bands were observed within the solution cell IR spectrum at 2048 cm^{-1} (w) and 2020 cm^{-1} (vs). The KBr spectrum showed a similar pattern however the strongest υCO band was more resolved and was split into two. These two separate bands were observed at 2007 cm^{-1} (vs) and 1992 cm^{-1} (vs), a third weaker band was also observed at 2060 cm^{-1} (m). These bands conform to the expected pattern for these compounds (refer to Figure 29) and correlate with the literature data[30].

Similarly the ESMS spectrum gave the expected $[M+OMe]^-$ peak at 728.917 *m/z*, which is a close match to the calculated value at *m/z* 728.913. NMR data was fully characterised with ^1H and ^{13}C signals readily assigned to the expected groups for (Vb).

4.4 Bis [benzyldimethylsilyl(tetracarbonyl)diruthenium] (Vc)

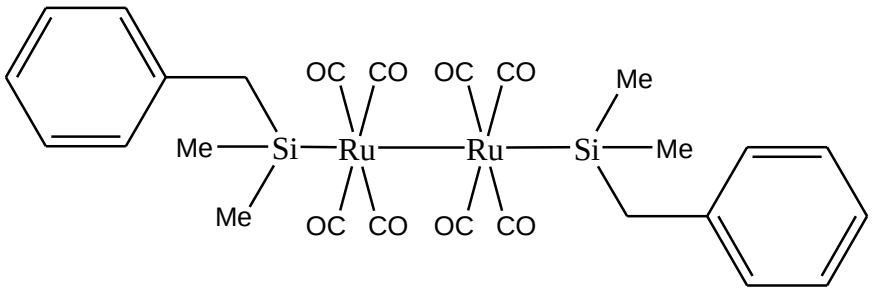

Figure 39: Proposed structure of (Vc)

The third dimer compound which consists of the linear-*trans*-Si-Ru-Ru-Si arrangement was prepared by placing $PhCH_2Me_2SiH$ and $Ru_3(CO)_{12}$ in an ampoule containing hexane. The ampoule was sealed and heated at 90 ^oC for 72 hrs to give a bright yellow solution. Cooling of the solution to room temperature resulted in the solidification of the yellow solution within the ampoule. The reaction mixture gave a high yield of the dimer (Vc), 90 %, which was purified through crystallisation techniques using warm petroleum spirits and cooling at -25 ^oC overnight.

This compound is much like (Vb) and (Va) however, contains a more flexible bulky group (refer to Figure 39). The new compound was further characterised using elemental analysis where its composition correlated well with the predicted values. Other spectroscopic methods conducted for (Vc) indicate that it is a direct analogue of (Va) and (Vb).

4.4.1 IR Spectroscopic Data

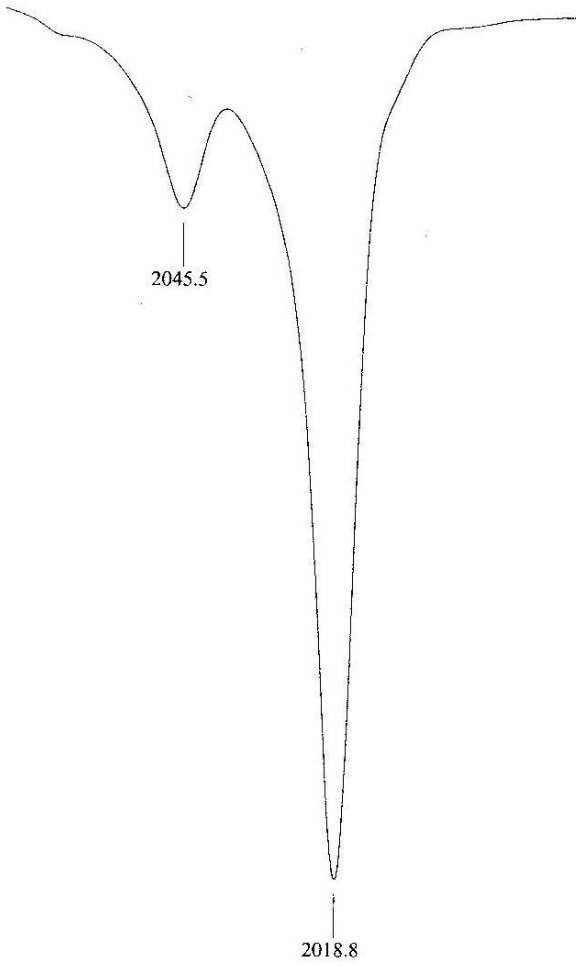

Figure 40: Transmittance solution cell IR spectrum of υCO region in (Vc)

The solution IR spectrum acquired showed the υCO bands with the same arrangement and with similar wave-number values comparable to that observed for previous examples (refer to Figure 40).

4.4.2 Electrospray Mass Spectrometry Data

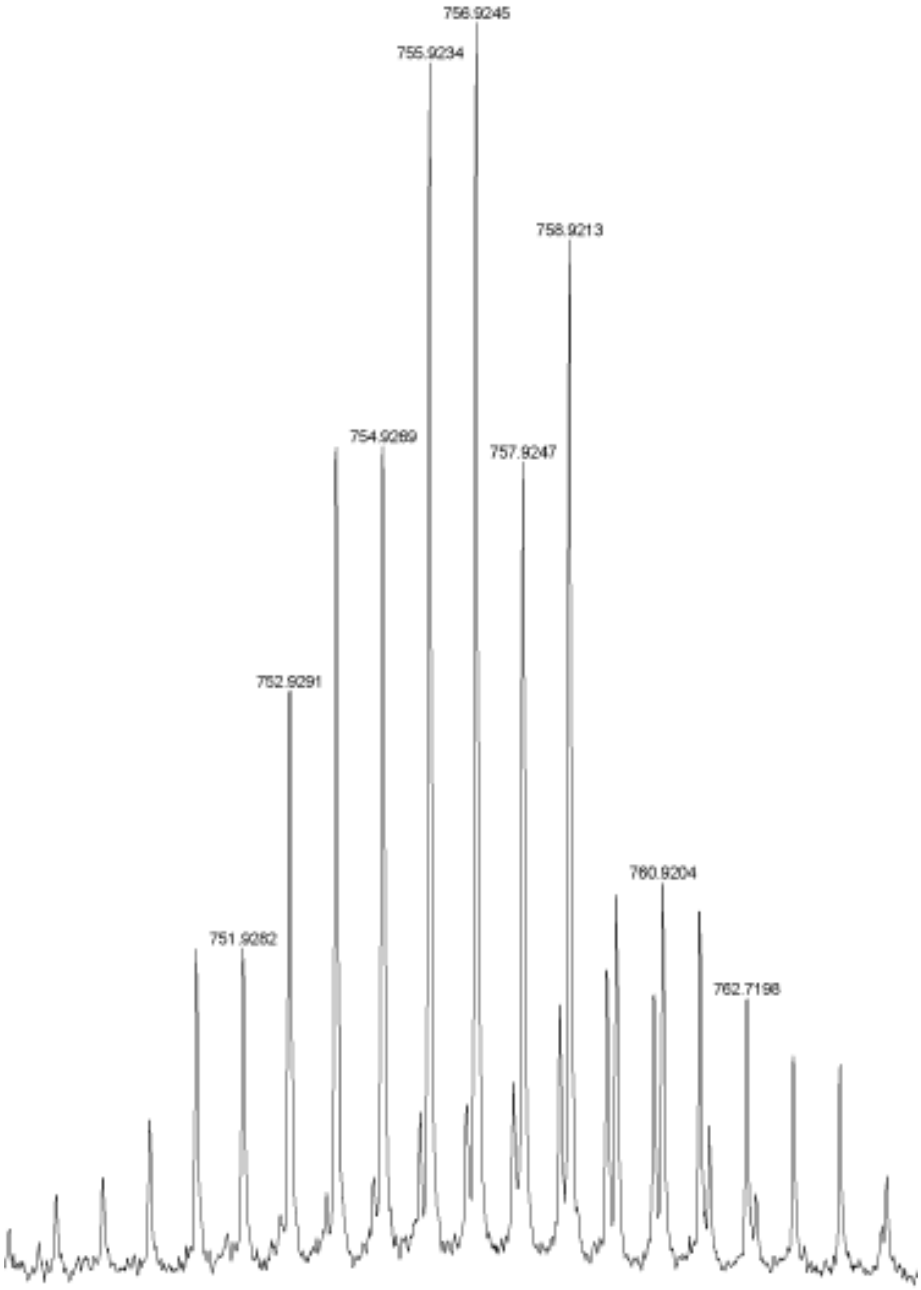

Figure 41: ESMS of [M +OMe] ⁻ ion for (Vc)

A mass spectrum was acquired for (Vc), where a $[M+OMe]^-$ peak is observed at *m/z* 756 (refer to Figure 41), this peaks correlates well with the calculated mass isotope (found: 756.924; calculated: 756.945). The peak at *m/z* 756 also showed the polynomial isotope pattern for a compound containing two ruthenium atoms (refer to Appendix 2).

4.4.3 Additional Spectroscopic Data

The NMR data acquired for (Vb) will be used as a template for the methyl and aromatics signals expected. The ^{1}H NMR spectrum for (Vc) contained one set of peaks at 7.0 ppm and two others at 2.5 ppm and 0.5 ppm. Comparing it to the spectra acquired for (Vb) the only differing peak is the one appearing at 2.5 ppm. Therefore, the signals have been assigned to belonging to the aromatics, CH_2 benzyl and Si-CH_3 groups respectively.

^{13}C NMR spectra acquired enforces that found within the ^{1}H NMR spectrum for (Vc). If the spectra for (Vc) is compared to that obtained for the prepared literature compound (Vb), only one peak differs within all NMR spectra. This differing peak occurs at 2.5 ppm (^{1}H) and at 34 ppm (^{13}C) and it is assigned to the CH_2 benzyl. Within the ^{13}C NMR spectrum there are four signals observed at 207 ppm, multiple singlets around 130 ppm, 34 ppm and 5.9 ppm. These signals have been assigned to belonging to CO, aromatics, CH_2 benzyl and Si-CH_3 groups respectively. The DEPT135 spectrum shows that the peak at 34 ppm becomes inverted which is further reasoning for the assignment of this peak to be the CH_2 benzyl group. Microanalysis results obtained for (Vc), based on C % and H %, correlate well with the calculated values.

4.5 Poly [1,1,3,3-tetramethyldisiloxane(octacarbonyl)diruthenium] (VIa)

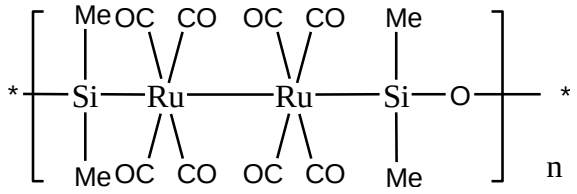

Figure 42: Proposed inorganic polymeric unit of (VIa)

Maintaining the same reaction conditions as that achieved for the synthesis of the dimer compounds, $HSiMe_2OMe_2SiH$ and $Ru_3(CO)_{12}$ were added to an ampoule containing hexane. The ampoule was sealed and heated at 85 ^oC for 96 hrs. The reaction mixture changed from a light-yellow to a very dark yellow solution. Removal of the solvent under vacuum resulted in a black opaque oil which was unable to be chromatographed using silica or alumina due to irreversible binding to the inert phase. Therefore, characterisation techniques used involve the crude black oil with a yield of 65 %.

This compound contains the Si-Ru-Ru-Si sequence and therefore, it is the same as that of the dimer compounds previously discussed. However, there exists a linkage between each four member sequence through the use of an oxygen (refer to Figure 42); thus, this is the first attempt at an inorganic polymer.

4.5.1 IR Spectroscopic Data

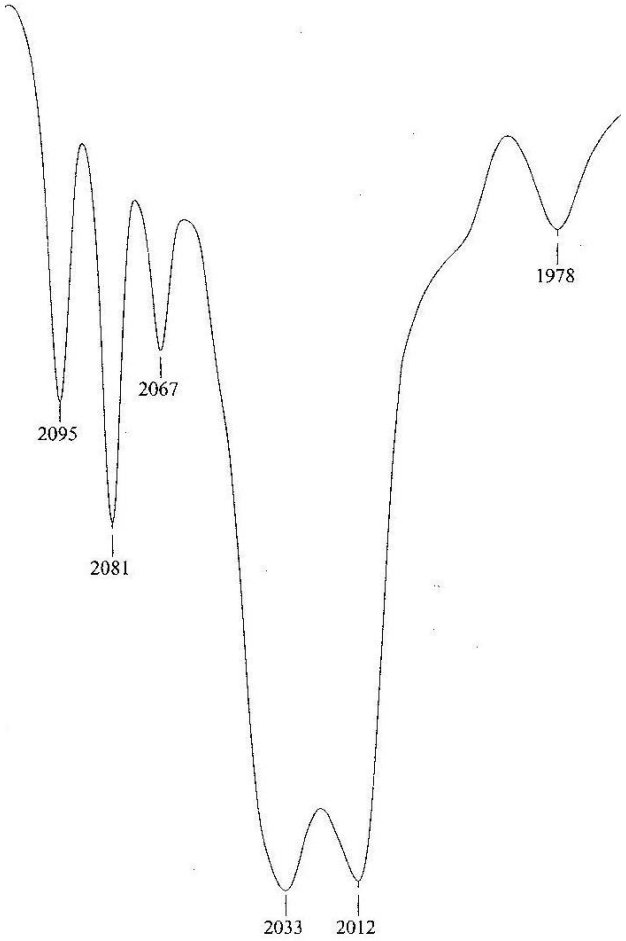

Figure 43: Transmittance solution cell IR spectrum of υCO region in (VIa)

A solution cell IR spectrum was acquired of (VIa) with the υCO region investigated giving a complex sequence of bands (refer to Figure 43). A full IR spectrum was also acquired in KBr which showed no change for the υCO complex bands. The pattern obtained for both IR spectra show a more complex arrangement of compounds present than the IR spectra of the dimer compounds previously discussed. The presence of more than one strong υCO band represents the possibility of both *cis* and *trans* forms existing.

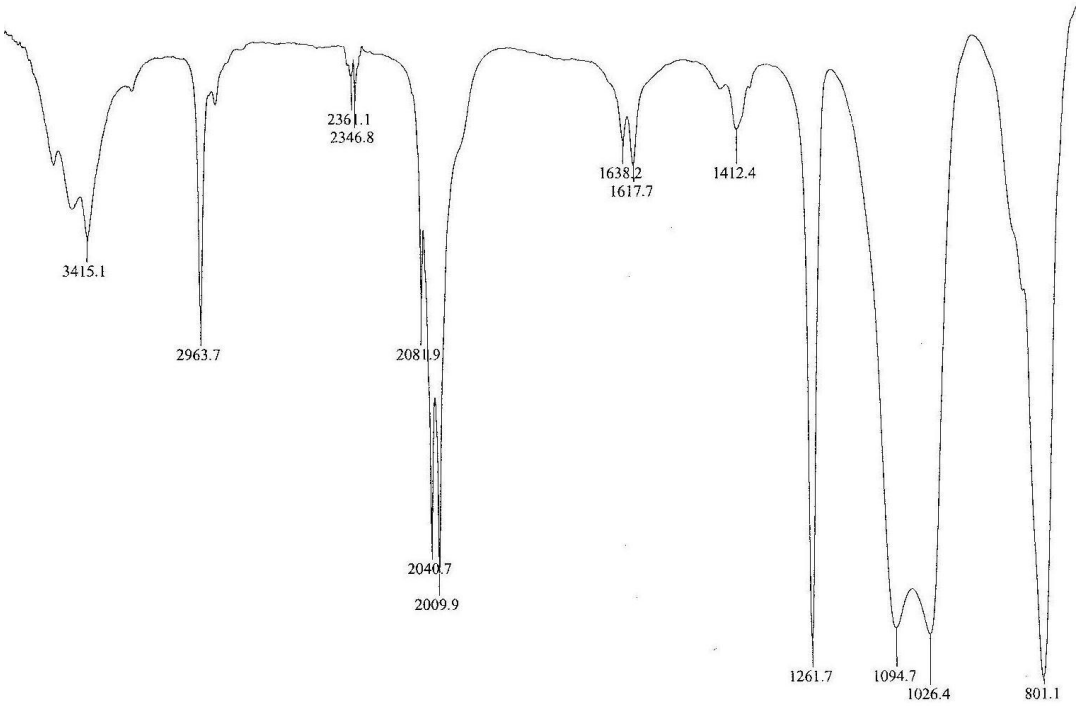

Figure 44: Full transmittance IR spectrum acquired in KBr of (VIa)

An interesting feature within the full KBr spectrum is the separation of the Si-O-Si stretching band occurring at 1026 – 1095 cm^{-1} (refer to Figure 44). The separation of the band is a result of good resolution of the Si-O-Si bonds symmetric and asymmetric modes, a feature not seen within the KBr spectrum of the parent siloxane.

4.5.2 Mass Spectrometry Data

ESMS did not prove a useful technique for finding potential lower mass compounds the only assignable peaks present were related to the expected $H_4Ru_4(CO)_{12}$ by-product impurity.

4.5.2.1 LDI-TOF Mass Spectrometry Data

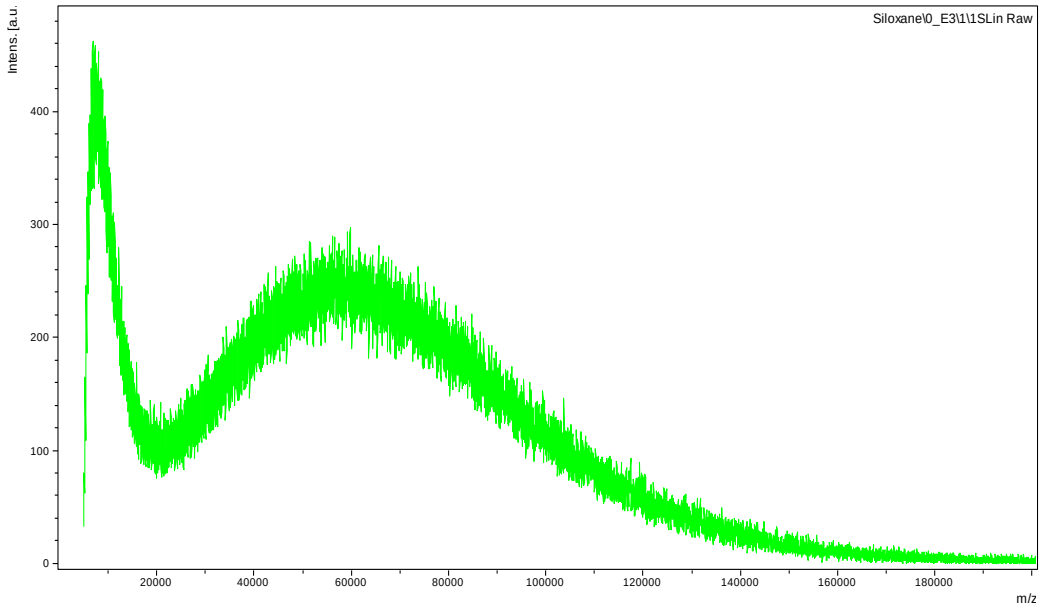

Figure 45: LDI-TOF mass spectrum of (VIa) on a polished steel plate

A polished steel plate was mounted, on which a dried solution of THF containing (VIa) without any ionisation matrix was prepared. The laser beam ionised the sample, in positive ion mode, and gave a broad curved peak with a maxima occurring around *m/z* 60,000 (refer to Figure 45). Further laser ionisations of the same mixture at lower mass ranges gave peaks that were only assignable to that of the by-product.

This data supports high molecular weight polymeric species however, due to the broadness of the curve observed there is no detail on how large one polymer is. The oil most likely consists of multiple polymeric units with no common chain length, which was unexpected. Therefore, it can be explained why a broad curve is observed in the LDI-TOF spectrum and why an oil is obtained, as opposed to crystals and solids which were acquired for previous examples.

4.5.3 NMR Spectroscopic Data

The ^{1}H-NMR spectrum of the crude oil showed a series of singlet peaks in the downfield region between 1.0 ppm and -0.5 ppm. The low downfield position of these peaks is somewhat an indication of Si-CH_3 groups to be present as observed in previous examples and for like compounds, for example tetramethylsilane (TMS).

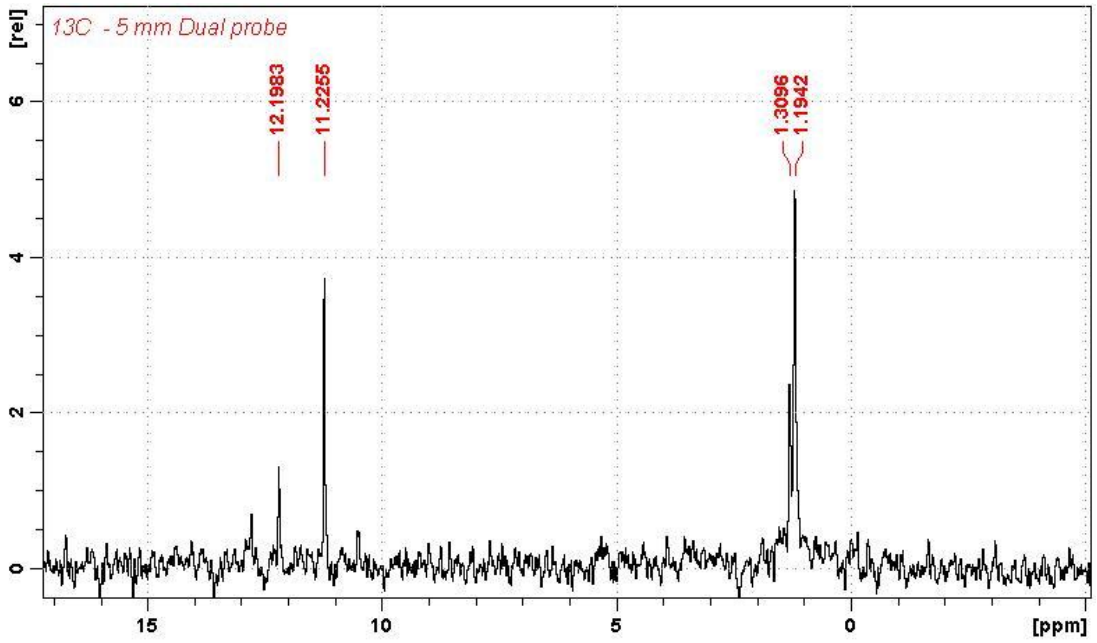

Figure 46: ^{13}C NMR of (VIa) in $CDCl_3$

Further data acquired using ^{13}C NMR and DEPT135 experiments gave spectra which contained multiple singlet signals, backing up the ^{1}H NMR spectrum (refer to Figure 46). The information gathered within these spectra all indicate that the ^{1}H signals observed must only be associated with Si-CH_3 groups. This is based on the fact that all ^{1}H and ^{13}C signals observed within the two spectra are singlets only, observed in the downfield aliphatic region and the DEPT135 contained positive phased peaks only.

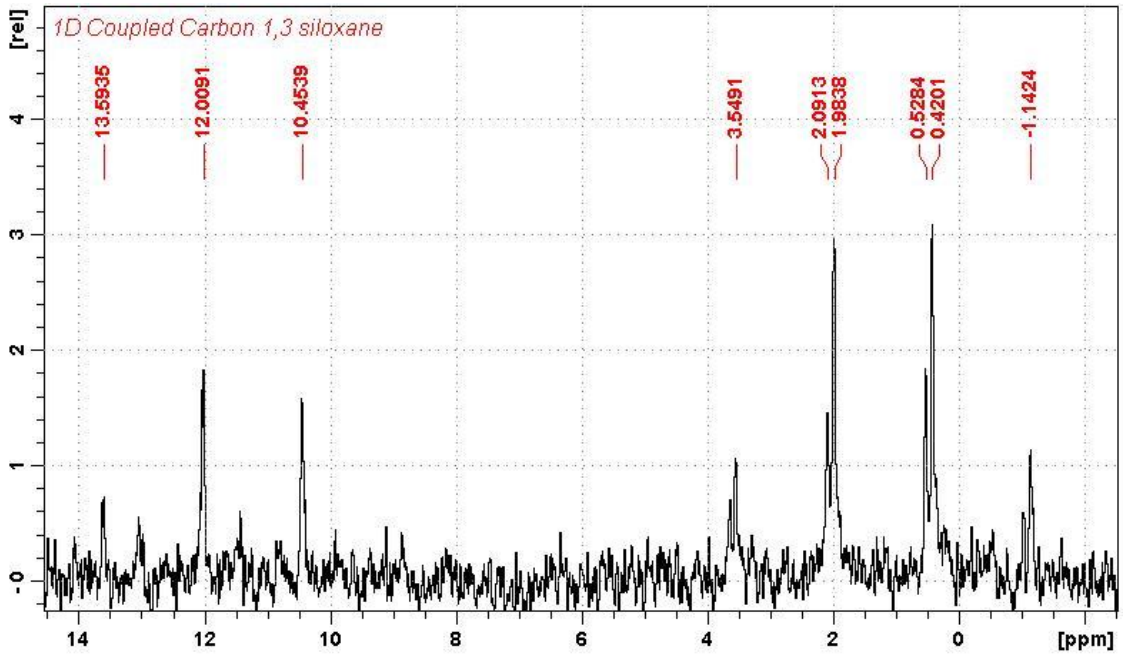

Figure 47: Coupled carbon NMR spectrum of (VIa) in $CDCl_3$

A further ^{13}C NMR experiment conducted involving a coupled carbon spectrum showed that each signal observed in the ^{13}C NMR spectrum split into a quartet (J = 118 Hz) (refer to Figure 47). This coupling constant value for a group of signals is proof of directly bound aliphatic groups to a silicon atom, as observed in previous examples.

The only conclusive result that can be obtained from the NMR spectra acquired is that the crude oil contains a mixture of differing polymeric ruthenium-siloxane compounds. These compounds appear to have no specific molecular mass and therefore, within the ^{1}H and ^{13}C NMR spectra, many singlet signals are obtained for each polymer present within the oil.

4.6 Attempted Chemical Characterisation of $[Si\text{-}Ru\text{-}Ru\text{-}Si]_n$ Polymer (VIa)

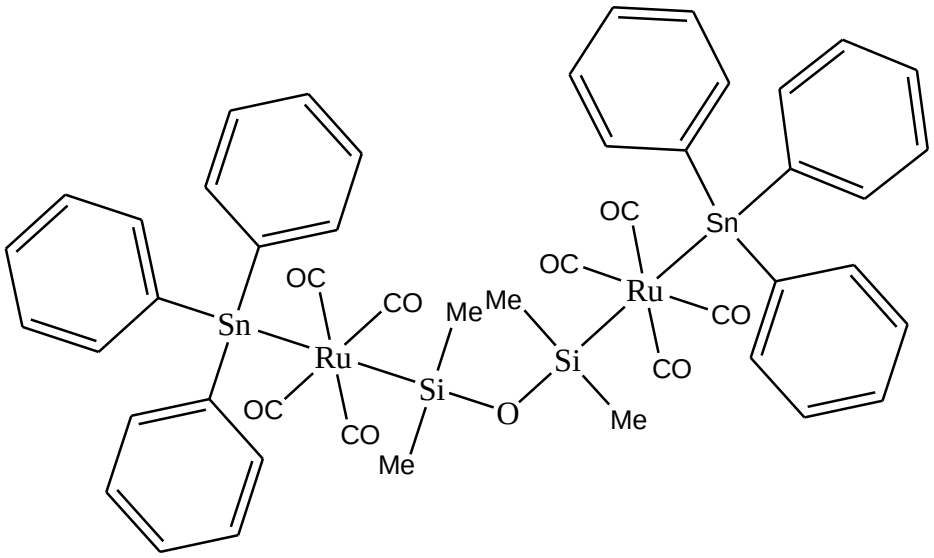

Figure 48: Proposed structural arrangement of (XVIa)

Knox and Stone discovered that the Ru-Ru bonds of the dimer compounds could be reduced using a sodium amalgam[22]. It is by this method that a chemical test for the formation of the linear-sequence Si-Ru-Ru-Si, which is in compound (VIa), could be determined. Formation of a dianion ruthenium compound should be possible which would then result in a salt elimination reaction, giving an end-capped ruthenium siloxane species with the arrangement of Sn-Ru-Si-O-Si-Ru-Sn (XVIa), (refer to Figure 48). This would confirm the presence of the proposed repeating Si-Ru-Ru-Si unit in the polymer (VIa).

A sodium amalgam was prepared under a di-nitrogen atmosphere in a Schlenk flask which had a THF solution containing compound (VIa) added. The solution was stirred at room temperature for 15 min to presumably generate the dianion Na_2(Ru-Si-O-Si-Ru) (XVa) before being transferred under nitrogen into another Schlenk flask containing a THF solution of triphenyltin chloride (Ph_3SnCl).

The second flask containing the two solutions was stirred at 0 ^{o}C for 2 hrs giving a slightly red coloured solution before having the solvent removed under vacuum. The red solid was re-dissolved in a 1:1 petroleum spirits:CH_2Cl_2 solvent mixture and filtered before having the solvent removed under vacuum to give an orange solid.

4.6.1 IR Spectroscopic Data

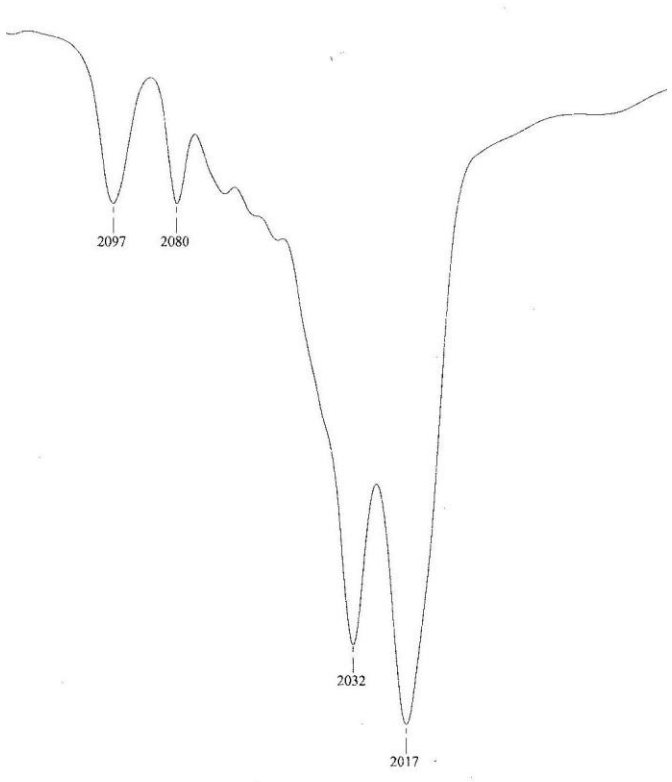

Figure 49: Transmittance solution cell IR spectrum of υCO region in (XVIa)

An IR solution cell using petroleum spirits was acquired and the υCO region investigated. There was the appearance of two weak and two strong υCO bands present (refer to Figure 49). The appearance of there being more than one strong band, as mentioned for (VIa), is the possibility of *cis* and *trans* species being present. The arrangement for the IR spectrum of (XVIa) to be complex is mostly due to the siloxane component only containing methyl groups. Therefore, there is not enough steric hindrance within the compound for there to be preference for one form only.

The full KBr spectra also contained peaks which were associated with the symmetric and asymmetric bands of Si-O-Si at ca. 1000 cm^{-1} also, there were bands present around 1400 cm^{-1} and 2900 cm^{-1} associated with aromatics.

4.6.2 Electrospray Mass Spectrometry Data

The spectrum acquired for (XVIa) showed higher mass peaks, cf. the by-product, that were not observed within the ESMS spectrum for compound (VIa). The main peaks from the ESMS spectrum have been solved and summarised in Table 9.

Table 9: ESMS peaks from (XVIa) spectrum

Compound	Calculated m/z	Found m/z
$[(Ph_3Sn)_2Ru(CO)_4 + OMe]^-$	944.943	944.952
$[Ph_3SnRu(CO)_4Ru(CO)_3SnPh_3 + OMe]^-$	1128.833	1128.856

There was one other higher mass peak within the spectrum at *m/z* 1278 however; this was unable to be assigned with the same accuracy as those in Table 9. Therefore, the ESMS shows a mixture of species that fit the generate isotope pattern formed for Ru – Sn compounds (refer to Appendix 5 and Appendix 6), but not the planned (XVIa) compound. The use of a sodium amalgam to generate the (XVa) dianion was less specific for the polymer (VIa), unlike that found by Knox and Stone for the dimer compounds[22].

4.7 Poly [1,1,3,3,5,5-hexamethyltrisiloxane(octacarbonyl)diruthenium] (VIb)

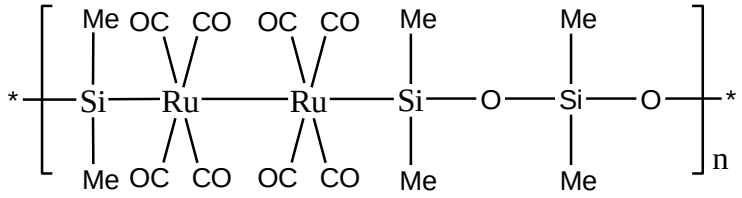

Figure 50: Proposed inorganic polymeric unit (VIb)

This extended polymeric compound had the same experimental procedures conducted as that achieved for the attempted synthesis of compound (VIa). An ampoule containing hexane had added to it $HMe_2SiOSiMe_2OSiMe_2H$ and $Ru_3(CO)_{12}$. The ampoule was sealed under vacuum and heated at 85 ^oC for 48 hrs resulting in a transparent yellow solution. The solvent was removed under vacuum leaving a viscous transparent yellow oil with a crude yield of 70 %. The flask containing the oil was flushed with nitrogen and stored overnight at -25 ^oC where it solidified. Warming of the solid to room temperature, as well as warming to 37 ^oC, did not result with solid melting to return the oil. However, re-dissolving the solid in petroleum spirits followed by vacuum removal of the solvent did return the yellow oil. The crude product was chromatographed using silica, eluting with a 1:1 petroleum spirits:CH_2Cl_2 solvent mixture. The fastest eluting yellow band was extracted using the same mixture and the solvent later removed under vacuum to give a pale yellow solid.

As an extension into the studies conducted for the first attempted synthesis of an inorganic polymer, compound (VIa). This attempted synthesis structure only differs from that of (VIa) within the siloxane bridging unit between Ru – Ru units. The addition of an extra O-$SiMe_2$ group should show greater flexibility, cf. (VIa), since the Si-O-Si bond would not contain large groups on both sides of the oxygen. Therefore, the siloxane bond will not be forced into a linear structure due to the central silicon remaining as a small group.

4.7.1 IR Spectroscopy Data

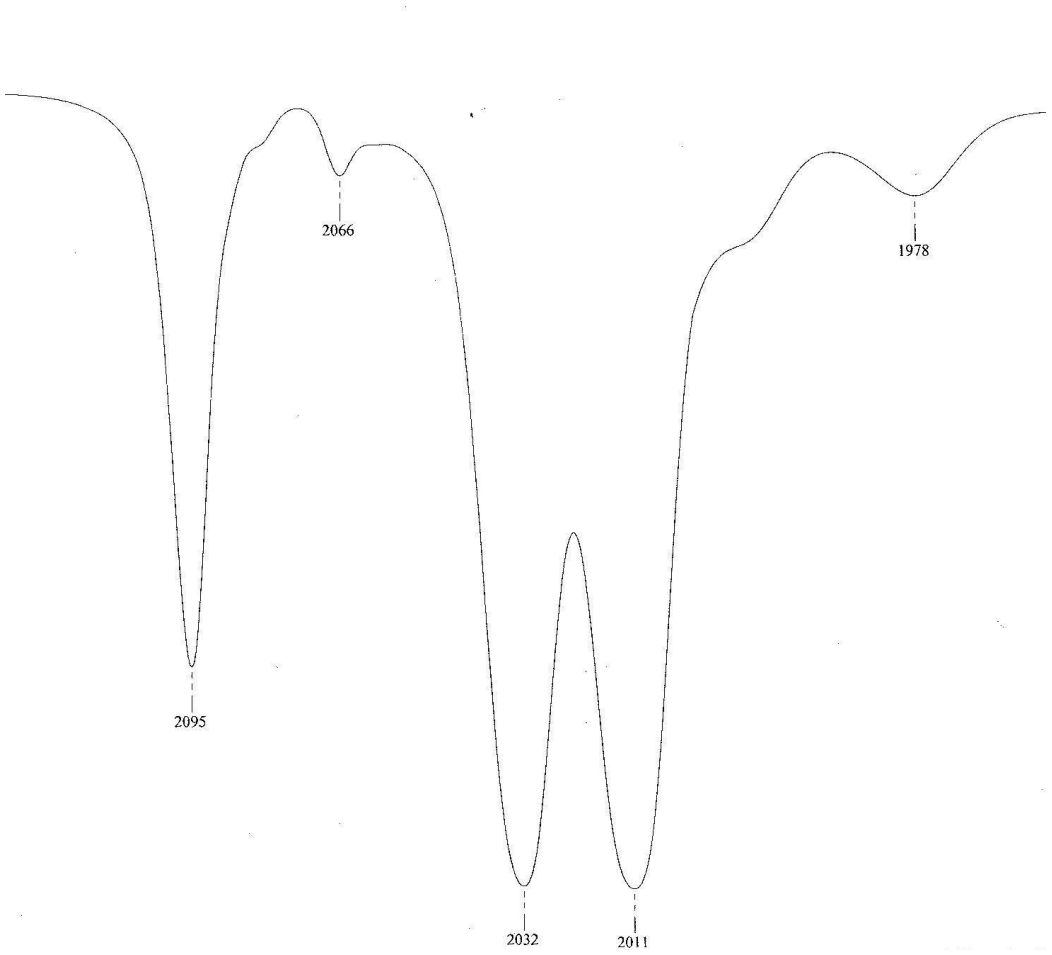

Figure 51: Transmittance solution cell IR spectrum of υCO region in (VIb)

The solution cell IR spectrum of (VIb) showed a new band pattern with three very strong υCO bands which was unexpected as the expected pattern was to somewhat like that acquired for (VIa). With the appearance of more than one strong υCO band, like that also observed for (VIa), the solid potentially contains a mixture of trisiloxane compounds that are in *cis* or *trans* forms (refer to Figure 51).

A full IR spectrum was also acquired in KBr with the Si-O-Si band, around 1000 cm^{-1}, having the same separation present for symmetric and asymmetric mode separation as observed in Figure 43.

4.7.2 Mass Spectrometry Data

4.7.2.1 Electrospray Mass Spectrometry Data

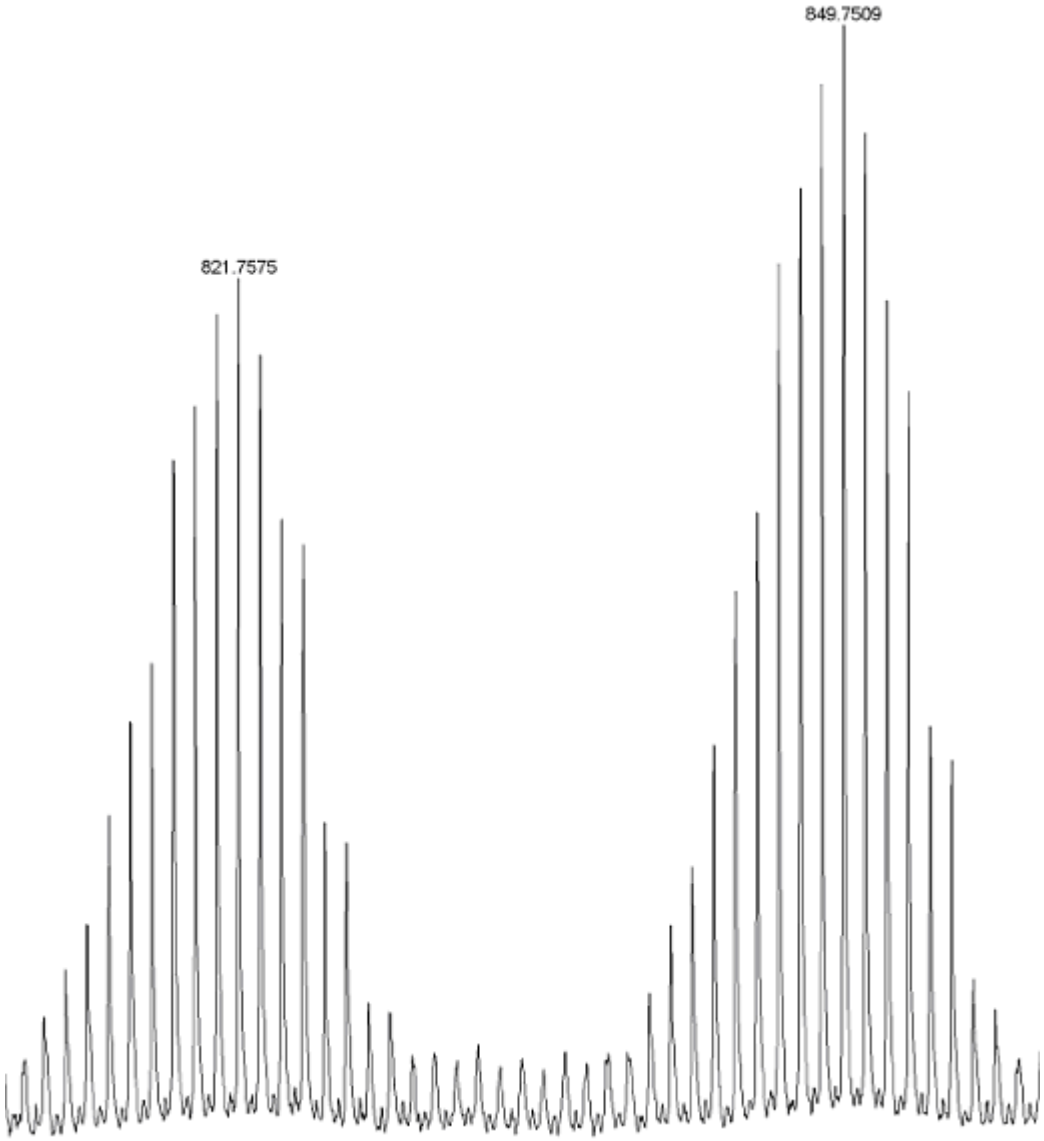

Figure 52: Major peaks in ESMS spectrum of (VIb)

The spectrum acquired does not show strong peaks for the by-product $H_4Ru_4(CO)_{12}$ at *m/z* 744 and related peaks, unlike the ESMS for compound (VIa). The two strongest peaks at *m/z* 849 and 821 are 28 mass units apart, this is equivalent to a compound losing a carbonyl (refer to Figure 52). The only other identifiable peaks present at higher *m/z* values (around *m/z* 1000) are also observed to be 28 mass units apart (refer to Figure 53).

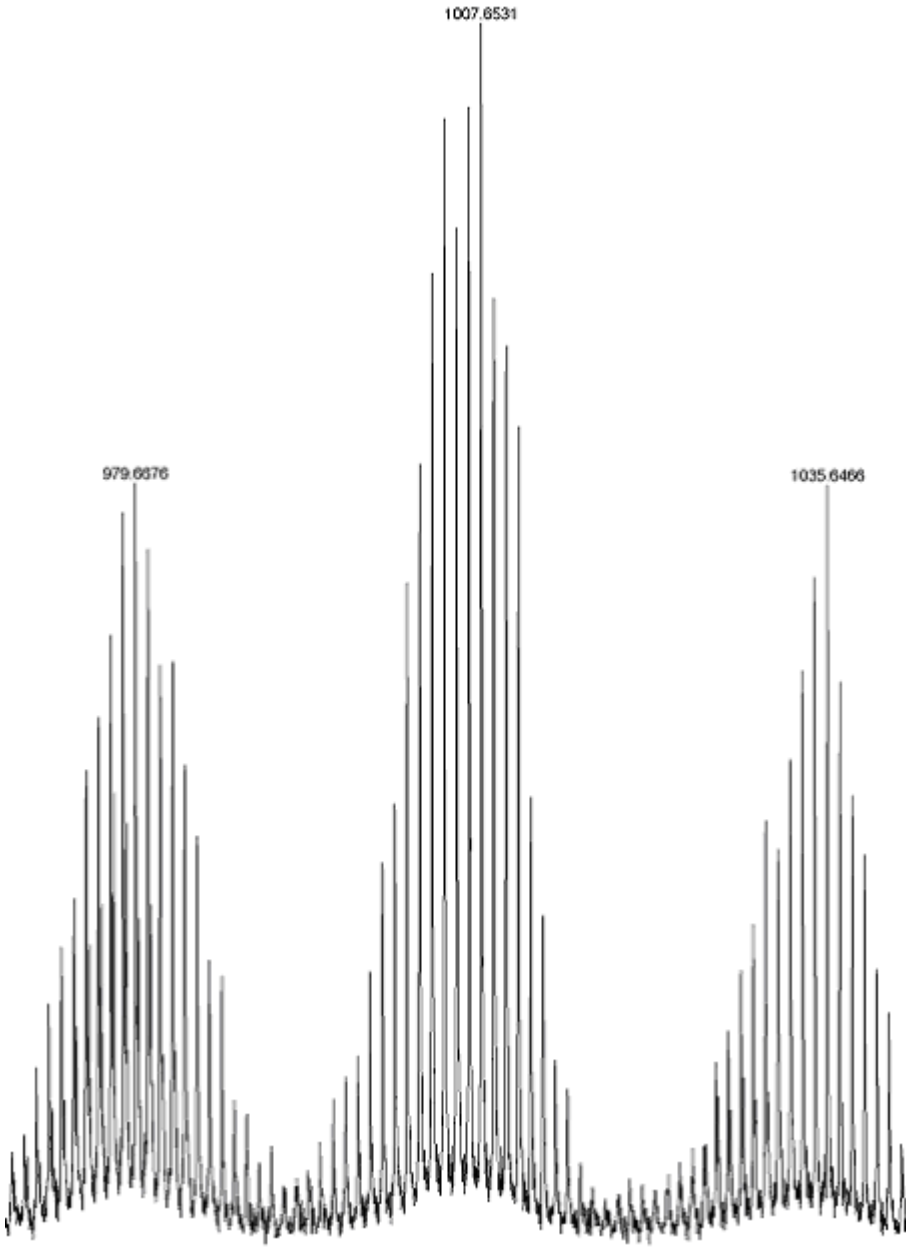

Figure 53: Minor peaks in ESMS spectrum of (VIb)

All these peaks appear to be associated with a high molecular weight metal carbonyl cluster which must contain silicon, as $Ru_3(CO)_{12}$ and $H_4Ru_4(CO)_{12}$ do not have molecular weights this high.

The two highest intensity peaks within the ESMS spectrum correlate well with the calculated values for multi-ruthenium atom containing species (refer to Table 10). Furthermore, all peaks observed fit the generated isotope patterns for their respective calculated multi-ruthenium species (refer to Appendix 3 and Appendix 4).

Table 10: Solved peaks of ESMS spectrum for (VIb)

Compound	**Found m/z**	**Calculated m/z**
Major		
$Ru_3(CO)_{11}(Si_3(CH_3)_6O_2)OCH_3$	849.751	849.739
$Ru_3(CO)_{10}(Si_3(CH_3)_6O_2)OCH_3$	821.758	821.744
Minor		
$H_4Ru_4(CO)_{14}(Si_3(CH_3)_6O_2)_2OCH_3$	1244.712	1244.721
$HRu_4(CO)_{14}(Si_3(CH_3)_6O_2)OCH_3$	1035.647	1035.637
$HRu_4(CO)_{13}(Si_3(CH_3)_6O_2)OCH_3$	1007.653	1007.642
$HRu_4(CO)_{12}(Si_3(CH3)_6O_2)OCH_3$	979.668	979.655

The result of increasing the siloxane chain length has given intermediate type compounds with the dodecacarbonyltriruthenium group remaining after addition of the siloxane. These cyclic compounds are probably similar to those made by Curtis et al.[33] however, the triruthenium group has remained after the attachment of the siloxane (refer to Figure 54). Therefore, with the extra flexibility it is presumed that the two oxygen atoms within the siloxane bridge allow a chelating arrangement rather than the formation of polymers. There also is the possibility of dative interactions between the siloxane O atoms and rutheniums, like those found by Braunstein et al. involving large bulky siloxanes and dodecacarbonyltriruthenium[31].

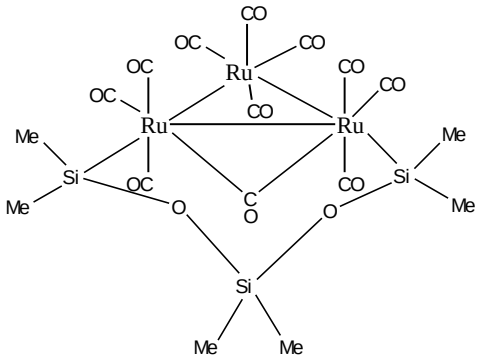

Figure 54: Proposed structure of (VIb)

There is however, some formation of the by-product, therefore these proposed Curtis-type intermediate cyclic compounds are not the only products formed from this reaction. Further ESMS conducted, without sodium methoxide, has given peaks that match *m/z* values for a parent by-product $H_2Ru_4(CO)_{13}$. This is not the same as the general $H_4Ru_4(CO)_{12}$ by-product observed in ESMS spectra for other ruthenium-silyl spectra[39]. $H_2Ru_4(CO)_{13}$ is the starting material for the series of minor compounds observed around *m/z* 1000 in Table 10. The silicon containing $H_2Ru_4(CO)_{13}$ compound has had similar compounds made within the literature however, none of these have involved the use of silicon to maintain an $18e^-$ compound[40, 41] (refer to Figure 55).

[39] Nagel, C. C.; Shore, S. G., J. Chem. Soc. Chem. Comm. (1980) 530
[40] Rheingold, A. L., Acta. Crystallographica, Sect. C. Cry. Stru. Comm. C49(8) (1993) 1458
[41] Rossi, S.; Puriainen, J.; Pakkanen, T., Organometallics 10 (1991) 1390

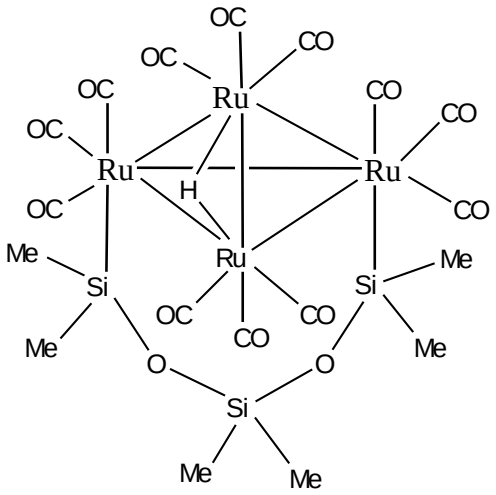

Figure 55: Proposed structure of $[HRu_4(CO)_{12}(Si_3(CH_3)_6O_2)]^-$

ESMS is capable of detecting these types of species, cf. the polymers, due to the increased flexibility of the siloxanes thus, resulting in smaller complexes.

4.7.2.2 LDI-TOF Mass Spectrometry Data

Mid mass spectral analysis using a dried THF solution containing a crude extract of (VIb) on a polished steel surface without an ionising matrix gave a broad curve with a maxima at a *m/z* of 50,000 like that observed for compound (VIa). The observation of the same broad curve is indication of polymeric species being present within the crude extract. Therefore, the increase in siloxane flexibility, due to the extra Si-O bond, can still possibly generate inorganic polymers. Lower *m/z* values did not give the same results as that observed within the ESMS spectra.

4.7.3 NMR Spectroscopic Data

4.7.3.1 ^{1}H NMR Spectroscopic Data

The ^{1}H NMR spectrum shows two peaks appearing at 0.6 ppm and 0.1 ppm in a 2:1 ratio, which was expected for this compound. The signals have been assigned as belonging to the two terminal Si-CH_3 groups and the central Si-CH_3 groups respectively. This is based on knowing that the two terminals silicon groups have equivalent environments, with the central silicon having its own environment, hence the 2:1 ratio.

4.7.3.2 ^{13}C NMR Spectroscopic Data

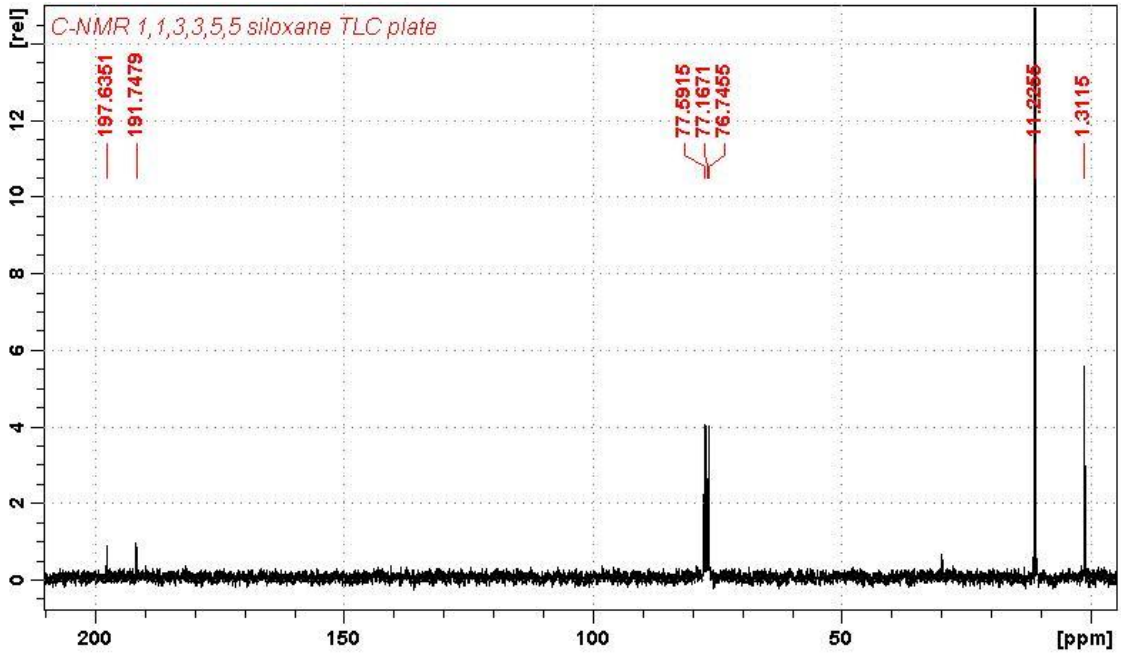

Figure 56: ^{13}C NMR spectrum of (VIb) in $CDCl_3$

^{13}C NMR, DEPT135 and 2D-XHDEPT135 experiments were conducted to further prove that the two ^{1}H NMR signals belonged to the two separate environments mentioned.

Within the ^{13}C NMR spectrum there appeared four peaks, two in downfield positions at 11.2 ppm and 1.3 ppm which are assumed to be the general

Si-CH_3 aliphatic signals. The other two peaks within the spectrum were at 197.6 ppm and 191.7 ppm which was unexpected as in previous examples the $Ru(CO)_4$ units were equal and only one signal was observed (refer to Figure 56).

DEPT135 spectra acquired showed the removal of the two peaks in the ^{13}C NMR spectrum at 190 ppm, with the two peaks in the downfield positions remaining in the positive phase. 2D NMR spectra showed the two peaks appearing at 11.2 ppm and at 1.3 ppm matched the ^{1}H NMR spectrum signals appearing at 0.6 ppm and 0.1 ppm respectively.

Investigating the IR spectra again, the bands observed initially indicated that there was an arrangement of *cis* and *trans* compounds present. However, with the ^{13}C NMR spectra showing two separate CO peaks the IR spectra could potentially be only one compound. Within the ESMS spectra the strongest peaks appeared at *m/z* 849 and 821 which match a multi-ruthenium atom siloxane compound that must containing a bridging trisiloxanes ($[M+OMe]^-$ and $[M-CO+OMe]^-$ respectively ($M = Ru_3(CO)_{11}(Si_3(CH_3)_6O_2)$) (refer to Table 10). The proposed structure of this compound (refer to Figure 54) shows that the ruthenium carbonyls are not all equivalent. Therefore, it is possible to get a separation of carbonyl bands within the ^{13}C NMR spectra. The peaks appear to be in a 1:1 ratio but physically they are not therefore, it is unclear why the CO peaks are observed in this manner. Furthermore, these peaks are unable to be assigned to which ruthenium carbonyl unit they originate from. However, it is suspected that the peak at 197 ppm is from the two $Ru(CO)_3$ groups as silicon is slightly electronegative and may force the peak to a more upfield position.

The appearance of more than one strong band within the IR spectra could be for the same reasons as why two carbonyl bands were observed within the ^{13}C NMR spectra. This is suspected as the $Ru(CO)_4$ and $Ru(CO)_3$ units differ thus, giving a complex band pattern within the carbonyl region of the spectrum. However, the possibility of *cis* and *trans* forms also being present cannot be ignored as chromatographic techniques used are unable to separate out compounds based on their structure, separation is achieved based on their mass.

4.8 Bis (triethylsilyl)-poly
[1,1,3,3-tetramethyldisiloxane(octacarbonyl)diruthenium] (VIIa)

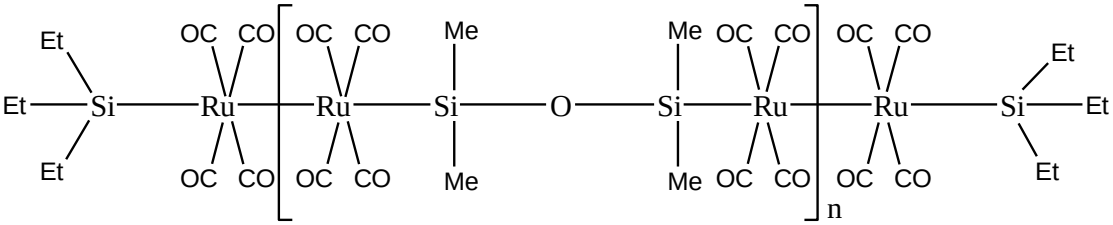

Figure 57: Proposed end capped siloxane polymer structure of (VIIa)

Further work conducted after the attempted synthesis experiments involving di- and tri - siloxanes to make polymers, an experiment involving both di- and mono-silicon hydrides was conducted in an attempt to synthesis a series of shorter polymeric units. The polymer formed in the attempted synthesis of (VIa) cannot be crystallised or chromatographed due to its size. Therefore, using small mono-silanes (Et_3SiH) the polymer can be stopped through end-capping (refer to Figure 57). This should result in smaller polymer fragments which could potentially be crystallised and chromatographed using techniques achieved in purifying the dimer compounds.

An ampoule containing hexane had added to it $Ru_3(CO)_{12}$, $HMe_2SiOSiMe_2H$ Et_3SiH. The ampoule was sealed and heated at 85 ^oC for 90 hrs to give a dark transparent amber solution of (VIIa). The ampoule was opened and the solvent removed under vacuum to give a dark brown oil, with a crude yield of 61 %.

The oil was unable to be chromatographed however, attempts made using silica with 1:1 petroleum spirits:CH_2Cl_2 solvent mixture eluted two bands with the majority of the compound remaining bout to the inert phase. The fastest band was pale yellow near the solvent front, with the majority of the compound remaining bound to the inert phase. The fastest band was extracted using the same solvent mixture and was subjected to IR and ESMS analysis.

The IR υCO band pattern was that of the by product $H_4Ru_4(CO)_{12}$ with the ESMS spectrum also showing strong peaks associated with this compound also. However, within the ESMS spectrum there also existed another peak observed at *m/*z 688, this has been assigned to a minute formation of the species (Va), which was expected. Due to no purification technique successfully working, all characterisation methods mentioned involves the crude material.

4.8.1 IR Spectroscopic Data

An IR solution cell spectrum using petroleum spirits gave multiple strong bands within the υCO region similar to that observed for (VIa). Therefore, as mentioned by Knox and Stone[22], and observed in previous compounds, the observation of more than one strong υCO band is an indication of *cis* and *trans* species possibly being present within the mixture. However, if the IR spectra for (VIa) and (VIIa) are overlapped there are large differences in the υCO band positions. Compound (VIa) contains three medium intensity bands >2050 cm^{-1}, with two very strong υCO peaks at 2033 cm^{-1} and 2012 cm^{-1}. Whereas, compound (VIIa) contains two strong bands at 2080 cm^{-1} and 2066 cm^{-1} and another strong band at 2025 cm^{-1} with a further two weaker bands between these three.

There are some physical similarities between (VIa) and (VIIa) however, the IR spectrum for (VIIa) shows a shift in the υCO bands towards higher wave-numbers, cf. (VIa). Clearly the addition of Et_3SiH into the reaction mixture has made the two oils different.

A full IR spectrum of (VIIa) acquired in KBr showed the presence of a Si-CH_3 band at 1200 cm^{-1} and the same separation of the Si-O-Si band around 1000 cm^{-1} into its symmetric and asymmetric bands, as observed for (VIa) (refer to Figure 44).

4.8.2 Mass Spectrometry Data

Using ESMS no $[M+OMe]^-$ peaks were observed with the exception of the by-product $H_4Ru_4(CO)_{12,}$ as seen in (VIa) mass spectra, and a minute quantity of (Va) $[M+OMe]^-$ at *m/z* 688 was also observed as mentioned.

4.8.2.1 LDI – TOF Mass Spectrometry Data

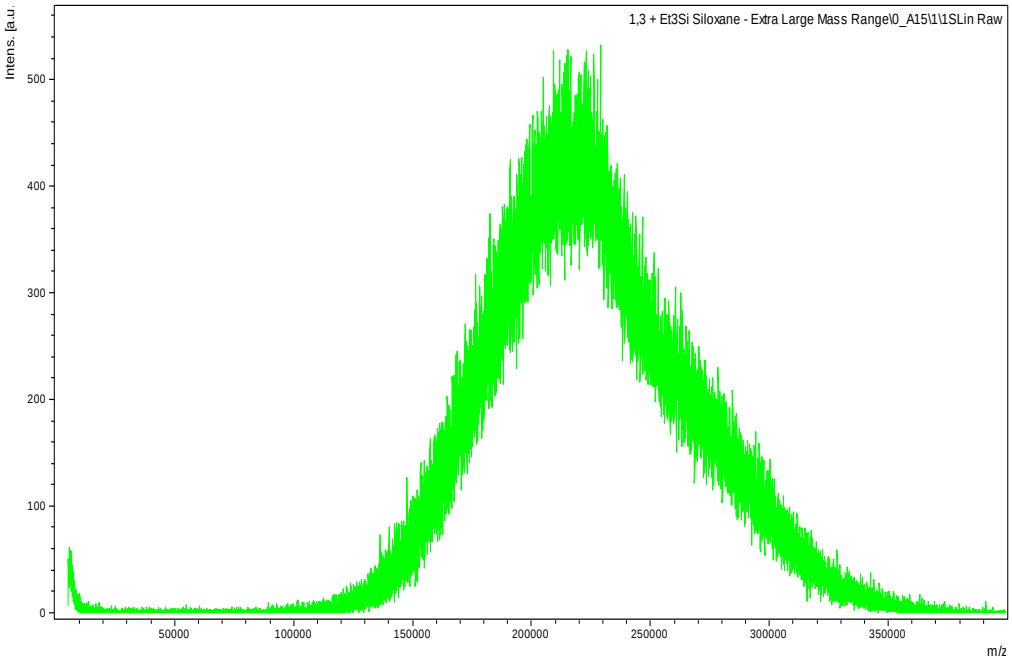

Figure 58: LDI-TOF mass spectrum of (VIIa) on a polished steel plate

A polished steel plate was mounted, on which a dried THF solution containing (VIIa) without any ionisation matrix was prepared. The laser beam ionised the sample and gave a very large broad peak from *m/z* 110,000 to 350,000 with a maxima at *m/z* 200,000 (refer to Figure 58). This peak is far different from that observed for (VIa), not only with *m/z* value but also with the intensity observed. Laser ionisations were also conducted at lower *m/z* value with no observable peaks present, with the exception of the by-product.

4.8.3 NMR Spectroscopic Data

NMR data acquired showed a complex spectrum however, all spectra acquired were different to that acquired for (VIa). The ^{1}H NMR spectrum showed three sets of peaks appearing, a singlet at 0.1 ppm with a triplet and quartet at 0.9 ppm and 0.5 ppm respectively.

When the crude mixture was removed from the ampoule the solvent was removed under vacuum which effectively should also have removed any remaining residual Et_3SiH. Therefore, it appears as though the crude mixture contains compounds that contain both silicon reagents. Further NMR experiments acquired involve ^{13}C NMR, DEPT135 and a ^{13}C-coupled carbon series of spectra. All carbon spectra acquired show the appearance of compounds which contain both silicon reagents like that observed within the ^{1}H NMR. As observed in previous techniques, the NMR data also shows that the (VIIa) oil differs substantially from compound (VIa).

Within the ^{13}C NMR there appears multiple peaks in the downfield region and one peak appearing at 189 ppm assigned to being a ruthenium carbonyl, which was not observed in the ^{13}C spectrum for (VIa). The DEPT135 spectra shows that the downfield region peaks at 6.7 ppm, 1.0 ppm and -0.3 ppm remain in the positive phase with one peak at 6.2 ppm becoming inverted. The ^{13}C coupled carbon spectrum acquired only shows one quartet (J = 118 Hz) present at 1.0 ppm, the coupling constant observed is that of a directly bound aliphatic groups to silicon. Furthermore, the appearance of this quartet, for (VIIa), overlaps perfectly with the largest quartet (J = 118 Hz) observed for the ^{13}C coupled carbon NMR spectrum acquired for (VIa).

It is therefore unclear what the structural arrangement of (VIIa) oil contains, based on the data acquired. The IR and NMR spectra are the only spectra that show some similarities to the original polymeric compound (VIa) with LDI-TOF being completely different to that acquired for (VIa).

4.9 Bis (triethylsilyl)-poly
[1,1,3,3,5,5-hexamethyltrisiloxane(octacarbonyl)diruthenium] (VIIb)

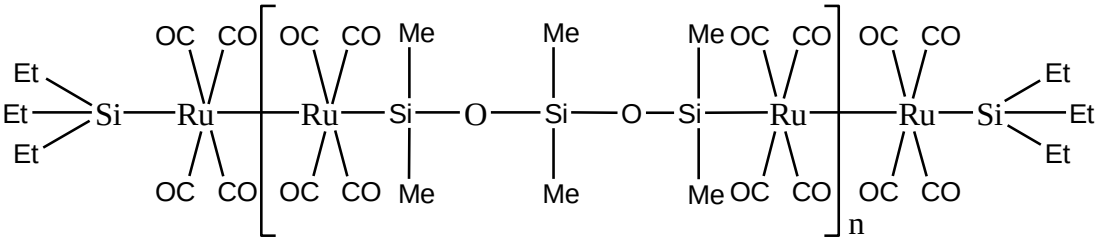

Figure 59: Proposed end capped siloxane polymer structure of (VIIb)

As conducted in an attempted synthesis of (VIIa), another end-capped polymeric ruthenium siloxane compound was attempted, involving the more flexible trisiloxane to generate (VIIb) (refer to Figure 59). Although it was found that (VIb) the more flexible siloxanes tended to form small cyclic ruthenium compounds, as opposed to polymeric compounds. The same broad band was observed in the LDI-TOF spectra and the generation of the by-product observed in ESMS are both indications of polymeric material synthesis.

Using the same method as conducted for (VIIa), $Ru_3(CO)_{12}$, $HMe_2SiOSiMe_2OSiMe_2H$ and Et_3SiH were added to an ampoule containing hexane. The ampoule was sealed and heated at 90 ^oC for 72 hrs resulting in a dark amber solution, which was extracted and the solvent removed under vacuum. The crude product was a dark oil, similar to that found for (VIb), where the oil solidified at low temperatures and would only return to an oil when re-dissolved in petroleum spirits.

The oil was chromatographed using silica eluting with a 1:1 petroleum spirits:CH_2Cl_2 solvent mixture. The fastest eluting brown/yellow band was extracted using CH_2Cl_2 followed by removal of this solvent under vacuum.

4.9.1 Spectroscopic Data

An IR spectrum of compound (VIIb) was acquired in petroleum spirits and the υCO region was investigated. The spectrum showed a complex mixture of compounds with the appearance of more than one strong υCO band present. The spectrum however, was the same as that acquired for (VIb) (refer to Figure 51).

Mass spectrometry acquired showed only the same peaks as that observed within the ESMS spectra acquired for (VIb) (refer to Figure 52 and Figure 53). LDI-TOF mass spectrometry techniques did not give any broad bands like that observed for (VIa), (VIb) or (VIIa) at higher *m/z* values. Lower *m/z* spectra did not show the same series of peaks as that observed within the ESMS spectra.

All NMR data acquired indicates that the oil formed consists of a mixture of compounds however; the main compound present is that of (VIb). ^{1}H and ^{13}C NMR data are identical to that obtained for (VIb) (refer to Figure 56). Therefore, it can be stated that no end capped polymeric compounds of the type in Figure 59 are formed by the thermal reaction between $Ru_3(CO)_{12}$, $HSiMe_2OSiMe_2OSiMe_2H$ and Et_3SiH. The thermal reaction between $Ru_3(CO)_{12}$ and the siloxanes appear to occur faster cf. the reactions between $Ru_3(CO)_{12}$ and the silanes.

4.9.2 Poly [1,4-(dimethylsilyl)benzene(octacarbonyl)diruthenium] (VX)

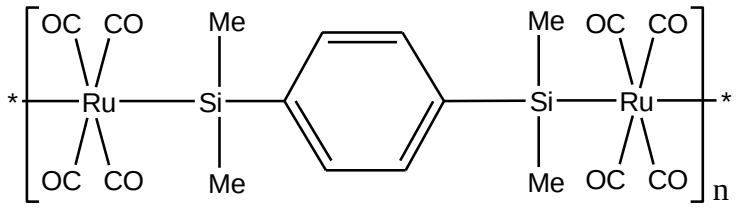

Figure 60: Structure of a singular polymeric unit for (VX)

The polymeric compound (VX) was previously made by Nombel et al. but was unable to be given a molecular weight due to its insolubility[30]. Other derivatives of (VX) were found to have *m/z* of roughly 15,000, using different techniques to that achieved in the literature, it is hoped that a molecular weight can be obtained for (VX).

$Ru_3(CO)_{12}$ and 1,4-bis(dimethylsilyl)benzene were added to an ampoule containing hexane. The ampoule was sealed under vacuum and heated at 85 ^oC for 90 hrs, resulting in a bright yellow solid and solution suspension. The ampoule was opened and the solvent removed under vacuum, giving a yellow solid. The solid was unable to be dissolved in common organic solvents and hence, was unable to be chromatographed. However, the solid was washed several times with petroleum spirits, removing the majority of the by-product $H_4Ru_4(CO)_{12}$ to give a dark yellow solid with a yield of 20 %.

4.9.3 Spectroscopic Data

IR spectra was acquired in KBr, due to the insolubility of the solid, showed a very strong υCO band that had separated into two. These bands occurred at 2005 cm^{-1} and 1995 cm^{-1}, there was one other medium intensity band observed at the higher wave function of 2050 cm^{-1}. These bands fit the general IR pattern for these types of compounds and are a good correlation with that found in the literature. The separation of the strongest band is possibly a result of increased resolution in the KBr disc for the $Ru(CO)_4$ bands. This is proposed as IR KBr spectra acquired for the polymer (VIa) observed the band separation of the Si-O-Si unit into its symmetric and asymmetric modes.

ESMS was conducted involving the solid (VX) product with the only peaks observed in the spectra assigned to the by-product $H_4Ru_4(CO)_{12}$.

LDI and MALDI-TOF mass spectrometry was conducted using a polished steel plate with the solid (VX). Laser ionisations did not result in any peaks for both techniques, within any *m/z* range.

As found within the literature, compound (VX) is insoluble in common organic solvents and its molecular mass was unable to assigned using other techniques that were not mentioned to have been used.

4.10 Poly [(tetracarbonyl)ruthenium] (VXI)

The inorganic polymeric ruthenium carbonyl compound (refer to Figure 11) was prepared in a Schlenk flask containing THF. The flask had $Ru_3(CO)_{12}$ added before the solution had $CO_{(g)}$ bubbled through it for 5 min. The carbonyl saturated solution and atmosphere was sealed and left in natural sunlight for three days[19]. An orange film developed on the walls of the flask with a high yield of >90 % as found by Masciocchi et al.

4.10.1 Spectroscopic Data

The orange solid was subjected to IR spectroscopy in the form of a KBr disc. The same bands observed within the literature were also observed for the synthesised compound (VXI)[19].

LDI and MALDI-TOF techniques were both conducted using a polished steel plate with the compound (VXI) (refer to Figure 11). Both techniques were used to determine a polymeric molecular mass however, due to the compounds low solubility, and potentially low ionisation, no peaks were observed.

4.1 Summary

Two known compounds containing the Si-Ru-Ru-Si linkage were prepared using the method of Knox and Stone, and full NMR data was acquired. Using the same method a new example, $[PhCH_2Me_2SiRu(CO)_4]_2$ was fully characterised.

Continuing on from the original work, polymeric species were synthesised through using siloxanes as bridging silyl groups between each Ru – Ru unit. Two separate polymers were synthesised, $[Ru(CO)_4SiMe_2OSiMe_2Ru(CO)_4]_n$ (VIa) and $Et_3Si[Ru(CO)_4SiMe_2OSiMe_2Ru(CO)_4]_nSiEt_3$ (VIIa). These two compounds were prepared in the same manner as that achieved for the dimeric compounds using di-functional silanes. Both compounds were black oils that slowly decomposed in solution and were unable to chromatographed or purified using crystallisation techniques. A chemical characterisation technique was attempted on (VIa) to determine that the repeating unit Si-Ru-Ru-Si was present. The crude mixtures showed very high molecular weight species having broad LDI-TOF curves with maxima at *m/z* 60,000 and *m/z* 200,000 respectively. All other spectroscopic data were consistent with the proposed structures, but complete characterisation was not achieved.

Using the more flexible siloxane $HSiMe_2OSiMe_2OSiMe_2H$ resulted in a compound where the siloxane attaches to the same cluster unit, giving molecular rather than polymeric species.

The compound was able to be purified using chromatography, resulting in a yellow solid which was characterised by spectroscopic methods.

5.0 Conclusion

The intent of this thesis was to develop an inorganic polymer that maintained metal – metal bonding without the use of large stabilising groups.

The end–capped iron silyl compounds had two new compounds that were not mentioned within the literature have now been synthesised. These did not give interpretable data by ESI-MS. New NMR data has been gathered for the known literature compounds that was not initially available.

Adding to the research that Knox and Stone had previously achieved, this thesis has uncovered new information that was not previously available regarding one of the literature compounds synthesised.

Synthesis of four new ruthenium silyl compounds has been achieved, one dimeric ruthenium silyl compound, (Vc); two inorganic polymers (VIa) and (VIIa). One other compound was characterised as being a new triruthenium compound containing a bridging siloxane.

The two polymeric species were unable to be chromatographed and were found to consist of high molecular weights. Other characterisation techniques were used in an attempt to determine that (VIa) consisted of multiple Si-Ru-Ru-Si units, but with limited success.

Future work involved with the synthesis of inorganic polymers that maintain metal – metal bonding may be want to investigate the accurate sizes using other instrumentation i.e. size exclusion chromatography.

6.0 Appendix

Isotope patterns for ruthenium.

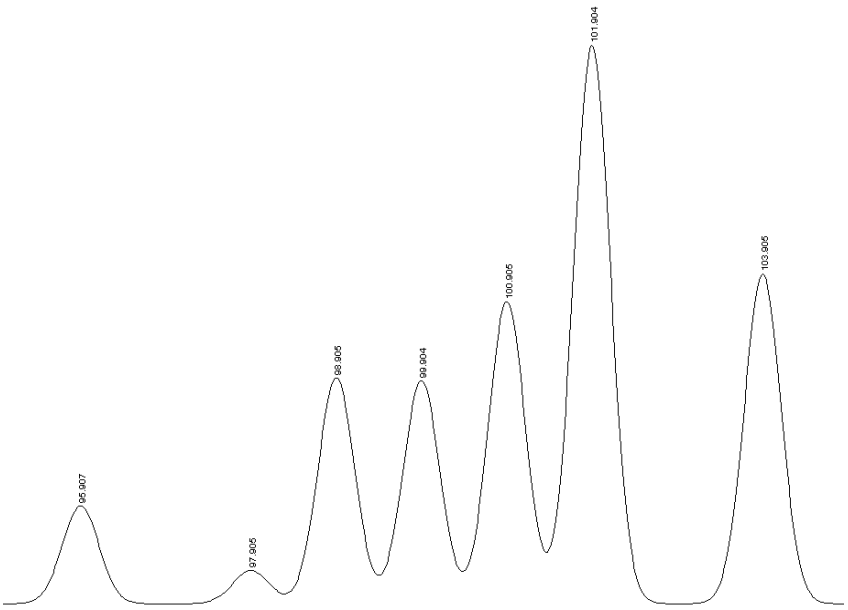

Appendix 1: Ru_1

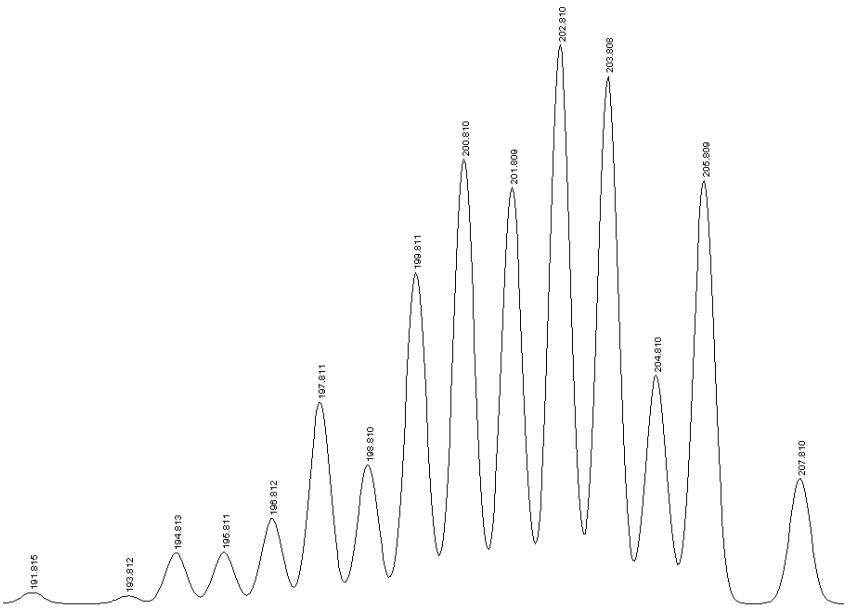

Appendix 2: Ru_2

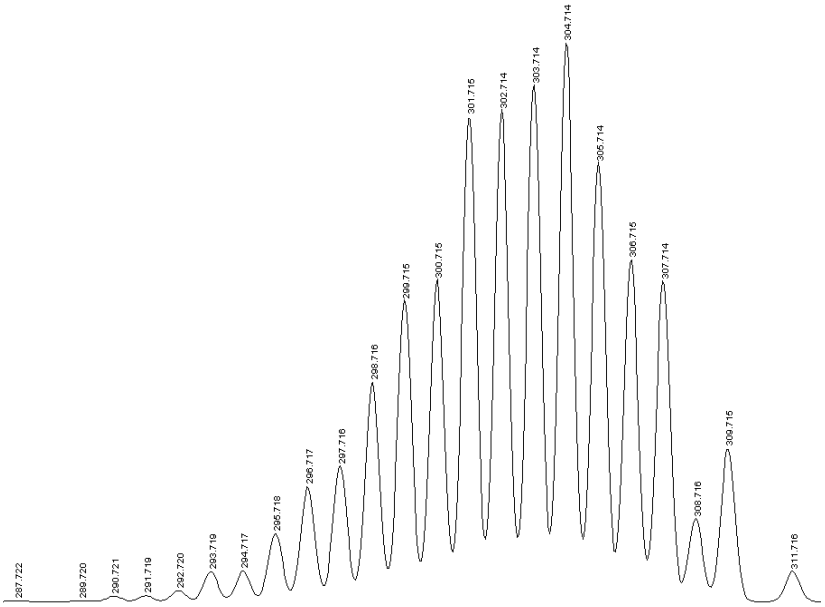

Appendix 3: Ru_3

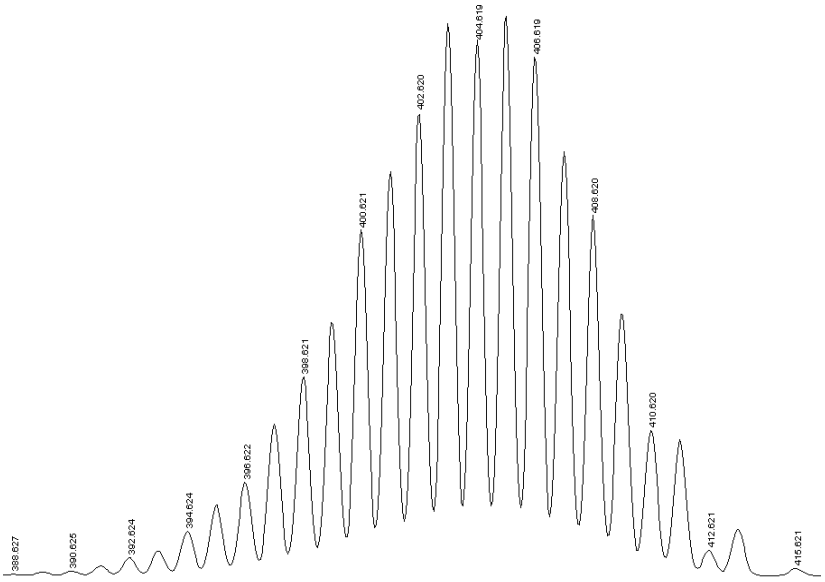

Appendix 4: Ru_4

Isotope patterns for ruthenium – tin compounds

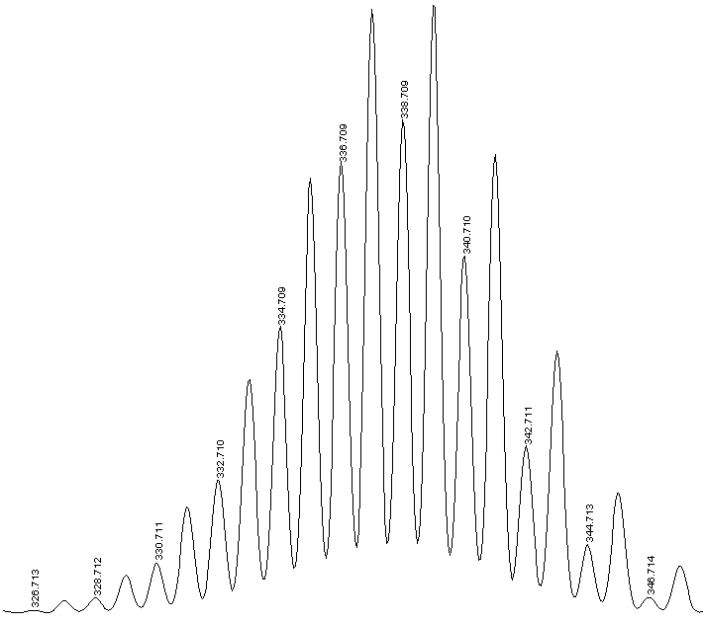

Appendix 5: Sn_2Ru

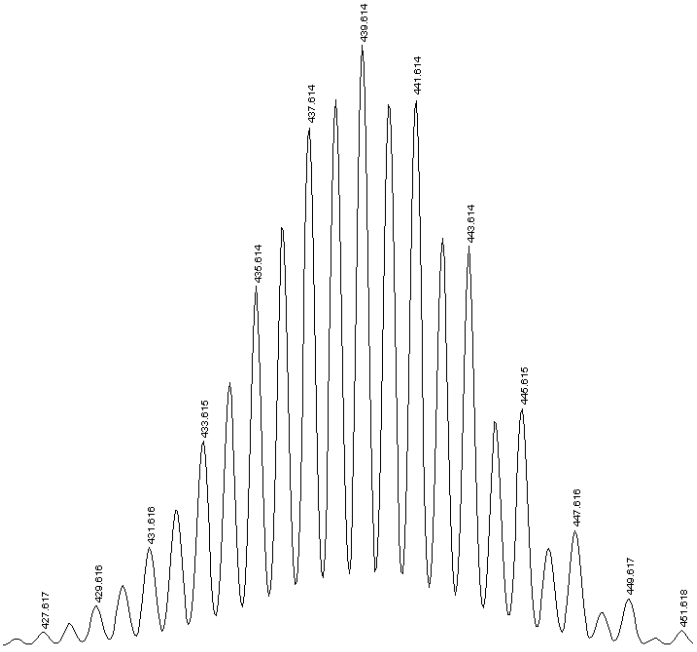

Appendix 6: Sn_2Ru_2

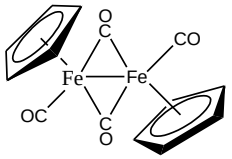

$(Fp)_2$

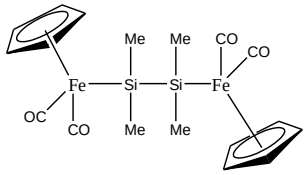

(Xa)

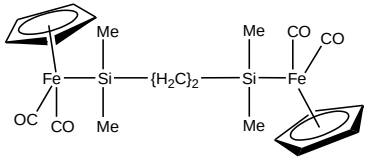

(Xb)

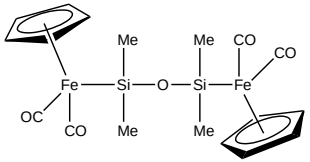

(Xc)

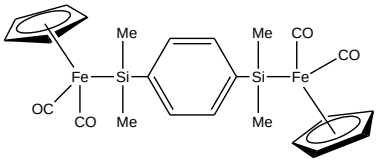

(Xd)

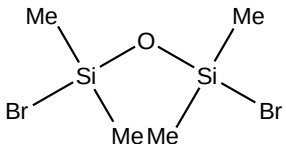

(Ia)

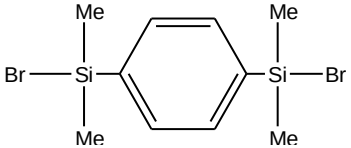

(Ib)

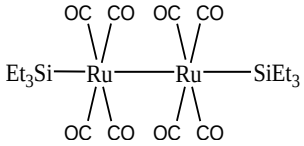

(Va)

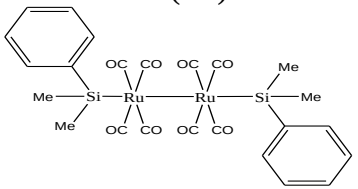

(Vb)

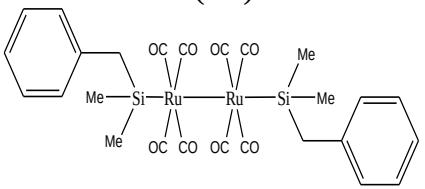

(Vc)

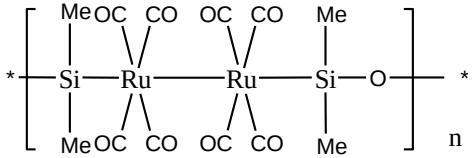

(VIa)

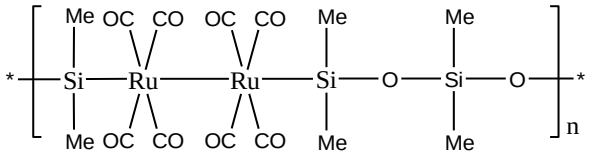

(VIb)

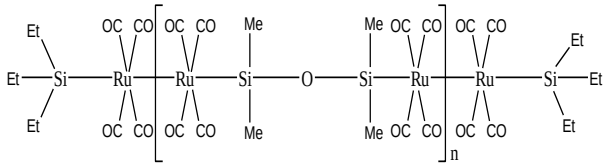

(VIIa)

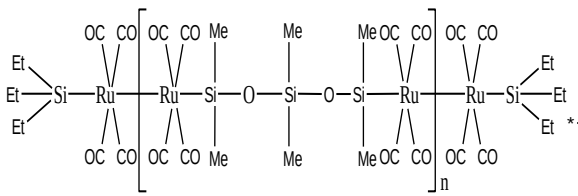

(VIIb)

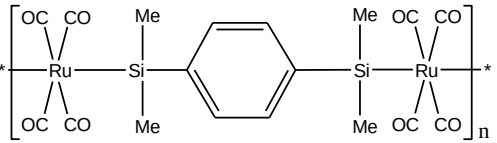

(VX)

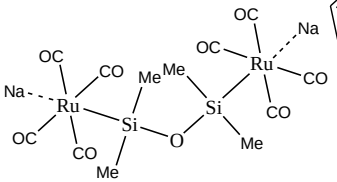

(XVa)

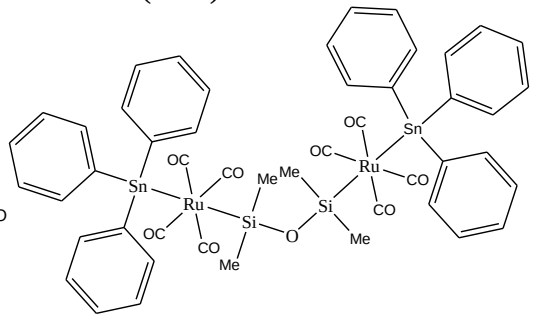

(XVIa)